

For Reference

NOT TO BE TAKEN FROM THIS ROOM

EX LIBRIS
UNIVERSITATIS
ALBERTAENSIS



T H E U N I V E R S I T Y O F A L B E R T A

RELEASE FORM

NAME OF AUTHOR	Jeffrey William Carr
TITLE OF THESIS	Laser Vaporization of Solid Samples into an Inductively Coupled Plasma
DEGREE FOR WHICH THESIS WAS PRESENTED	M.Sc.
YEAR THIS DEGREE GRANTED	1980

Permission is hereby granted to THE UNIVERSITY OF ALBERTA LIBRARY to produce single copies of this thesis and to lend or sell such copies for private, scholarly or scientific research purposes only.

The author reserves other publication rights, and neither the thesis nor extensive extracts from it may be printed or otherwise reproduced without the author's written permission.

THE UNIVERSITY OF ALBERTA
LASER VAPORIZATION OF SOLID SAMPLES
INTO AN INDUCTIVELY COUPLED PLASMA

by



JEFFREY WILLIAM CARR

A THESIS

SUBMITTED TO THE FACULTY OF GRADUATE STUDIES AND RESEARCH
IN PARTIAL FULFILMENT OF THE REQUIREMENTS FOR THE DEGREE
OF MASTER OF SCIENCE

DEPARTMENT OF CHEMISTRY

EDMONTON, ALBERTA

FALL, 1980

THE UNIVERSITY OF ALBERTA
FACULTY OF GRADUATE STUDIES AND RESEARCH

The undersigned certify that they have read, and
recommend to the Faculty of Graduate Studies and Research,
for acceptance, a thesis entitled LASER VAPORIZATION OF
.....
SOLID SAMPLES INTO AN INDUCTIVELY COUPLED PLASMA submitted
.....
By JEFFREY WILLIAM CARR in partial fulfilment of the
.....
requirements for the degree of Master of Science.

To my wife Janice and my parents for
their support through the years

ABSTRACT

Laser vaporization has long been used in spectroscopic analysis as a sampling technique. This method has been used to produce a vapor that could be viewed directly or excited by another source. The inductively coupled plasma (ICP) is now a most promising source for emission spectroscopy, however few people have attempted to introduce solid samples into the plasma. The system developed in this study uses a laser vaporizer or atomizer as a solid sampler for an ICP.

In this system the sample to be vaporized is placed in an airtight sample holder inside the shielded plasma chamber directly underneath the torch. The laser, when fired, vaporizes a small portion of the sample. The vapor produced is carried into the plasma with a stream of argon, resulting in a transient emission signal. The signal is measured using a self scanning photodiode array which provides 500 Å spectral coverage over the region of interest. This viewing area permits the observation of several spectral lines simultaneously and facilitates the use of internal standards.

The laser used in the initial work was a pulsed ruby operated in the free running mode as well as in the Q switched mode using a KDP Pockels cell. The laser's specified power output is as high as 100 MW when operating in the Q switched mode and the maximum energy delivered per pulse is as high as 2 Joules. Vaporization reproducibility was tested over

a range of laser power and intensities.

Aluminum alloys have been studied extensively and calibration curves of the concentration of trace components have been obtained. The precision of the ruby system is in the range of 5%. Using this system we have been able to achieve detection limits below one picogram in some cases, depending on the size of the sample being injected into the plasma and the element being investigated. Sample sizes vary depending on the material vaporized and the mode of laser operation. A typical size of aluminum sample vaporized in the free running mode is 0.5 mg and in the Q switched mode about 25 μg .

The greatest problems with the system are the ruby laser's inherent power fluctuations and inhomogeneity of the sample. The power fluctuations are responsible for selective volatilization introducing significant error into the system. Another problem caused by power fluctuations is large shot to shot signal intensity variation. This has been overcome by using another element in the sample with an emission line nearby the element of interest as an internal standard. In the case of aluminum with only trace impurities (less than 0.5%) a weak aluminum line can be used as a constant internal element.

Other types of samples such as brass, steel and biological materials have been investigated and are discussed briefly.

ACKNOWLEDGEMENTS

I would like to acknowledge the guidance and assistance given to me by many people during my stay at the University of Alberta, foremost among these being Dr. G. Horlick. In addition, I would like to thank Eric Salin for his help with the initial stages of the research, the shop personnel for their expert advice and Elizabeth Stubley for typing and proof reading the manuscript.

Also included in this acknowledgement should be a list of individuals who through their personal efforts have made my stay at this university as difficult as possible. From these people, I have learned a valuable lesson in dealing with the outside world.

Table of Contents

Chapter	Page
I Spectrometric Techniques for Solid Sampling	1
A. Introduction	1
B. Solid Sampling Techniques	1
1. D.C. Arc	1
2. A.C. Spark	3
3. Electrothermal Atomization	4
4. Inductively Coupled Plasma Emission	6
5. Laser Vaporization	7
a) Introduction	7
b) Interaction of Lasers with Solids	11
i) The Crater	11
c) Spectral Methods	23
i) Introduction	23
ii) Atomic Emission	24
a) Laser Vaporization and Excitation	24
b) Cross Excitation	26
iii) Atomic Absorption	30
II Instrumentation	37
A. Lasers	37
1. Introduction	37
2. Principle of Laser Operation	37
3. Q Switching	43
4. Ruby Laser	47
B. Radiofrequency Inductively Coupled Plasma	56
1. Introduction	56
2. Instrumentation	57
C. Sample Chambers	57
1. Introduction	57
2. Rod Sample Chamber	58

Chapter	Page
3. Disc Sample Chamber	60
D. Optical System	63
E. The Diode Array Detector	65
1. Introduction	65
2. Instrumentation	65
F. Data Collection	66
1. Introduction	66
2. PDP-11 System	66
3. PDP-8 System	67
III Sample Types	68
A. Aluminum Samples	68
B. Brass Samples	68
C. Nonconducting Samples	68
IV Initial System Characterization	72
A. Time Studies	72
1. Introduction	72
2. Experimental	72
3. Spectral Results	73
4. Conclusions	76
B. Qualitative Wavelength Studies	77
1. Introduction	77
2. Experimental	78
3. Spectral Results	78
4. Conclusions	78
V Sampling Technique	83
A. Introduction	83

Chapter	Page
B. Laser Operation	83
1. Timing and Number of Shots	83
i) Introduction	83
ii) Experimental	84
iii) Results	85
2. Q Switched Versus Free Running	85
i) Introduction	88
ii) Experimental	90
iii) Spectra and Results	91
3. Effects of Focus	93
4. Summary	94
C. Plasma Conditions	96
1. Introduction	96
2. Height of Observation	97
3. Flow Rate of Aerosol	99
4. Summary	101
VI Analytical Results	104
A. Introduction	104
B. Aluminum Samples	104
C. Detection Limits	119
D. Brass Samples	122
E. Nonconducting Samples	125
F. Sample Inhomogeneity	125
G. Conclusion	131
Bibliography	133
Appendix A	138

List of Tables

Table	Description	Page
1	Detection Limits for D.C. Arc, A.C. Spark, Electrothermal Atomization and ICP-DSIT	7
2	Comparison of Q switched, Semi Q switched and Free Running Laser Specifications	16
3	Detection Limits for Laser Sampling With and Without Cross-Excitation	28
4	Detection Limits for Laser Vaporized AA and Standard AA	32
5	Inrad Pockels Cell Q switch Model 212 Specifications	49
6	Inrad Q switch driver Model 2-015 Specifications	50
7	Korad Ruby Laser Specifications	53
8	Korad Power Supply Specifications	54
9	High Alloy Aluminum Samples	69
10	Low Alloy Aluminum Samples	70
11	Brass Samples	71
12	Time Behavior of Sample HA	77
13	Relative Standard Deviations of the Emission Peaks for Various Spaces of Time Between Laser Pulses	85
14	Statistical Data for Aluminum Samples	110
15	Precision of Peak Heights for Various Samples and Ratios	117
16	Detection Limits for Selected Elements	121
17	Analytical Data for Brass Samples	124
18	Sample Inhomogeneity: Measurement of Peak Heights	129

List of Figures

Figure	Description	page
1	Crater Volume as a Function of Laser Energy	13
2	Crater Diameter as a Function of Laser Energy	14
3	Change of Reflectivity of Some Materials as a Function of Laser Power Density	17
4	Plume of Ejected Material Resulting from Laser Sampling	19
5	Craters Produced by Free Running, Semi Q switched and Q switched Lasers	21
6	Laser Probe with Cross Excitation	27
7	Energy Levels for the Ruby and the Nd:YAG Lasers	39
8	Flashlamp Output as a Function of Time and Wavelength	42
9	Pulse Output of the Free Running and Q Switched Laser during One Flashlamp Burst	44
10	Inrad Pockels Cell Model 212-150	48
11	Q Switch Interface Circuit	51
12	Korad Laser Model K-1	55
13	Rod Type Sample Chamber	59
14	Disc Type Sample Chamber	61
15	Optical Arrangement of the Laser, Plasma and Spectrometer	64
16	Time Behavior of the Laser Solid Sampler	74
17	Emission Signal from Sample HA	79
18	Effects on the Emission Signal by the Number of Laser Shots	86
19	Comparison of the Emission Signals for Free Running or Q switched Modes of Laser Operation	92
20	Effects of Focus on Aluminum Sample HG	95

Figure	Description	page
21	Vertical Emission Profiles of Aluminum as a Function of Time	100
22	Calibration Curve of Mn/Si in the Free Running Mode	104
23	Calibration Curve of Mn/Mg in the Free Running Mode	105
24	Calibration Curve of Si/Mg in the Free Running Mode	106
25	Calibration Curve of Mn/Si in the Q switched Mode	107
26	Calibration Curve of Mn/Mg in the Q switched Mode	108
27	Calibration Curve of Si/Mg in the Q switched Mode	109
28	Calibration Curve of Low Alloy Aluminum Samples with all Points Included	113
29	Calibration Curve of Low Alloy Aluminum Samples with LB not included	114
30	Calibration Curve of Low Alloy Aluminum Samples with LB and LH not Included	115
31	Spectra showing the Reproducibility that can be Obtained with Homogeneous Samples	118
32	Calibration Curve for NBS Brass Standards	123
33	Brass Spectra	126
34	Wood Spectra	127

CHAPTER I

SPECTROMETRIC TECHNIQUES FOR SOLID SAMPLING

A. Introduction

Atomic spectrographic techniques are some of the most powerful methods available for the qualitative and quantitative analysis of the elemental composition of a large variety of materials and samples. The modern methods including flame atomic emission, absorption and fluorescence, D.C. arc and spark spectroscopy, inductively coupled plasmas and electrothermal atomic absorption spectroscopy provide an easy method of producing accurate and precise results. For these methods, sample types can be presented in solid or liquid (solution) form but for the most part, atomic spectrometric methods are more precise and accurate for solution samples. However, in many analytical situations direct analysis of solid samples is desirable as often very significant savings in time can be achieved in the area of sample preparation. These methods will now be briefly reviewed with respect to their capability for the analysis of solid samples.

B. Solid Sampling Techniques

1. D.C. Arc

The D.C. arc, one of the first widely used spectrometric tools, was also the first system to conveniently handle solid samples. An industry standard for a long period of time, the D.C. arc handles solid samples in the form of a powders. Typically a sample will be diluted in a matrix of LiCO_3 or some other suitable spectroscopic buffer and a small percentage

of internal standard will be added. Other forms of solid samples have been used but powders are by far the most common.

D.C. arc provides a good qualitative measurement of the spectrum; about 70 elements can be qualitatively identified in routine analysis. Semiquantitative results can be obtained fairly easily and produce results within one-half of an order of magnitude of the true value. Full quantitative results are generally more difficult to obtain. Reasonable quantitative results can be obtained with direct reading spectrometers.

Aside from being a difficult and not very convenient quantitative tool, the D.C. arc has suffered from problems that are still to be alleviated. Problems such as self absorption reduce intensity of the lines at high concentration which results in non linear calibration curves. Erratic wandering of the arc over the sample surface produces imprecise results, though the problem has been partially corrected by the use of spectroscopic buffers. After considerable improvement, the precision of a D.C. arc is still only 1% relative standard deviation (RSD). Selective volatilization results in different time behavior for elements and a long exposure time is needed to correct this. Spectral interference from other elements in the sample can be great enough to render all emission lines of the sample of interest useless. Methods such as carrier distillation for suppressing elements with many emission lines have been developed but are not totally successful in all cases.

Sample preparation for the D.C. arc is lengthy in comparison to other techniques. A sample must be finely ground and completely homogeneous with the internal standard and dilution matrix. As well as the long period needed for mixing, time must be spent accurately weighing the samples and packing the electrodes before the sample can be examined.

In spite of its faults the D.C. arc provides good qualitative and semiquantitative results (Table 1) and has the ability to handle conducting or nonconducting samples. A complete review on D.C. arcs has been published by Harvey (1,2).

2. A.C. Spark

An alternating current across an analytical gap produces a spark capable of removing a small portion or sample of the surface of the electrode. Each piece of sample removed is examined with a spectrograph similar to the one used for D.C. arc and an emission spectrum is obtained.

Solid sample types in the A.C. spark are for the most part limited to conducting substances. The system therefore has found wide applicability as a tool for quality control in the metals industry. At present the spark source is the technique of choice for the sampling of aluminum, steel, brass and metal alloys. As a routine technique, it provides accurate and precise information on major components in conducting samples. Nonconducting samples must be ground into powders and pressed into a hard graphite disc for sampling. The main drawback to spark systems is their inability to handle any samples other than conductors. The preparation of conducting

samples is simple; in most cases only the oxide film on the sample surface must be removed.

Advantages of the spark over the D.C. arc in addition to increased precision are good sensitivity for ion lines, low self absorption and linear calibration curves. Unlike the D.C. arc, the sampling mechanism of the A.C. spark is not thermal in nature and so problems in selective volatilization or fractional distillation do not arise. Unlike the steady burn of the D.C. arc, the high rate of sampling improves the precision of the spark source. Coupled with a direct reader the precision of this system is 2% to 5%. Detection limits for the A.C. spark are shown in Table 1.

Reviews of spark sources have been published by Walters (15) and a collection of benchmark papers on spark emission spectroscopy have been published in a book by Barnes (3).

3. Electrothermal Atomization

The major emphasis in generating an atomic vapor from solid samples for atomic absorption measurement is in the area of electrothermal atomization. Flames, the classic tool for atomization, have not been used for the direct analysis of powders except for one attempt to introduce solids into a flame with a spatula (7). Using electrically heated graphite tubes or rods, metal strips or braids, an atomic vapor is produced that is spectroscopically examined to determine the concentration of a single variable.

The advantages of absorption methods for solid sample determination are low detection limits for some elements and

a wide range of elements that can be determined. The disadvantages of this method are most of those common to classical flame atomic absorption as well as some specific to the solid sampling techniques. The method is generally a single element technique, a source is needed for each individual element. There are chemical and spectral interferences as well as incomplete sample atomization. A complete discussion of atomic absorption is beyond the scope of this text but several review articles are available that cover the topic in detail (4,5,6,7).

Problems specific to solid sampling are sample preparation, matrix interferences and precision. In order for the sample to vaporize completely it must be as finely divided as possible. This is accomplished by laborious grinding with an agate mortar and pestle or by putting the sample in solution and evaporating the solvent. In either case, time is needed to prepare the sample for determination. Solid sampling with electrothermal atomization is greatly affected by the matrix of the sample, with varying degrees of atomization achieved depending on the form of the matrix. The temperatures needed to vaporize a certain matrix may be high enough to boil the element to be determined right out of the sample cell resulting in a low concentration reading. Depending on the matrix and the heating cycle used the sample may be vaporized slowly or rapidly. Peak heights, the more common method of sample measurement, cannot be used in this situation. Instead the area under the curve must be measured. Even with area measurement, the precision of a sample in the part per million (ppm)

range is 5-10% and in the part per billion (ppb) range 10% to 30%. The detection limits of this technique are shown in comparison to others discussed in Table 1.

4. Inductively Coupled Plasma Emission

The inductively coupled plasma (ICP) has solved many of the problems of previous spectroscopic methods. Its use as a multielement source has been well documented (8,9), however the capability of the ICP for solid samples has not been fully developed.

Many methods for the introduction of solids have been attempted. Powdered samples have been blown into the plasma with the aerosol gas (10,11) or dropped in from above. Electrothermal atomization of solids into the plasma for emission spectroscopy has been tried with various results (13,14). Dissociation of the sample with a spark source (33) was another attempt to introduce solid samples into the plasma, however none of the above methods have been entirely successful to date.

A new technique that shows promise but has some of the sample handling problems of the D.C. arc is the direct solid insertion technique (DSIT) (12). A sample similar in form to one used in a D.C. arc is placed into a D.C. arc electrode and inserted into the center of the plasma from below. The heat of the plasma volatilizes the sample into the plasma where it is further excited for emission.

The main drawback of this system is the type of samples used. Only a powdered solid sample or a desolvated solution

will work. As with the D.C. arc sample, the time needed for sample preparation is a significant portion of the entire determination time.

The ICP as an emission source is superior to previous methods in most aspects. As a hotter source, the problems of selective volatilization and chemical interference are largely removed. The hot argon surrounding the sample also reduces the amount of self absorption. The precision is better than the D.C. arc or the A.C. spark, generally better than 1%. The detection limits of the ICP coupled with the DSIT are shown in Table 1,

A convenient method for solid sampling into an ICP has yet to be developed. Sample volatilization, the major problem, may be simplified by the use of a high powered laser. Laser vaporization is already a proven technique that has been used to generate vapor from solid samples.

5. Laser Vaporization

a) Introduction

After the invention of the ruby laser by Maiman in 1960 (16) it was soon realized that high powered lasers could be used to vaporize small amounts of materials. The radiation emitted by the laser vaporization plume, with or without additional excitation, could be viewed spectroscopically for analytical analysis. The main attraction of laser vaporization is its ability to handle conducting as well as nonconducting samples by direct vaporization of the material. In addition the small sample area examined by the focused laser beam could

TABLE 1

Detection Limits for D.C. Arc, A.C. Spark, Electrothermal
Atomization and ICP-DSIT

Element	D.C. Arc	Detection Limits (ppm)			ICP-DSIT
		A.C. Spark	Electrothermal Atomization		
Cd	.02	1	.01	.02	
Zn	.01	.5	.003	.001	
Sn	.01	.30	.2	.01	
Cu	.0003	-	.06	.0003	
Mg	.007	.05	.04	.007	
Mn	.003	.01	.02	.003	
Mo	.006	.03	.3	.6	
V	.02	.02	.3	.2	

perform local or in situ microanalysis yielding information not available by standard macroanalytical techniques. The laser alone could be used for excitation as well as sampling or additional excitation from standard techniques such as flames or sparks could be used if necessary.

The first laser microprobe developed by Breck and Cross (17) and marketed by the Jarrel-Ash company for routine analytical use was built for its microsampling capabilities. It employed a passive Q switched ruby laser using cross excitation by a spark source for additional signal intensity. The first system met with limited success and only 125 units were sold. Many other workers began investigating laser sampling systems with a large portion of the work being conducted by Russian and East German scientists. Commercial laser probes, manufactured in Moscow and Jena, Germany became available in 1963 and by 1966 eight different commercial laser sampling systems were available (19). These systems were diverse in design using ruby or Nd:glass lasers, with and without cross excitation, using all types of Q switches, spectrometers and detectors that were available at the time.

In spite of the large number of commercial instruments available, only eight references are found in the literature up to 1966 (56) but by 1968 (57) there were forty references in the literature. The field has increased yearly and at this writing nearly 1500 papers have been published on spectroscopic applications of laser vaporization.

It is not the intention of this section to review the

entire field of laser vaporization but instead to present a summary of the general findings that have been reported. Several complete reviews are available; the first, a review in German by Moenke and Moenke-Blankenburg, is now available in an English translation (18). More recent reviews by I. Harding-Barlow et al. (19), Laqua (20) and Margoshes (21) are now available as well as biannual reviews by Barnes and Kelihar in Analytical Chemistry (22,23,24,76). A bibliography containing 916 references of laser vaporization in medicine and biology was published by Eichler and Lenz (25).

A beam of laser light has more energy at its specific frequency than any other source of visible radiation known. We would not expect the interaction of the beam with a material to be a simple process. Indeed we find it a complex function of several variables including energy of the beam, number of pulses of the beam, time between pulses in the beam, type of sample and the atmosphere above the target.

Many attempts have been made to derive a theoretical model for the vaporization process. Most notable among the early investigators was Ready (26,27,28). Later more sophisticated models were developed by Bogerhausen and Vesper (29), Klocke (30) and others. The results of these investigations were not completely successful. We will discuss mostly the experimental aspects of the phenomena.

Unfocused, a normal laser beam will vaporize little if any material (56). Since the beam is parallel and essentially

monochromatic, focusing through a simple single element lens is an effective way of increasing the energy density produced by the laser. Typical gains achieved are in the order of 1000 (19).

The ability to focus to a diffraction limited spot size is of major importance in the microsampling capabilities of the laser system. The diffraction limited spot size is

$$d = 1.2 \frac{f}{D} \lambda \quad 1-1$$

where d is the spot size, f is the focal length of the focusing system, D is the beam diameter and λ is the wavelength of the laser. For the ruby in our system the calculated minimum spot size is 7 μm in diameter for the focusing system currently in use. Sampling areas of 0.5 μm have been achieved with frequency doubling and shorter focal length focusing lenses. In practice lasers do not emit exactly parallel beams and the spot size is generally larger than the calculated size (Equation 1-1) due to the beam divergence.

b) Interaction of Lasers with Solids

i) The Crater

The condition of the crater; depth, size and shape as well as the amount of sample removed depends on the properties of the sample and the condition of its surface as well as the properties of the laser. The diameter of the focal

spot is important in determining the diameter of the crater but the two of them are not the same. The crater is always larger than the focus size because of heat transfer from the focal point to the surrounding areas. The major factor in determining crater size up to a certain limit is energy of the laser beam (45) (Figure 1). After a certain beam energy is reached the crater does not increase in size regardless of an increase in laser energy (59,60). This is attributed to absorption of energy by the plume and will be discussed later.

By decreasing the energy of the beam, the crater diameter approaches that of the focal area of the beam. From Figure 2 (20) it is evident that a crater will be produced anywhere above the vaporization threshold and as the laser energy increases the diameter and depth of the crater also increases. It can also be said that with increasing energy the depth of the crater increases more rapidly than the diameter.

Interaction with the target is complex but it is believed that part of the radiation is absorbed, giving rise to a luminous plume, and the remainder of the energy is reflected. The amount of energy reflected or absorbed depends on the sample and the condition of its surface as well as the power and mode of operation of the laser. For the fraction of radiation absorbed the absorption takes place in the first few hundredths of a millimeter of the sample. The material is quickly raised above its boiling or decomposition point and vaporization begins.

The actual mechanism of sample removal depends on the

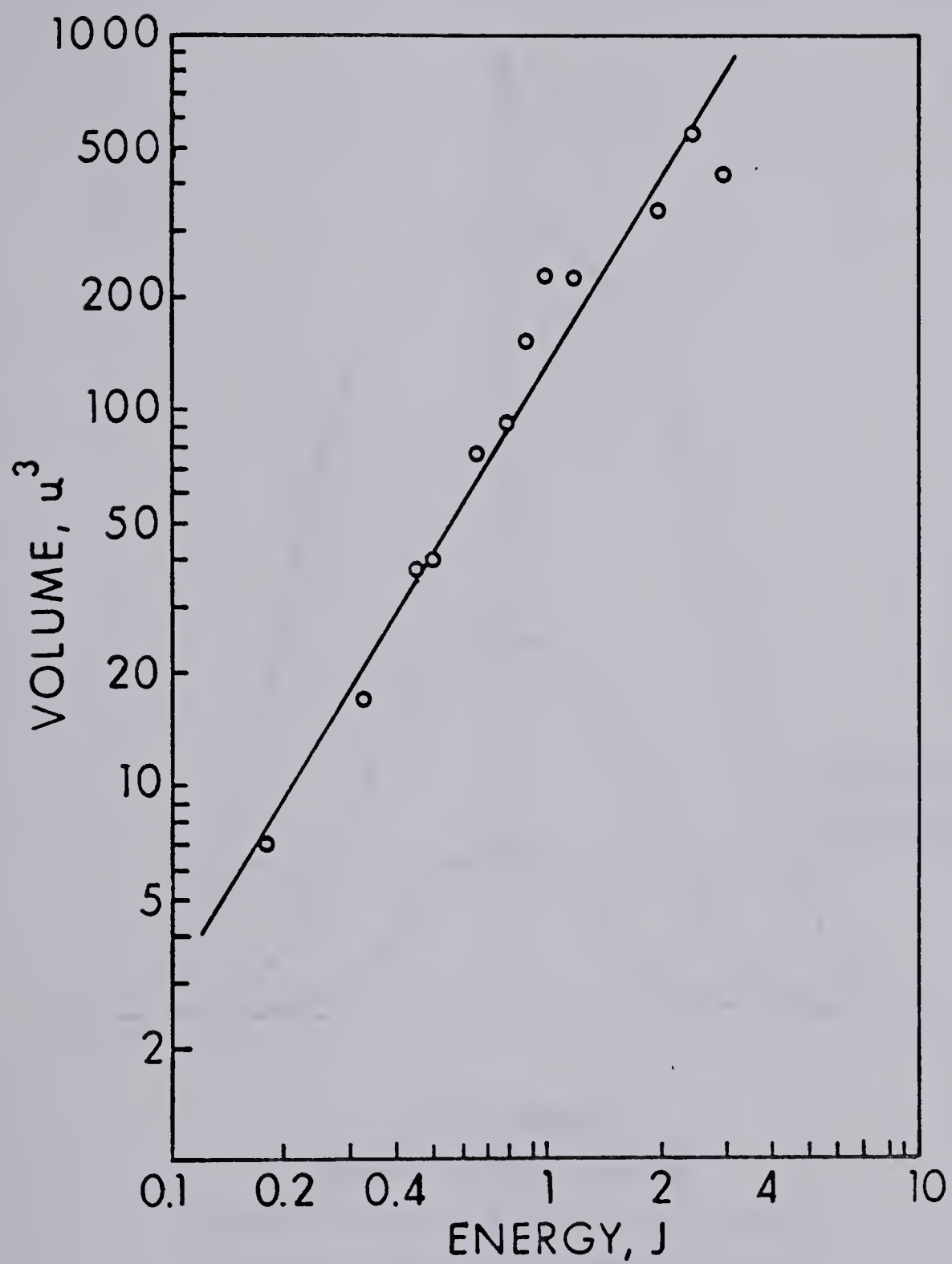


FIGURE 1. Crater Volume as a Function of Laser Energy

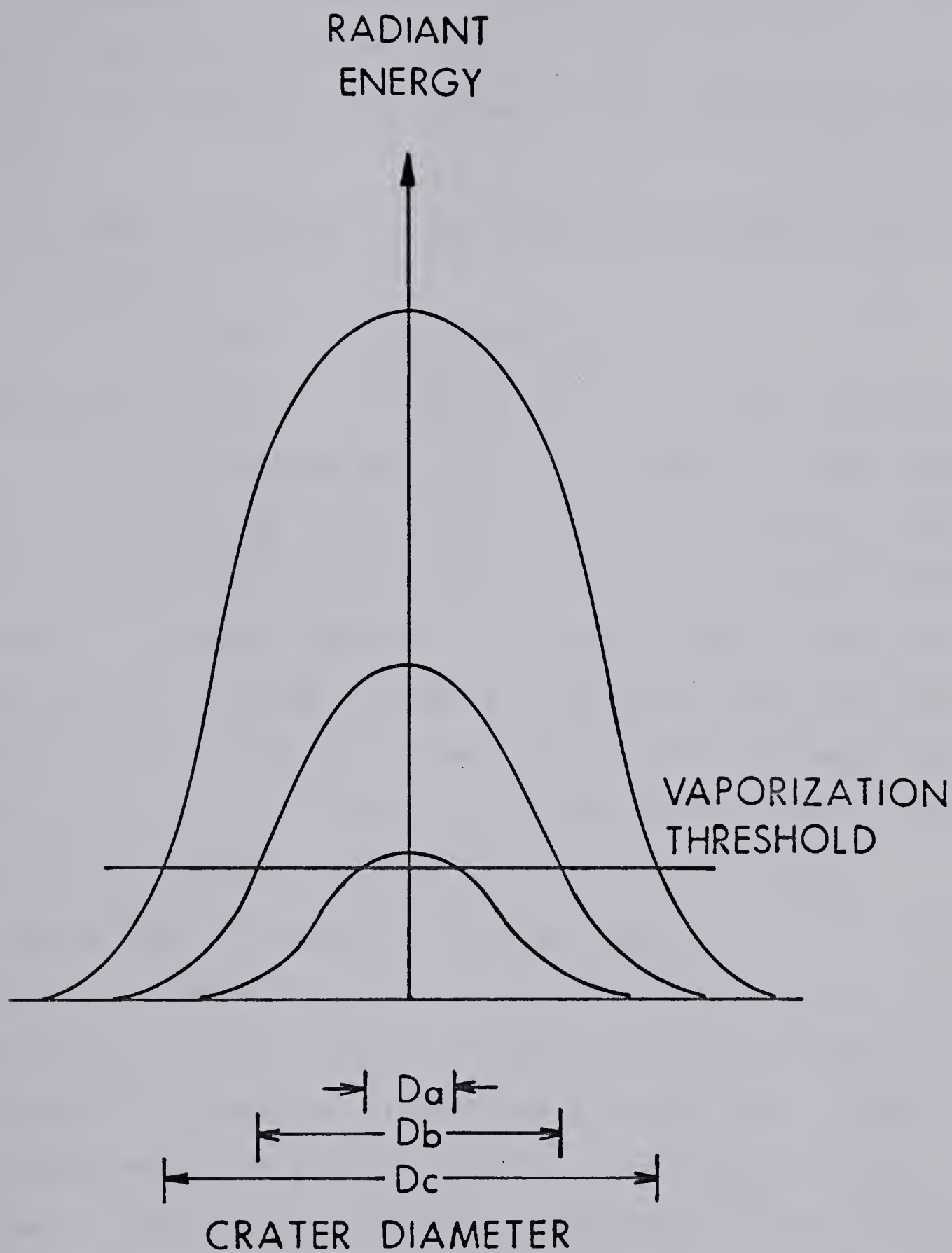


FIGURE 2. Crater Diameter as a Function of Laser Energy

mode of operation of the laser. Three principle modes of operation have been defined (19):

- 1) Free Running - many pulses of low energy and random timing,
- 2) Semi Q switched - a few high energy pulses also randomly spaced and
- 3) Q switched - a single giant pulse.

A comparison of typical values can be seen in Table 2 (19).

In the free running mode the power density of the laser is usually less than 10^8 W/cm^2 . With this power density, reflection of the light can play a significant role in determining the amount of energy absorbed. A change in reflectivity vs. energy density is shown in Figure 3(20). In the case of aluminum this reflectivity can be as high as 85% for energy densities produced by the free running mode but the exact value depends on the sample surface as well as the material.

The portion of radiation that is absorbed produces cratering and a plume approximately 30 μsec after lasing. From 40 to 100 μsec a fine stream of particles with a velocity of 10^4 cm.sec^{-1} is observed (34,35) and at about 200 to 300 μsec molten metal is ejected and the plume appears to be striated. Approximately 400 μsec after firing vaporization and spectral emission cease although lasing may continue. The large amount of sample removed during the free running mode is responsible for the scattering of laser radiation and the quenching of excited species. The temperature of the plume has been reported at 5000 to 8000 $^\circ\text{K}$ (29).

TABLE 2

Comparison of Q switched, Semi Q switched and Free Running Laser Specifications

	<u>Free Running</u>	<u>Semi Q switched</u>	<u>Q switched</u>
Maximum Energy	3 J	0.4 J	0.4 J
Time Duration	850 μ sec	25-30 μ sec	50 nsec
Number of Spikes	550	20	1
Mean Energy Density	6.4 kJ/cm ²	0.84 kJ/cm ²	1.5 kJ/cm ²
Mean Power Density	7.6 MW/cm ²	31 MW/cm ²	30,000 MW/cm ²
Crater Diameter in Al	340 microns	500 microns	60 microns
Mean Power	3.5 kW	14 kW	8 MW

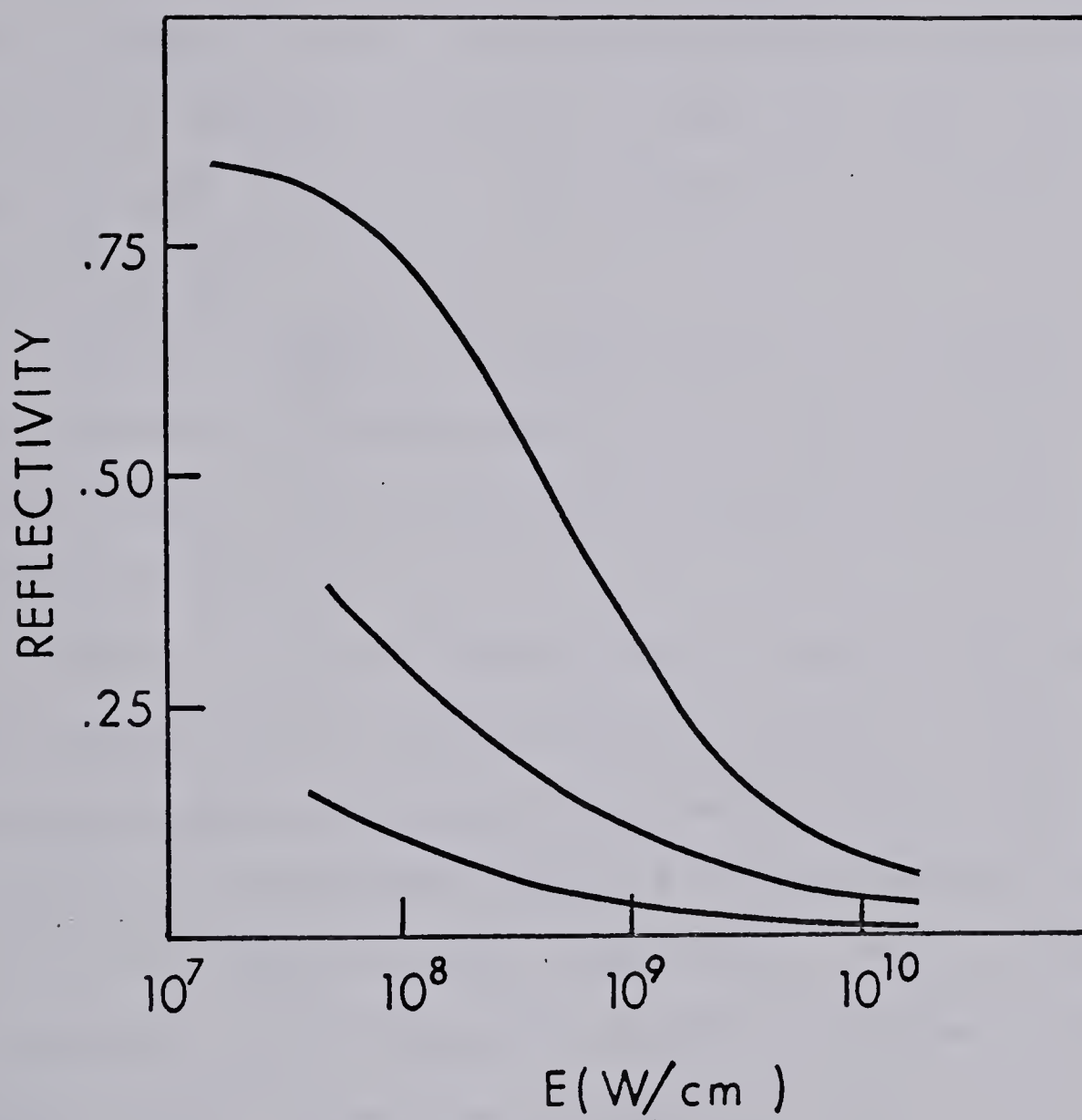


FIGURE 3. Change of Reflectivity of Some Materials as
a Function of Laser Power Density

In the semi Q switched mode, a rotating prism or a dilute bleachable dye Q switch allow a short train of high energy pulses out of the laser cavity. These spikes are randomly spaced but are emitted with higher energy over a shorter period of time than the free running mode. A typical number of spikes is about 20 with each spike having its own surface interaction, usually lasting for about one μsec . The overall plume produced lasts about 50 μsec and has a velocity of about $10^5 \text{ cm}\cdot\text{sec}^{-1}$ (34,35).

It can be assumed that the action of the semi Q switched mode is somewhat intermediate between free running and Q switched modes. No time studies of the cratering process have been reported.

A fully Q switched laser emits a single high energy pulse usually with an energy greater than 10^9 W/cm^2 . This high energy heats the target well beyond its boiling point and reducing the fractionating. At these powers, the reflectivity of the sample becomes negligible. The material ejects at a velocity of $10^6 \text{ cm}\cdot\text{sec}^{-1}$ (34,35) but values as high as $2 \times 10^7 \text{ cm}\cdot\text{sec}^{-1}$ have been reported by Basov et al. (37). In this case, none of the material ejected from the crater exists in the liquid state.

The plume lasts for about 15 μsec and temperatures from 10,000 to 15,000 $^\circ\text{K}$ have been reported (29). The shape of the plume (Figure 4) is essentially the same for all modes of sampling (36). However, the chemical and physical composition

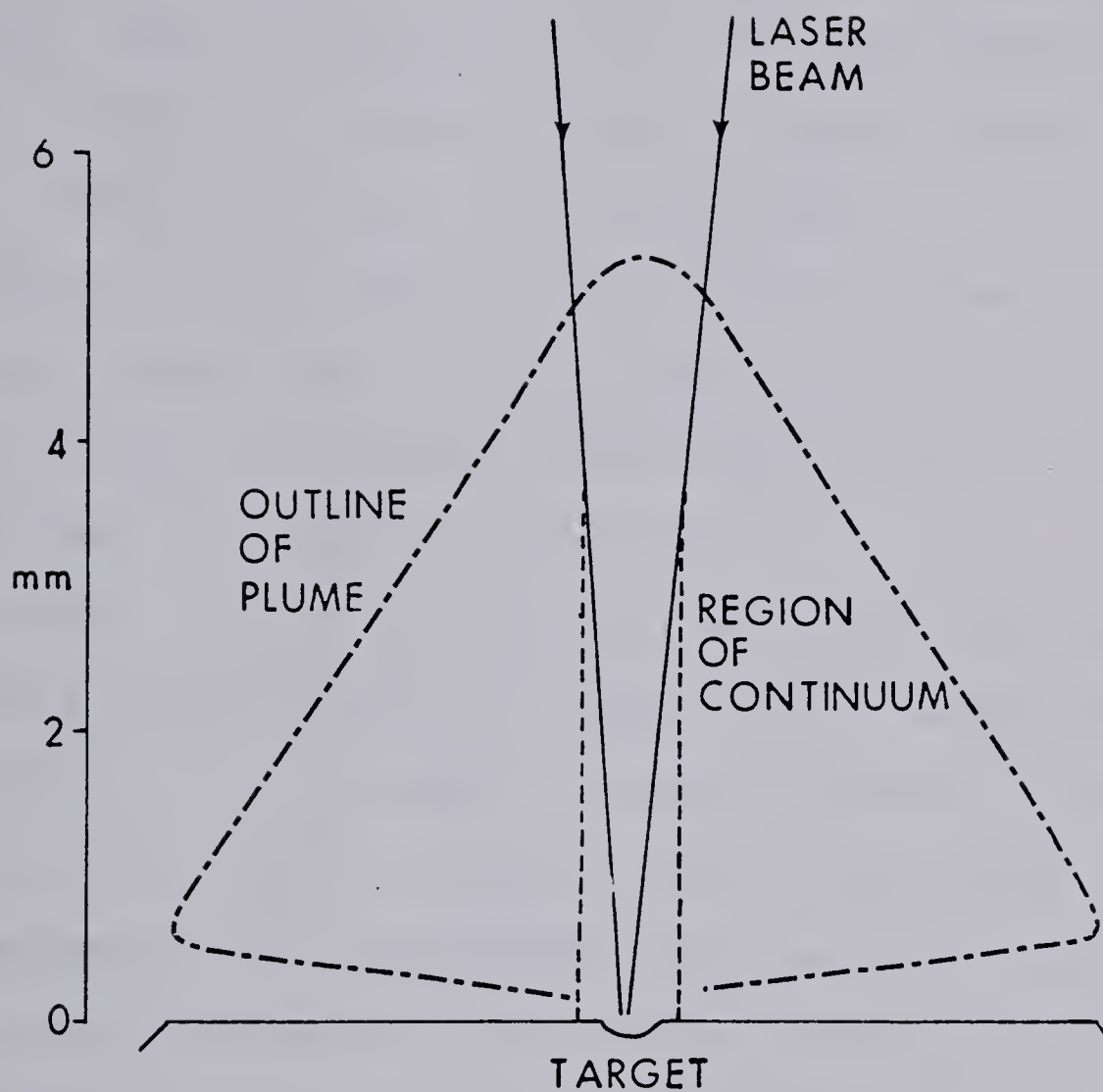


FIGURE 4. Plume of Ejected Material Resulting from Laser Sampling

as well as the temperature, rate of expansion and electron pressure are strongly time and space dependent and are governed by the process of vaporization.

The three modes of operation produce different types of craters. Free running and semi Q switched lasers produce larger craters and create molten or liquid ejecta that forms a wall around the crater (Figure 5a and b). A Q switched pulse gives a very clean crater with no evidence of molten material (Figure 5c). In the free running laser the application of many low energy pulses drills a hole that is much deeper than it is wide (Figure 5a).

If the lifetime of the laser plume is long enough to produce a plume before it is over (free running and semi Q switched) or if the pulse is powerful enough to produce a plume in a very short period of time (Q switched) there will be absorption of laser radiation by the plume. This prevents the energy from reaching the surface of the sample and causing additional vaporization. The atmosphere and its pressure over the sample has been found responsible for the absorption of laser radiation and the limit on crater size (36). If the pressure is reduced so that the plume can expand quickly away from the surface, the crater size will increase with increasing power. An atmosphere of argon has been found to decrease the plume absorption.

As noted earlier, the crater is dependent on the sample material indicating the possibility that the sample matrix may affect the emission of trace components, however it is

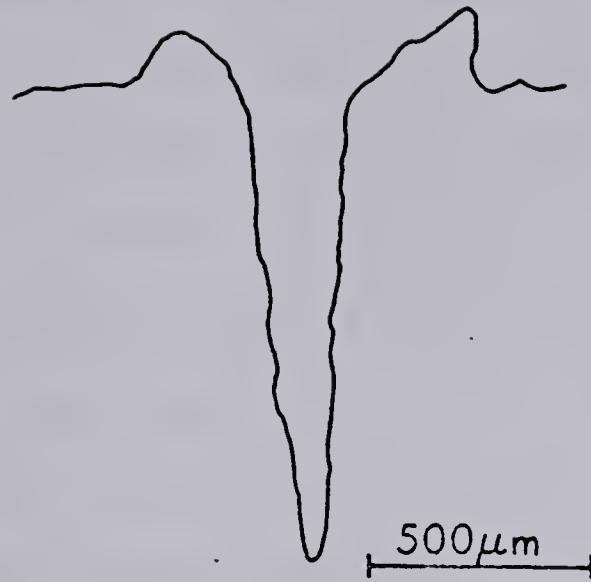


FIGURE 5a. Crater Produced by Free Running Laser

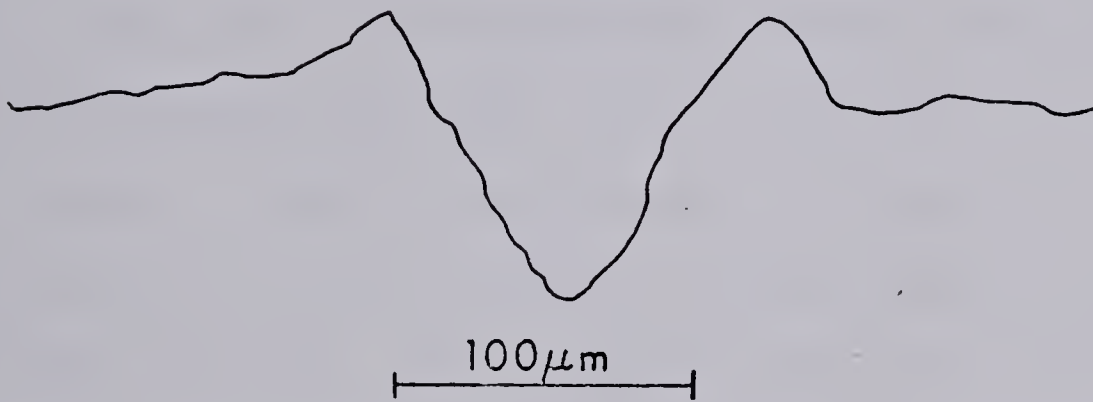


FIGURE 5b. Crater Produced by Semi Q switched Laser

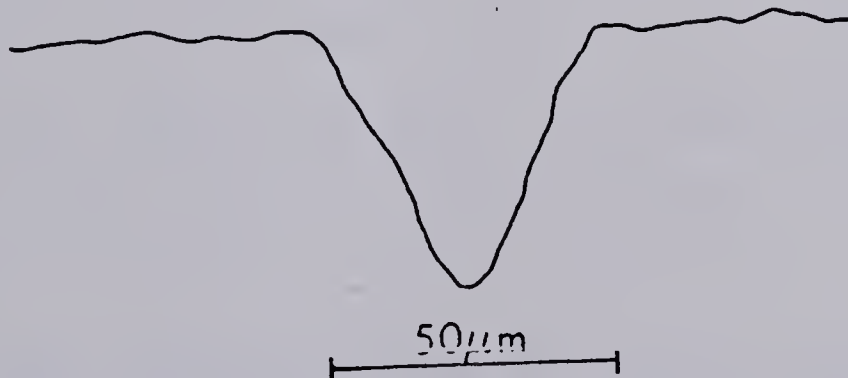


FIGURE 5c. Crater Produced by Q switched Laser

not clear what effect the matrix has on the vapor composition. Rasberry et al. (38) found minimal matrix effects upon the determination of manganese in high temperature alloys containing 12% to 72% nickel. Whitehead and Heady (39) studied the effects of powdered BaF_2 , Al_2O_3 , Yb_2O_3 and WO_3 matrices in D.C. arc and laser probe excitation. Small effects were seen with the laser vaporizer but these were significantly less than D.C. arc matrix effects.

In other studies the composition of the vapor produced by the laser was collected and analysed by conventional methods to determine its concentration. Baldwin (40) found the condensed vapor and the resolidified molten fraction differed in concentration and were both different from the original sample. Similar results were obtained by Pantaleev and Yankovokii (41) in the study of Cu-Zn alloys, some of which contained silicon. The collected vapor was found to be considerably enriched in Zn. The degree of enrichment appeared to depend on the silicon content of the specimen and the ratio of Zn content of the vapor to that of the specimen increased from 1.3 to 3.7 as the percentage of silicon increased from 1.6% to 5.5%. Unlike Baldwin, the resolidified molten ejecta was found to be similar in concentration to the original specimen.

This data indicates that the matrix can have a profound effect on the quantitative determination of an element. Since these results conflict with other reports further studies are needed in the area.

Another effect of cratering is the amount of material removed and available for sampling. Reported sample sizes vary from 10^{-3} gram to 10^{-12} gram depending on the laser type, mode of operation and the type of material being examined. The sample sizes are determined by weighing an object before and after a sampling pulse.

Not all of the material removed in the vaporization step is useful for spectroscopic examination. For absorption experiments the only usable portion of the removed material is ground state atomic vapor, while in emission experiments only excited atomic vapor species are important. In either of these two spectrometric areas the material removed as a liquid and/or recondensed solid is not of any use. By coupling to a cross excitation source the liquid and/or recondensed solid sample can be further excited and enhance signal intensity markedly.

c) Spectral Methods

i) Introduction

The laser atomizer has found a variety of applications in analytical chemistry. The special property of microsampling and the use of nonconducting samples have made the laser probe useful in the study of biological (67) and geological (68) samples. From the time of the first laser probe until 1974 there were 916 articles (25) in the literature on biological and medical samples alone. Samples included bacteria, rat brains, teeth, bone, blood cells, viruses, plant material and tumors.

Art objects have been successfully examined to determine their authenticity. An examination of trace metals in paint pigments or the components of a bronze alloy can be used in dating the object as well as determining its point of origin. The microsampling feature of the laser probe makes it a virtually nondestructive technique.

The laser vaporizer has special properties outside of its obvious microsampling capabilities and its ability to handle nonconducting samples. The laser has been used as a remote sampling system for determination of the composition of molten steel in a blast furnace (43) and for determination of radioactive or poisonous materials through an optical window. Because of the production of ions the laser can also be used as a source for mass spectrometry. An instrument using a quadrupled Nd:YAG is now commercially available (44).

The majority of analytical investigations have involved absorption or emission spectroscopy of biological and medical samples. The plume produced by the laser can be examined directly or after additional atomization or excitation is introduced.

ii) Atomic Emission

a) Laser Vaporization and Excitation

The first fundamental studies of optical emission from a laser plume were carried out using the laser for atomization and excitation. When used as an emission source the plasma must contain a suitable concentration of emitting species. It

is therefore desirable to use a Q switched or semi Q switched laser to provide as much excitation energy as possible. Unlike most analytical excitation sources it is possible for a laser in some cases to ionize an atom above the XV ionization state, producing emission lines as energetic as 25 nm.

Several authors have examined emission from laser plumes (34,38,45) and have found that emission of various species depends strongly on observation height above the sample surface. For a Q switched laser the best viewing height for atomic and ion emission is approximately 3 to 5 mm above the surface. Molecular band emission can be seen above and below this region.

A large amount of line broadening and some wavelength shifts due to doppler effects are evident (34,38,46). The high velocity plasma created by the Q switched laser is responsible for these phenomena.

With only laser excitation the intensity of the plasma is quite low. Generally multiple exposures are used to increase the signal level and for this reason an integrating detector such as a photomultiplier tube or photographic plate is required. The best results are obtained by semi Q switching the laser and producing plumes 1 to 100 μ sec apart. The production of several independent plumes with similar characteristics adds to the spectral intensity.

Rapid cooling of the plasma enhances problems of self absorption and self reversal. From an analytical viewpoint, the spectrum produced by laser vaporization and excitation is

inferior to that from other spectrometric sources. The detection limits are poorer than most methods (Table 1) but for elements with concentrations within the detectable range the precision of this system is better than 10% with reports as good as 2% (34). Rasberry et al. (38) have found better detection limits with multiple spikes (semi Q switched) but better precision with single spikes (Q switched).

Most researchers have used internal standards for quantitative analysis, ratioing the intensity of the standard emission signal against the intensity of the element under investigation. The log of this ratio is plotted against the log of the concentration of the element to be determined. If the element to be determined is a trace component in a nearly pure matrix, a weak emission line of the matrix can be used as an internal standard with a fixed concentration of 100%. Slopes of the analytical curves in these log-log plots range from 0.5 to 0.75 indicating self absorption (38).

The matrix effects of this system have been various. In many cases the effects are severe with the fraction of atoms excited being very dependent on the matrix material.

b) Cross Excitation

The first commercial laser system employed spark cross excitation for increased signal strength (17). A diagram showing a typical layout of the electrodes and sample surface is shown in Figure 6. The emission source became 15 times as intense and a corresponding decrease in detection limits was found (Table 3). The addition of the spark source also

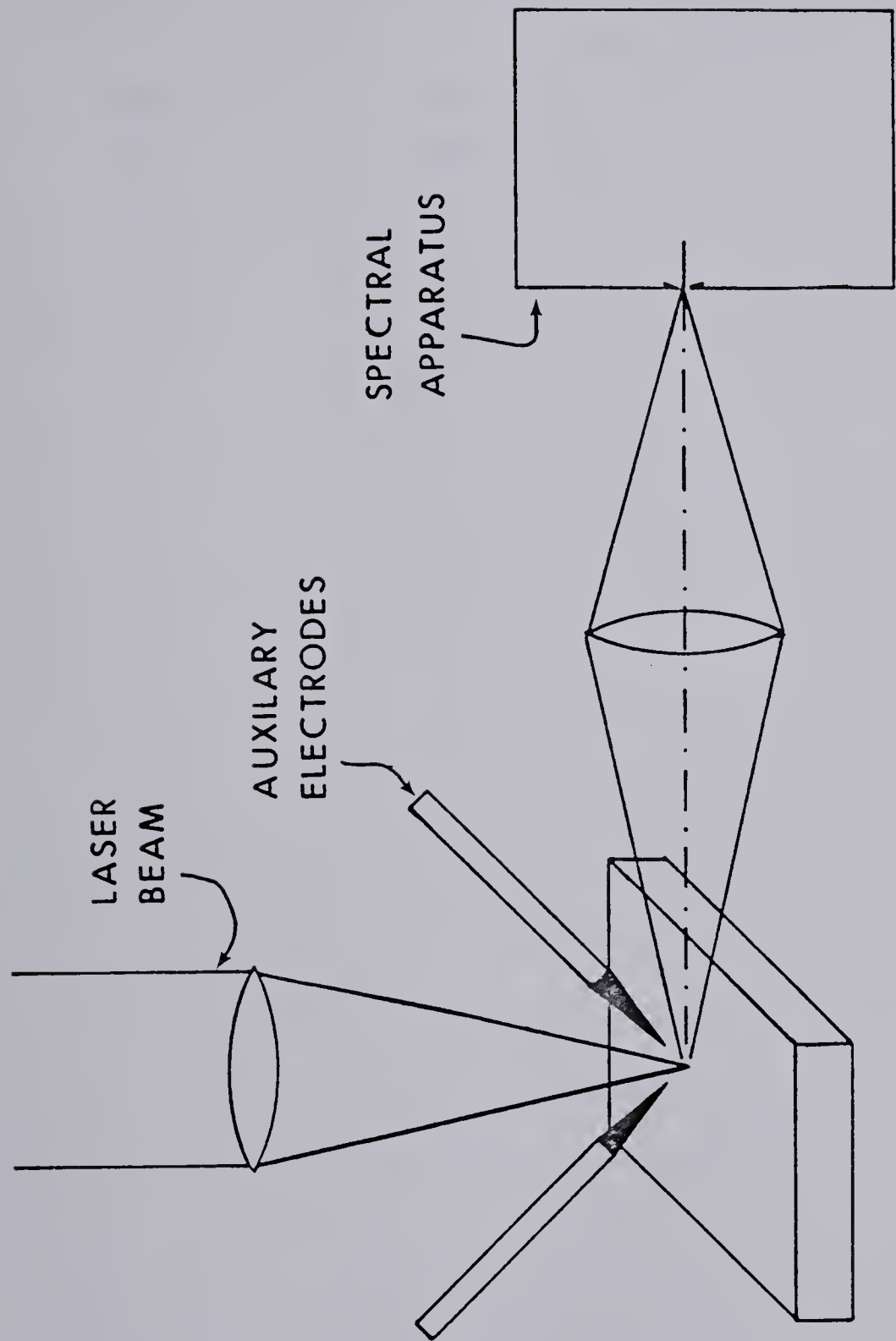


FIGURE 6. Laser Probe with Cross Excitation

TABLE 3

Detection Limits for Laser Sampling With and
Without Cross-Excitation (ppm)

Element	Laser Alone	Spark Cross-Excitation
Mg	10	0.9
Mn	20	1.0
Si	35	1.6
Zn	8	0.7
Cu	25	1.0
Al	20	6.0

reduced the problem of line broadening by the expanding plasma. The major drawback to simple spark excitation was the drop in precision from 10% to approximately 30%.

An attempt to increase precision by monitoring laser power has produced conflicting results from different authors. In one report, Pepper et al. (32) found an improvement in precision and in a later study Saffir et al. (47) found monitoring laser power to be useless or to actually decrease precision.

Initially the spark was triggered by the region of electrons in front of the plasma. It was thought that the spark was triggered too soon and that the bulk of the sample material had not yet reached the spark gap. A time delay spark gap was developed with a resulting improvement in precision to 15% to 20% (42).

Aside from poor precision, the spark cross excitation suffered from several other problems (19). Cyanogen bands are introduced by the carbon electrodes obscuring weaker spectral lines and trace impurities on or included in the graphite can obscure quantitative information. This is a common problem due to the condensation of a portion of the plume on the electrodes. If the electrodes are placed close to the sample surface an arcing can occur to the surface of a conducting sample, with the resulting spark sampling overshadowing the signal produced by laser sampling.

The main advantages of cross excitation are lower detection limits and an apparent reduction in matrix effects. In spite of the drawbacks the laser microprobe with cross

excitation remains a valuable qualitative or semiquantitative tool largely due to its ability to handle nonconducting samples.

An inductively coupled radio frequency plasma (ICP) as an excitation source was tried briefly. In this method developed by Mode (20) the laser produced vapor is excited in an induction coupled rf discharge at a frequency of 80 MHz. It was supposed that the plasma would have a low spectral background and sharp spectral lines. Unfortunately ICP technology was in its infancy and the plasma produced was unstable and erratic. The sample was difficult to get into the plasma and the overall results were disappointing.

A system built by Leis (20) in 1976 used a microwave cavity and avoided most of the problems of the early ICP's. In this work the low optical density of the plasma and consequently its low irradiance prevented an intense signal even with high speed spectrographs.

In 1980 Ishizuka and Uwamino (48) used a similar arrangement with a ruby laser and a microwave cavity. Using a photomultiplier tube as an integrating detector for the transient signal they were able to achieve precisions of 1.2% to 13.8% for peak height measurements and 2.3% to 12.1% for area measurements. Linear calibration curves over two orders of magnitude and detection limits as low as 0.7 picograms were obtained. No mention was made of matrix effects.

iii) Atomic Absorption

The large percentage of ground state atoms produced by

laser atomizers has made this sampling technique useful for atomic absorption. It has been shown that atoms capable of absorbing radiation outlast light emission from the plume (49). It would seem that duration, temperature and size and shape of the laser plume produce conditions that are not very favorable for atomic absorption but procedures have been developed that allow analytical measurements with features not attainable by any other method.

Two approaches can be taken for the spectral observation of atomic vapor. The vapor can be viewed immediately after the excess radiation from the plume subsides or it can be subjected to heat to prolong its life in the atomic state. In both cases the analytical signal must be corrected for nonspecific absorption, usually by the use of a deuterium lamp.

Several examples of laser generated atomic vapor absorption are found in the literature (49,50,51). Analytical curves have been obtained over two orders of magnitude and unlike most atomic absorption techniques these curves are straight at the higher concentration end (50). Precisions of 2% to 10% for peak height measurements and 1% to 12% for area measurements are among the best values found (50). In some cases, precision as poor as 20% to 30% has been reported (51). Examples of reported detection limits are compared in Table 4(77) with values obtained in standard methods of atomic absorption. Since the detection limits are related to the population of neutral absorbing atoms it is desirable to vaporize as large a sample as possible.

TABLE 4

Detection Limits for Laser Vaporized AA and
Standard AA

Element	Detection Limits (ppm)	
	Laser AA [*]	Standard AA
Al	7.3	0.1
Cu	7.2	0.004
Mg	1.8	0.003
Mn	2.1	0.0008
Fe	1.9	0.004
Cr	2.7	0.002
Ni	4.7	0.005
V	16	0.02

^{*}Limits will improve with a better spectrometer

Optimization of the spectral signal when viewing the atomic vapor depends on the height of observation above the sample surface. This is a factor that is dependent upon the individual laser system. Without additional energy in the system stable oxides are formed rather quickly and for this reason Osten and Pepmeier (51) suggest the use of an argon atmosphere for optimization of the spectral signal.

Additional energy has been applied to the sample with flames (52), microwave generators (20) and carbon furnaces (49). The performance of the laser atomizer with additional flames and carbon furnaces is similar to standard flame atomic absorption and electrothermal atomization with common atomizer-nebulizers.

When coupled with a high quality monochromator, laser atomization has allowed the use of some rather special and unusual sources. The use of glowing walls of the crater (54) or the two step method proposed by Kaporskii and Musatova (53) are two examples. In the two step system, the laser is focused to a diffraction limited spot in air. When using a high power laser the focused beam is sufficient to cause the breakdown of air. The spark produced at the point of breakdown is used as the primary source for absorption by the plume produced by the remainder of the laser pulse.

A study of matrix effects on atomic absorption was carried out by Mossotti, Laqua and Hagenah (49). The absorption signal for a given element varied widely when different alloys were studied and there was no apparent correlation with the

size of the crater produced by the laser. This indicates that the free atom fraction of material removed from the crater changes considerably and is quite variable from one matrix to another.

Overall the laser vaporization technique has a wider linear range than any other atomic absorption technique with no danger of sample contamination. A direct analysis is possible and very little sample preparation is necessary. The laser sampler also allows the determination of solid samples. In spite of what appear to be some very desirable features laser atomization for atomic absorption spectroscopy has seen limited success. Other standard techniques such as flame and electrothermal atomizers provide similar results and are commercially available at a price much less than a custom laser system.

It was felt that addition of an ICP as a subsequent excitation source would solve most of the problems of the previous laser excitation studies as well as permit the use of the ICP for solid sampling. This system coupled with a diode array detector was expected to provide low detection limits and precise data on a large variety of solid sample materials with little or no sample preparation.

6) Laser Vaporization into an ICP

This study is an investigation of the analytical capabilities of laser vaporization into an inductively coupled plasma. One of the major limitations of laser vaporization

in emission spectroscopy is the low signal level produced when the laser alone is used for excitation. At the expense of precision other sources have been used to increase the spectral intensity. These other excitation sources generally have such poor precision that the system is semiquantitative at best.

The state of the ICP has improved significantly since it was first coupled to a laser vaporizer (20). Commercially available ICP's now offer a precision of approximately 1%. It was felt that when coupled with a stable ruby laser and used with internal standards, the precision of the laser vaporizer/ICP system could be as low as 3%.

As an additional improvement to the system it was thought that a silicon photodiode array detector would improve the signal detection capability of the system. The signal produced by a pulsed laser is inherently transient in nature and for this reason integrating detectors such as photographic plates and photomultiplier tubes with integrating electronics have been used. The diode array possesses most of the desirable characteristics of photographic and photomultiplier detectors and at the same time overcomes most of their difficulties. The diode array's wide spectral coverage, good dynamic range, fast response time and reasonable spectral sensitivity were used to make use of the plasma's multielement capabilities and to gain maximum utility from the transient signal.

To achieve the best possible detection limits it seemed reasonable to have the greatest possible sample size. For

this reason a free running ruby laser was used to vaporize a large sample. Since the ICP provides additional vaporization and excitation it did not matter whether the sample was a true atomic vapor or microscopic droplets of molten or condensed material.

CHAPTER II

INSTRUMENTATION

A. Lasers

1) Introduction

The primary source for vaporization was a ruby laser designed and built by the Korad Corporation, a division of Union Carbide. The reason of choice for the ruby laser was one of convenience; other lasers could have done the job but are not as well suited to the sampling of metals.

High power, one of the laser's prime characteristics, is of major importance in its application to vaporization. Other important aspects of laser radiation such as coherence, high directionality and monochromaticity were small factors in the choice of a laser as a vaporization tool. Hundreds of other users in spectroscopy, communications and industry have made use of these unique properties.

2) Principle of Laser Operation

A laser consists of three basic components:

1. a medium with a suitable energy level system in which population inversion and lasing can occur
2. a method of pumping or population inversion
3. a cavity to provide optical feedback.

Many mediums have been shown to exhibit population inversion and lasing has been achieved using a variety of excited species in solids, gases and liquids from the ultraviolet

to the infrared.

A typical solid lasing medium similar to the one used in this experiment would consist of a host material or matrix such as Al_2O_3 or glass with a small percentage of the active lasing species being substituted for Al^{3+} in Al_2O_3 . A typical concentration of the active element is 0.05%. In solid lasers two types of energy level systems are common. The three level system as in the ruby laser and the four level system exemplified by the Nd:YAG or Nd:glass lasers.

In the ruby three level system (Figure 7a) the active element is a Cr^{3+} atom trapped in the crystal lattice of sapphire. Incoming radiation from the pumping system is absorbed by the chromium atoms promoting them to a higher electronic state. This excited species then decays to a metastable state where it can undergo either spontaneous emission or stimulated emission. Its lifetime in this state is determined by the number of photons available to stimulate decay or its spontaneous emission lifetime. In this system, since the lower state that the system is lasing to is the same energy level as the ground state, a large percentage of the chromium atoms must be excited to create a population inversion.

As a result of the difficulty in achieving a population inversion, the pumping efficiency of the ruby laser is not very high. Typically only 0.1% conversion efficiency of flashlamp energy into laser energy is achieved. Of 1000 Joules produced by the flashlamp pumping source only 1 Joule is

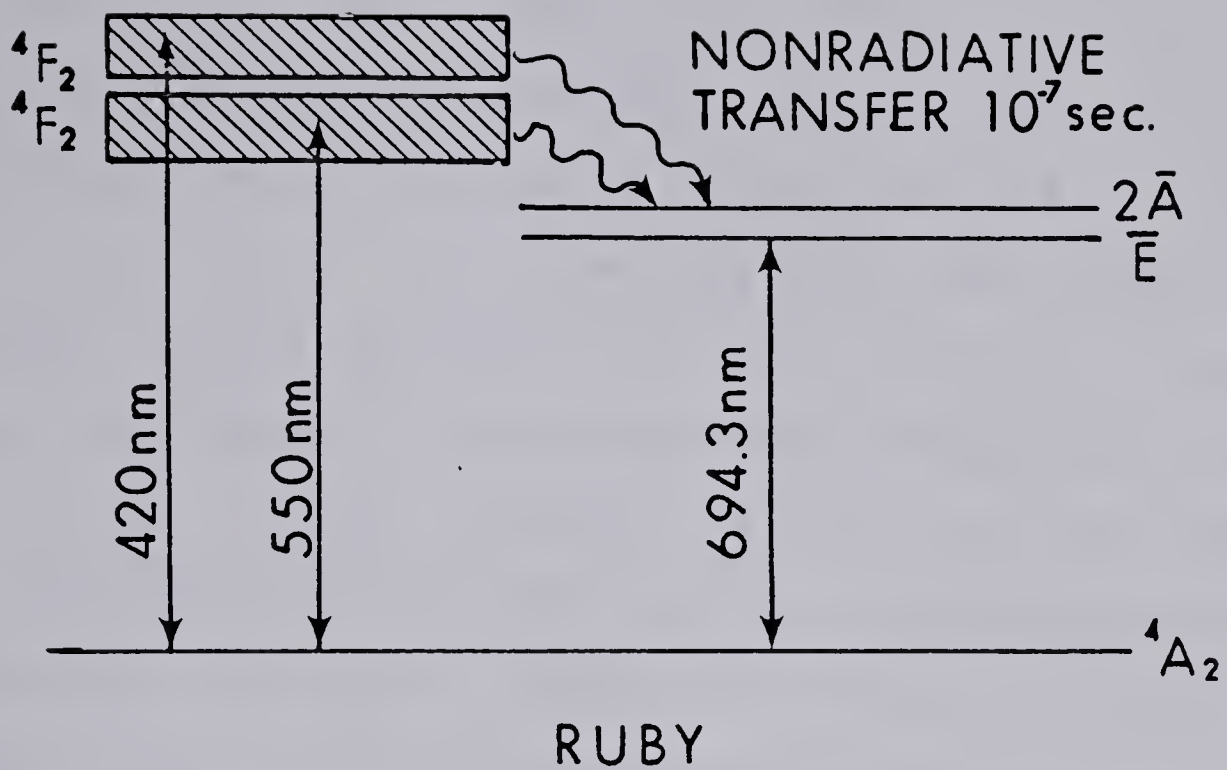


FIGURE 7a. Energy Levels for the Ruby Laser

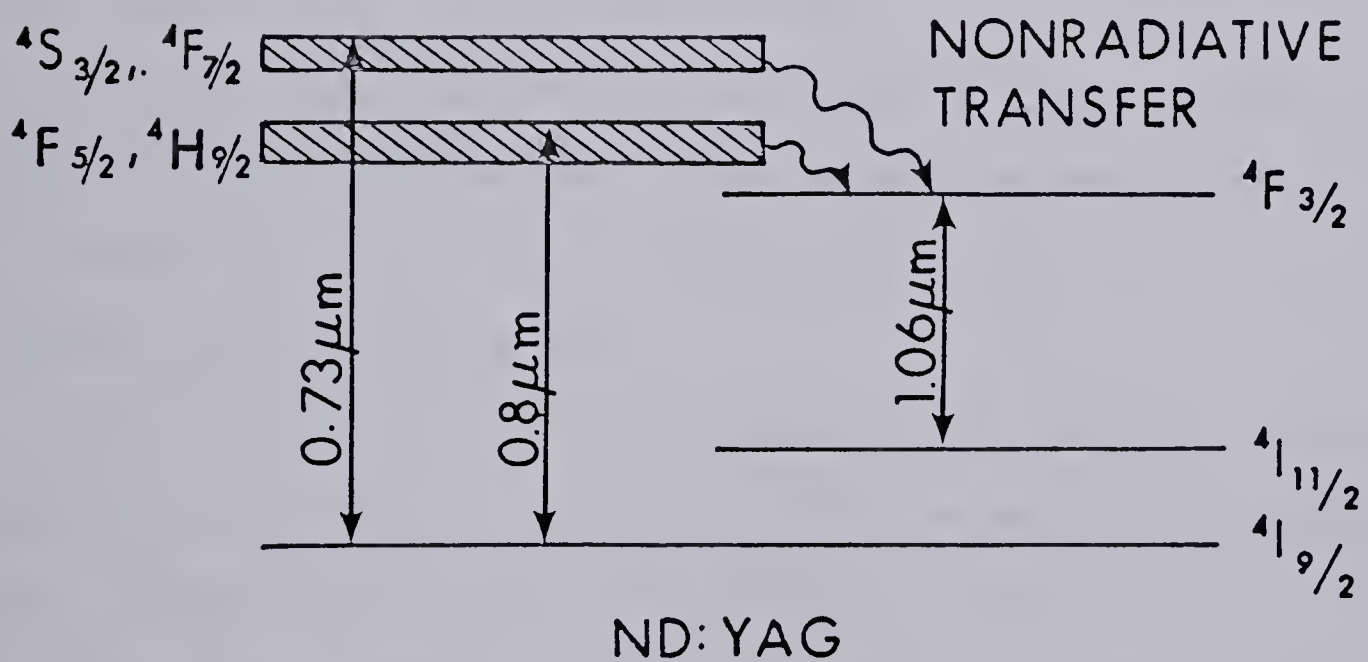


FIGURE 7b. Energy Levels for the Nd:YAG Laser

emitted as laser radiation.

In the four level system (Figure 7b) of the neodymium laser, Nd^{3+} is the active medium. Like the ruby, it absorbs energy supplied by the pumping system promoting it to an upper energy level. After reaching this upper energy level it decays rapidly through nonradiative transfer to a metastable state where it can spontaneously decay or be stimulated to emit. Unlike the ruby, the neodymium laser decays to a state above ground state and as a result the lower state is generally empty and a population inversion or laser threshold can be achieved with greater ease.

Neodymium lasers are commonly found in glass or yttrium aluminum garnet (YAG) host crystals. The characteristics of these two systems are similar but the glass laser is slightly lower in cost and is the more common.

The ruby and neodymium lasers are the most common ones used in laser vaporization. Some work has been done with CO_2 and argon ion lasers but these appear to be inferior for many reasons and are seldom seen.

The second component of a laser is a pumping system or method of population inversion. Many methods have been developed. Examples of these are electric discharge as in a CO_2 or He-Ne laser, chemical reaction as in a hydrogen chloride laser and flashlamps as in ruby or Nd:YAG lasers. Another common type of pump is another laser; most dye lasers are pumped by nitrogen gas lasers. A flashlamp was used to pump the ruby and will be the only one discussed here.

A high voltage discharge across a tube filled with xenon gas will produce an intense burst of light over a period of a millisecond (Figure 8a) covering a wide region of the spectrum (Figure 8b). The low efficiency of flashlamp pumped systems is because the emission band of the flashlamp is so much wider than the absorption band of the lasing medium. A typical emission spectrum may be 500 nm wide while a very wide absorption band as in the ruby laser is only 50 nm wide. Even with a great difference in band width, flashlamp pumping is the most convenient method.

The cavity of a simple solid laser system consists of two mirrors at either end of the laser rod. The rear mirror is 100% reflecting, all of the energy reaching the mirror is reflected back towards the laser rod. Front mirrors range from 99% to approximately 10% depending on the laser system. Energy not reflected back into the cavity by the partially reflecting front mirror is emitted as a highly directional coherent beam. The front mirror on the ruby system used in this experiment is a low reflectivity uncoated sapphire window.

The oscillation of the reflected radiation within the laser cavity is provided by amplification, a photon travelling through the laser rod will stimulate other photons to emit. As these photons travel down the laser rod, they will stimulate additional photons to emit and the result will be a monochromatic coherent packet of photons travelling in exactly the same direction. If the photons are going in

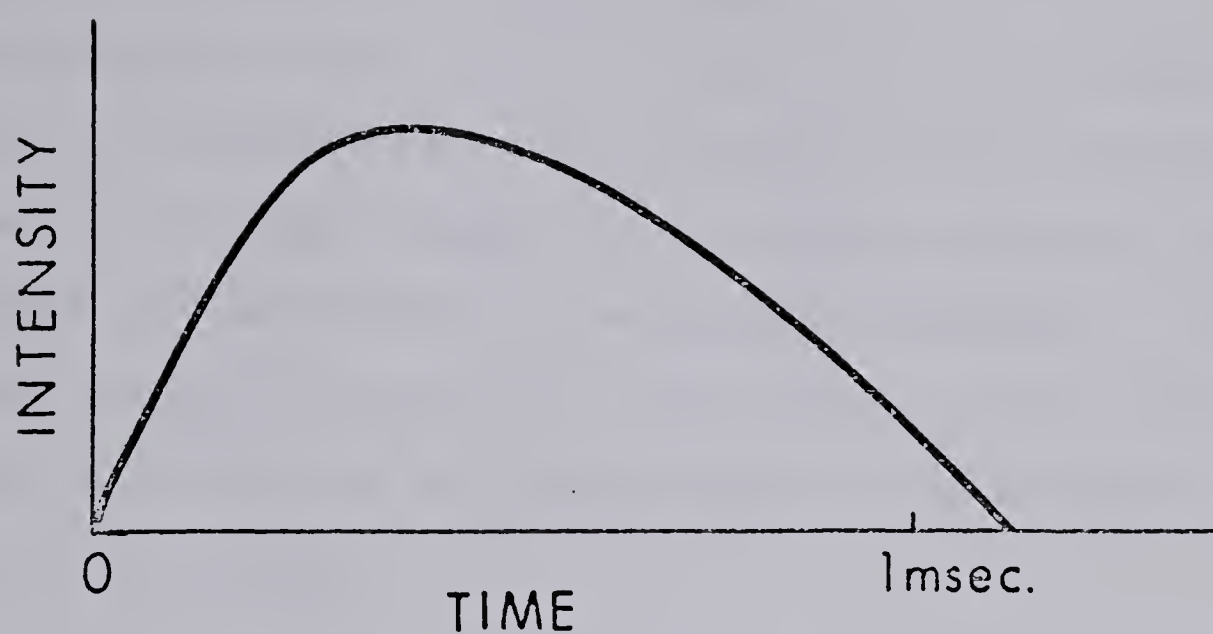


FIGURE 8a. Flashlamp Output as a Function of Time

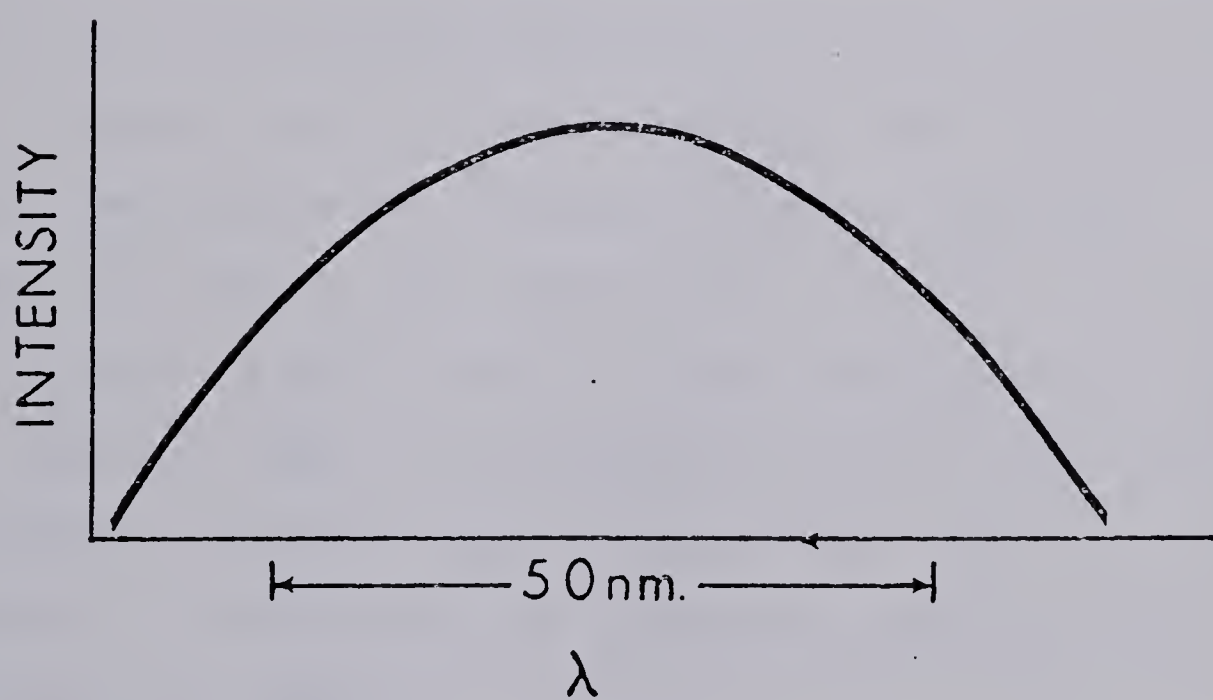


FIGURE 8b. Flashlamp Output as a Function of Wavelength

the correct direction to be reflected back from the mirror into the cavity, the stimulation process will continue amplifying the intensity of the photons.

The length of the cavity varies from 30 cm to approximately 70 cm depending on accessories such as Q switches that may be included inside. An increase in cavity length decreases the band width of the emitted radiation. Since the monochromatic properties of the beam were not important the cavity length was not determined and was changed as needed.

3) Q Switching

For the comparison of free running versus Q switched operation, a KDP Pockels cell and bleachable dye Q switches were used.

In the free running mode the laser produces many pulses within a single flash of the flashlamp. The lifetime of a typical flashlamp pulse is approximately 1 msec and the time of a single ruby laser pulse is 10nsec to 20 nsec. Since the laser pulse is much shorter than the flashlamp pulse, there is time for the medium to lase, repopulate and lase again for several cycles (Figure 9a). The result is many pulses of relatively low intensity; generally 500 to 1000 pulses are emitted.

In the Q switched mode all of the energy that is absorbed by the lasing medium is stored until it is emitted as one giant pulse. The energy of this giant pulse is many times greater than that of a pulse in the free running mode (Figure 9b).

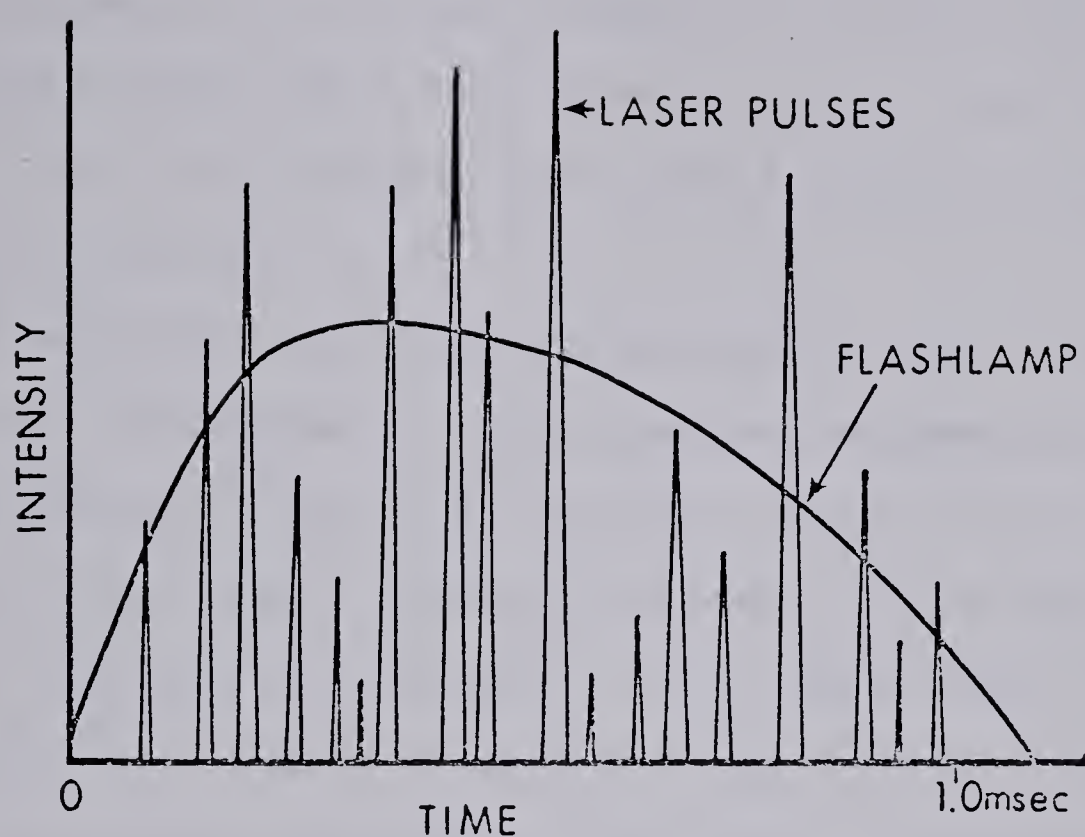


FIGURE 9a. Typical Pulse Output of the Free Running Laser during a Single Flashlamp Burst

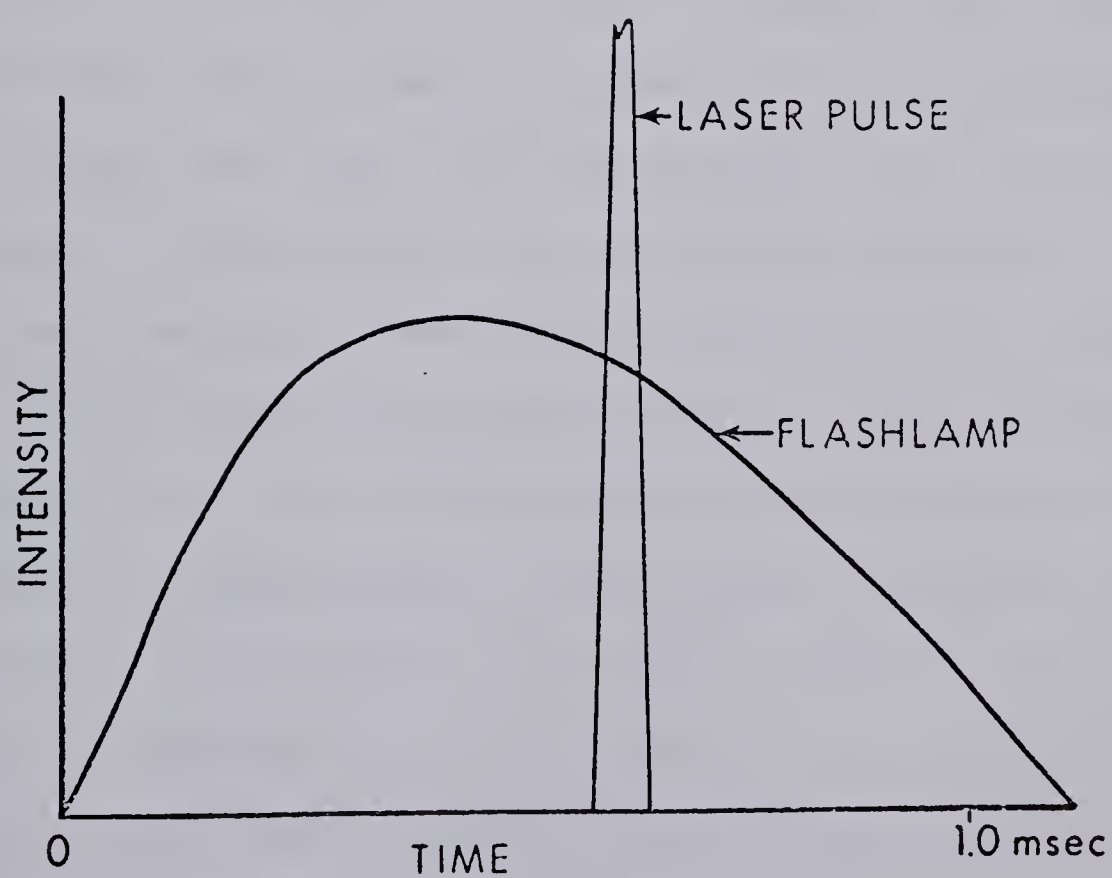


FIGURE 9b. Single Pulse of the Q switched laser during one Flashlamp Burst

The semi Q switched mode is somewhat intermediate in that the pulses are fewer in number and higher in energy than the free running mode, but lower in energy than the Q switched mode. The number of pulses emitted is usually somewhere between 50 and 5.

Q switching has been accomplished in many ways. The two basic categories of Q switches are active and passive. In the passive Q switch a bleachable dye is put into the cavity of the laser. Photons emitted early in the period of the flashlamp are absorbed by the dye as they travel towards the rear mirror. Being absorbed by the dye prevents them from reflecting off the rear mirror stimulating additional photons to emit. As the dye absorbs more photons it begins to bleach and become optically transparent. The photons can then pass through the transparent liquid, making many passes through the laser rod and stimulating a large amount of emission. After depletion of the upper state of the lasing medium, the energy density in the beam drops and the dye returns to its original absorbing state. The absorbed energy is dissipated as heat and the dye is again capable of blocking photons or rebleaching. The Q switch is called passive because there is no control over the timing of the pulse. The delay in bleaching can be slightly controlled by the concentration of the dye and in the initial set up of this experiment, a cryptocyanine dye of 5×10^{-6} M was used as a Q switch.

With an active Q switch, the timing of the pulse can be

accurately controlled with the electronics used to control the Q switch. The type of active Q switch used in this experiment was a potassium dihydrogen phosphate (KDP) crystal (Pockels cell). KDP crystals rotate polarized light, the amount being dependent on the voltage applied to the crystal. Light emitted by the laser is vertically polarized. Initially a voltage is applied to the Pockels cell sufficient to rotate light 90° out of the vertical plane. A polarizer included in the laser cavity then removes the nonvertical component of the radiation; in the initial phase 100% of the light is removed and the throughput is zero. After a period of time during which energy is stored in the laser rod, the voltage across the KDP crystal drops to zero and the photons pass through, retaining their vertical polarization. This vertically polarized radiation is then able to pass through the polarizer with little loss, reflect off the rear mirror and stimulate other photons to emit. The voltage on the Pockels cell is held long enough to allow the production of a single giant pulse of 20 nsec half width. The voltage is then removed, rendering the cavity opaque to remaining photons.

The so called semi Q switched mode utilizes a rotating prism as a switching device. Often referred to as mechanical shutters, these prisms operate as rear mirrors in the laser cavity. A pulse can propagate during the time in the rotation that the prism reflects the light back into the cavity. For single pulses the prisms must operate at 30,000 rpm or greater. If a slow-

er speed of rotation is used more than one pulse can be emitted during a single revolution; for semi Q switched operation the prism is rotated at a speed of 3000 rpm. Rotating discs in the cavity or rear rotating mirrors have also been used with success.

Other types of Q switches such as Kerr cells and Acousto-Optical Shutters have been designed and found successful. Since they have seen limited use in laser vaporization, they will not be discussed.

The Pockels cell used in this experiment was a model 212-150 from Interactive Radiation Inc. The specifications and dimensions of this Q switch are presented in Figure 10 and Table 5 respectively.

The Q switch driving electronics were also from Interactive Radiation Inc., model 2-015. Specifications are shown in Table 6.

To make the Q switch output signal of the Korad laser power supply compatible with the TTL input of the Q switch driver, an interface circuit was needed (Figure 11a). The output of the Korad power supply was a variable pulse 50 to 100 volts in height with a 10 μ sec width (full width half maximum). The signal used to test the circuit was a sine wave, 50 volts peak to peak, 1 μ sec per cycle.

4) Ruby Laser

As stated previously, the laser used in this experiment was a Korad K-1 ruby laser. The laser was used in the free

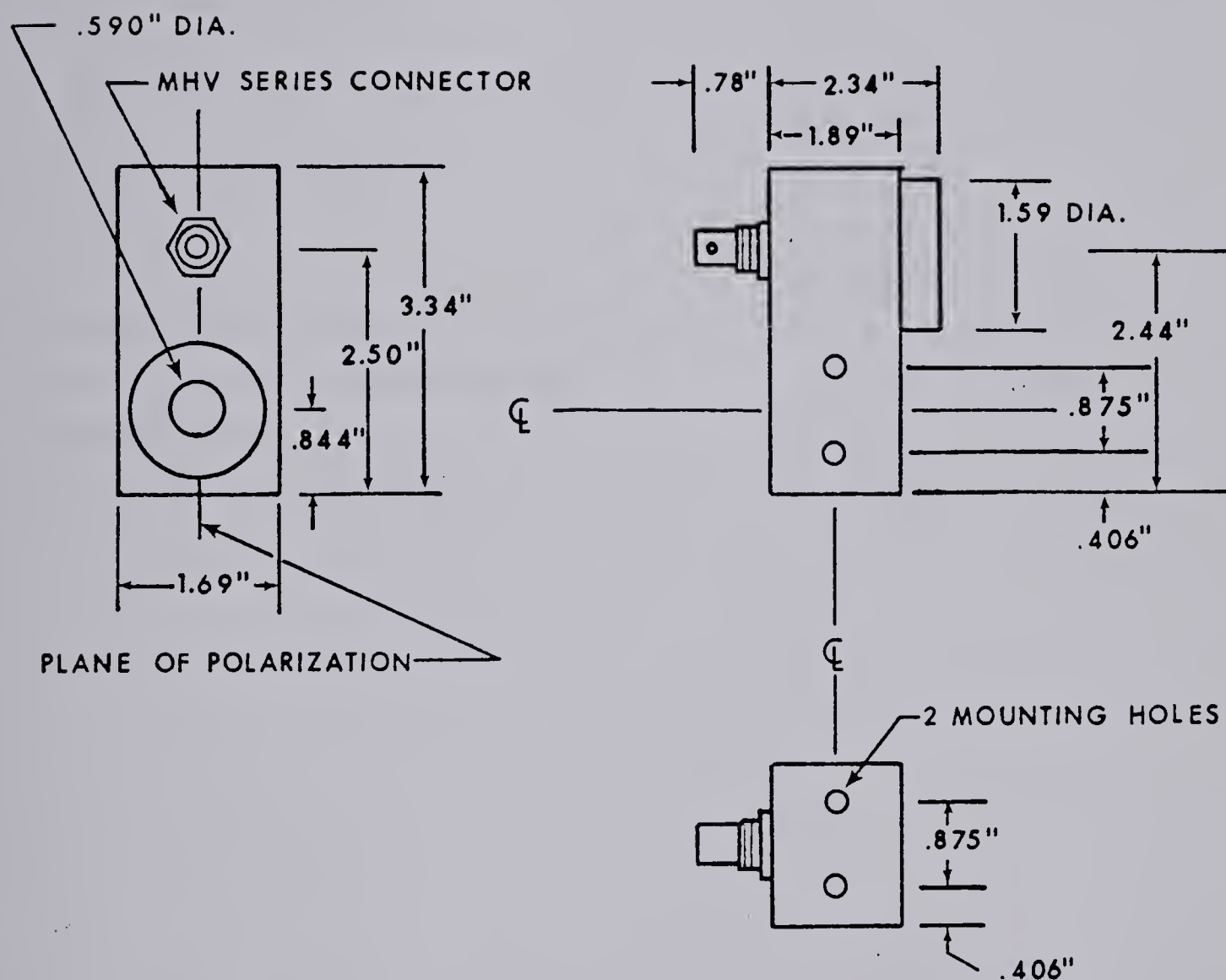


FIGURE 10. Inrad Pockels Cell Model 212-150

TABLE 5

Inrad Pockels Cell Q switch
Model 212 Specifications

Aperture Size	15.0 mm
Half-Wave Voltage	
@ 1.06 m	6.6 kV
@ .6943 m	4.4 kV
Quarter-Wave Voltage	
@ 1.06 m	3.3 kV
@ .6943 m	2.2 kV
Optical Transmission	98 %
Optical Transmission Range	.25 to 1.17 μ m
Capacitance	11 pf
Electrical Rise Time	1 nsec

TABLE 6

Inrad Q switch Driver Model 2-015
Specifications

Switched Voltage	1 to 8 kV (7990 V)
Switched Voltage Selection	Direct Reading thumbwheels
Switched Voltage Resolution	10 V
Switched Voltage Regulation	$\pm .05\%$ over full temperature and input range
Switching Time	10 nsec
Recovery Time	3 msec (RC with 100 pf load)
Repetition Rate	Single Pulse to 40 pps
Delay, Variable	0 to 16 msec
Delay Resolution	1 μ sec
Delay Accuracy	$\pm .5\%$ of setting + 1 μ sec
Delay Jitter	$\pm .01\%$ + 5 nsec typical
Trigger Input Voltage	$\pm .2$ to $.5$ V
Trigger Input Impedance	50 Ohms
Post Delay Trigger Output	TTL, drives 50 Ohms

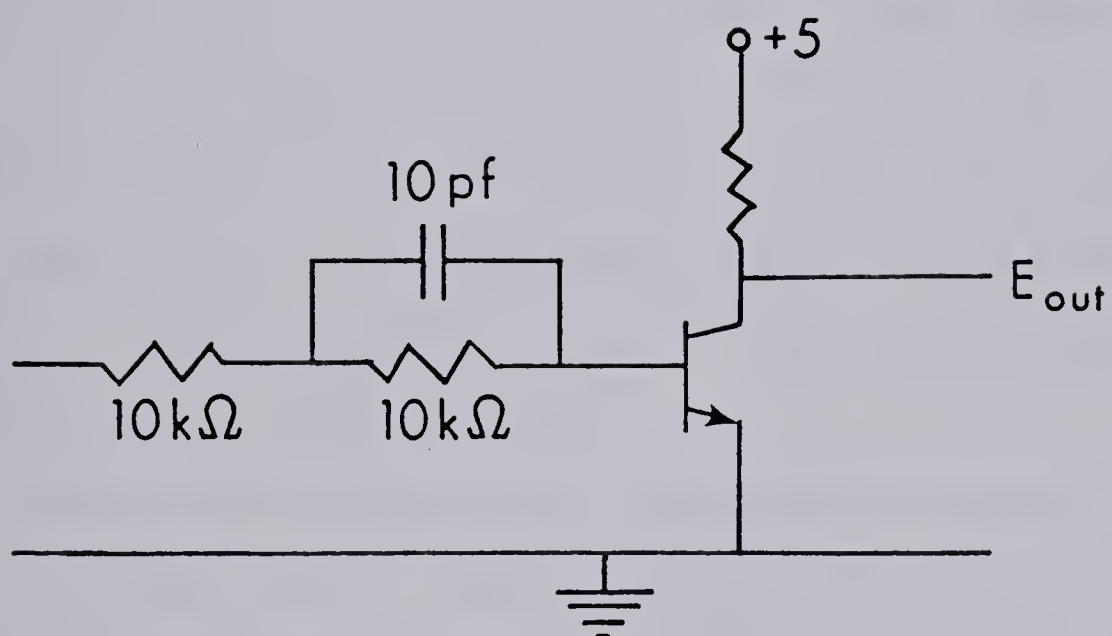


FIGURE 11. Q switch Interface Circuit

running mode for the majority of the work and a comparison was carried out between free running and Q switching with a KDP Pockels cell. The main reason for using a ruby laser was the availability of one in the lab. Fortunately, for other reasons the ruby is also the laser of choice. Ruby crystals are thermally robust and are good heat conductors; insuring dependability and a long lifetime. The 694.3 nm radiation produced by the ruby is also advantageous because it is absorbed to a greater extent than other common vaporizing lasers such as CO_2 (10.6 μm) or Nd:YAG (1.06 μm).

Power output of the free running laser was rated by the manufacturer at 1 to 2 Joules per pulse, 50 to 150MW intensity and a pulse width of 10 to 20 nsec. The output power can vary greatly from pulse to pulse.

In determining sample size, vaporization should be a function of power only. The use of an internal standard should allow compensation for any variation in laser power. For this reason, the laser power was not monitored and the absolute intensity was not determined. Literature values suggest fluctuations from 5% to 25% to be common. The procedure used by the manufacturer to keep laser power constant is temperature control. The manner of operation is also important in keeping the output constant. This will be discussed in a later section.

The basic specifications of the Korad laser are presented in Table 7 and Table 8. A general layout showing the position of the components is shown in Figure 12.

TABLE 7

Ruby Laser Specifications

	<u>Q switched Mode</u>	<u>Free Running</u>
Pulse Energy	1-2 J	1-2 J
Pulse Width	10-20 nsec	pulse train 1 msec 100, 10-20 nsec pulses
Peak Power	50-150 MW	1 MW per pulse
Beam Divergence	4-10 mrad	same
Beam Diameter	9/16 "	same
Wavelength	6943 Å	same
Linewidth	.01 Å	same
Pulse Repetition Rate	4 ppm	same
Jitter	\pm 50 μ sec	same
Polarization	0-180° Adjustable	same

TABLE 8

Korad Power Supply Specifications

OUTPUT

Voltage, Adjustable	5 kV maximum
Power	60 ppm @ 5 kJ for 2 hrs 50 ppm @ 5 kJ continuous
Load	Requires Capacitive load

INPUT

Voltage	208/220 V, 60 Hz
Average RMS current	50 amps
Average Line Power Required	17 kVA

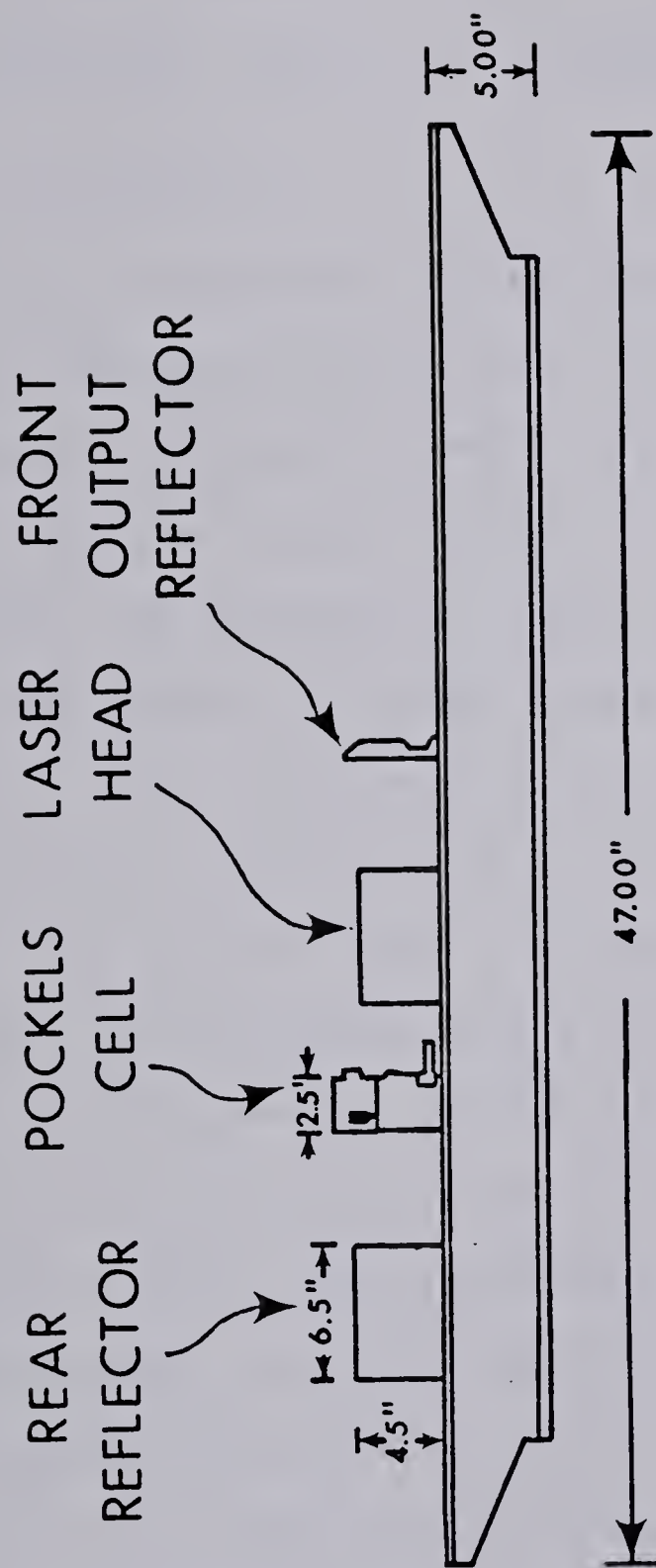


FIGURE 12. Korad Laser Model K-1

This system was found to be very stable over 3000 pulses. Little realignment was necessary. The original alignment was carried out by aligning the multiple reflections of a He-Ne laser.

B. Radiofrequency Inductively Coupled Plasma

1) Introduction

The first development of the atmospheric radiofrequency inductively coupled plasma (ICP) for use as an analytical source began in the early 1960's with development by two independent research groups, Wendt and Fassel (61) in the United States and Greenfield, Jones and Berry (62) in England. A steady development in plasma spectroscopy has occurred over the period of time since its initial introduction, resulting in a fundamental understanding of the ICP as an emission source and the availability of commercial instrumentation.

The ICP was developed as a solution to the inherent physical problems of previous analytical sources. As a high energy source, it most closely approaches the goal of an ideal multielement source. The problems of self absorption, chemical interference, poor stability and the formation of refractory oxides found in D.C. arc, A.C. spark and flame methods are, to a large extent, alleviated. In addition, the high temperature of the source results in excitation of elements that could not be achieved in flames. When coupled with laser sample vaporization the ICP is able to introduce additional energy for vaporization.

The linear dynamic range, precision and accuracy of the plasma source is generally taken to be superior to previous atomic emission sources. A linear dynamic range of at least five orders of magnitude can be expected and is often limited only because of detector response. Reviews on ICP spectroscopy have been published by Greenfield (8) and Boumans (9) and an overall assessment of the ICP coupled to a laser vaporizer will be made in the following chapters.

2) Instrumentation

A Plasma-Therm Inc. (Kreston, N.J.) argon RF-ICP was used for additional vaporization and as an emission source for this experiment. The system consists of a model HFP-2500D 2.5 KW R.F. generator (27.12 MHz), a model ADC5-3 automatic power control, a model AMN-2500E automatic matching network and a model PT-2500 plasma torch assembly. The plasma torch geometry corresponds to that used by Fassel and Knisely (63). Typical flow rates used for the coolant, auxiliary and aerosol gases were 18.0 l/min, 0.0 l/min, and 0.8 to 1.2 l/min respectively. The flow rate for the aerosol was more accurately controlled than the others with a Matheson model 603 rotameter. The plasma was operated at 27.12 MHz with 1.5 KW power output.

C. Sample Chambers

1) Introduction

The connection of the sampling chamber to the torch of the ICP must be kept as short as possible if the majority of

molten liquid sample produced by the laser is to reach the plasma. For this reason, the sampling chambers utilized in this experiment were designed to fit inside the shielded plasma chamber directly below the torch. Radiation produced by the laser was focused through a quartz window onto the surface of the sample, the focal point being approximately 0.5 mm below the surface. The resultant plume was swept vertically into the plasma with a stream of aerosol gas. The sample atoms and droplets entered the central channel of the plasma where they underwent further vaporization and excitation.

The sample chambers were designed around common sample sizes typically found in industry. Two chambers, designed to accept different sample geometries, were built.

2) Rod Sample Chamber

The first chamber to be used was built to handle samples in the form of rods or tubes $3/8$ " in diameter or less and from $1/2$ " to 4" in length (Figure 13). To present a new surface for sampling, the sample was moved up or down with a threaded rod screwed into the teflon base. The upper part of the chamber was constructed out of $1\frac{1}{2}$ " diameter machinable glass rod. The transparent chamber simplified alignment, sample rotation and focusing of the laser. Various geometric configurations of argon inlets were tested to determine the best position for sweeping the sample into the plasma. The two positions tested were found to have identical performance

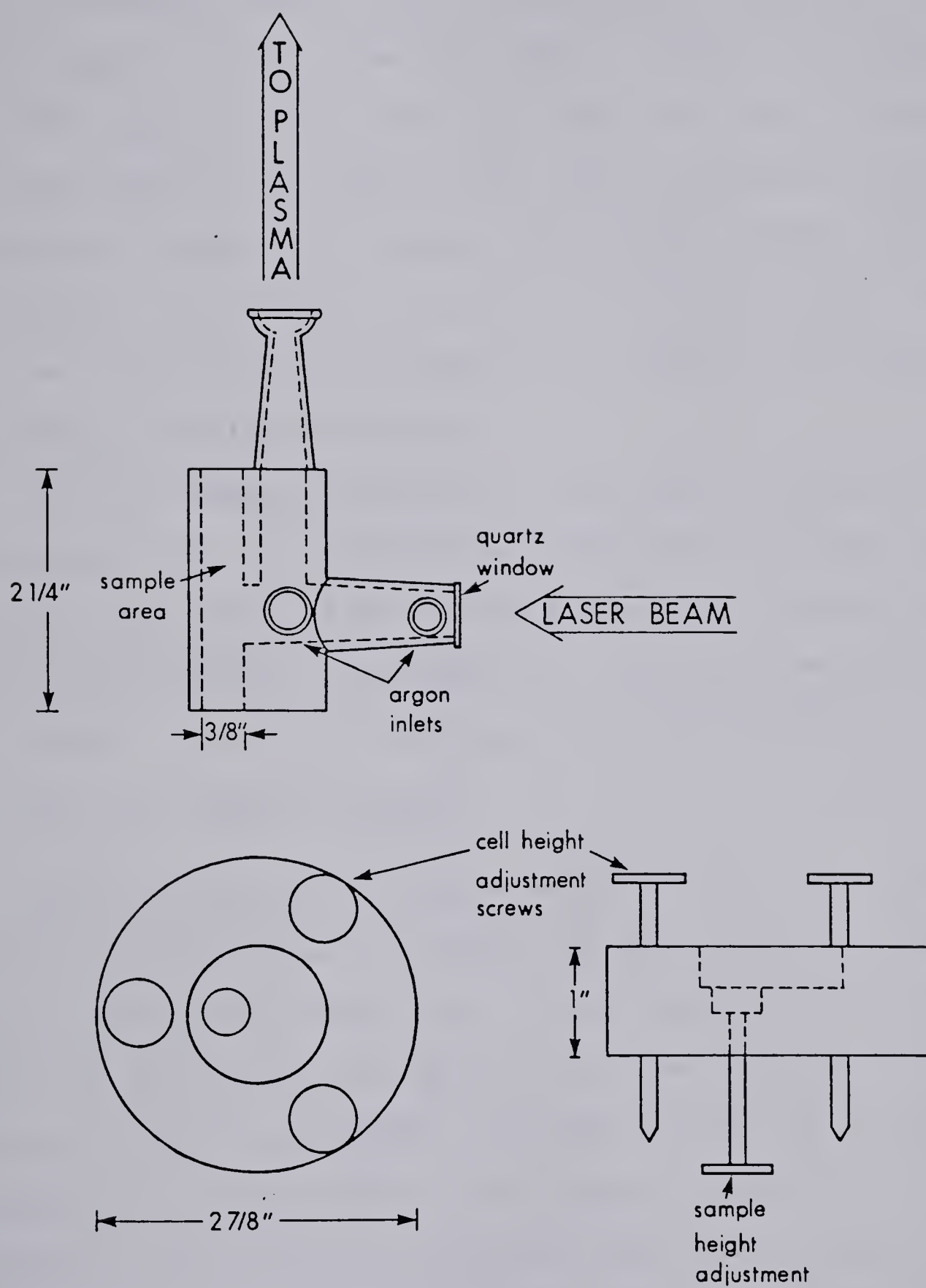


FIGURE 13. Rod Type Sample Chamber

within the experimental error of the system.

An aluminum adapter for the analysis of powdered samples was designed to fit in the rod sample chamber. It consisted of a 3/8" rod with its upper half machined down to accomodate the extra width of a layer of two sided tape with a coating of powdered sample. The adapter was placed inside the sample chamber in the same manner as a solid rod sample. The laser was defocused to prevent penetration of the tape and the removal of aluminum below.

The rod sampler was used in the initial phases of the experiment only. It showed the feasibility of laser vaporization but the lack of suitable standards limited its use to characterization of the system. For this reason, a sample chamber capable of handling discs was designed.

3) Disc Sample Chamber

The availability of many samples in the form of discs promoted the design and construction of a sample chamber capable of handling that type. Discs from 1/2" to approximately 5" in diameter and 1/32" to 2 1/2" in thickness can be handled by the disc sampler. A large variety of aluminum standards from Alcoa and an even larger selection of steel, stainless steel and brass standards from the National Bureau of Standards are available in this size range. Most of the samples produced by the metals industry fall within this range and can be used with little or no sample preparation.

As with the rod sampler, the disc sample chamber (Figure 14) mounts inside the plasma chamber directly beneath the

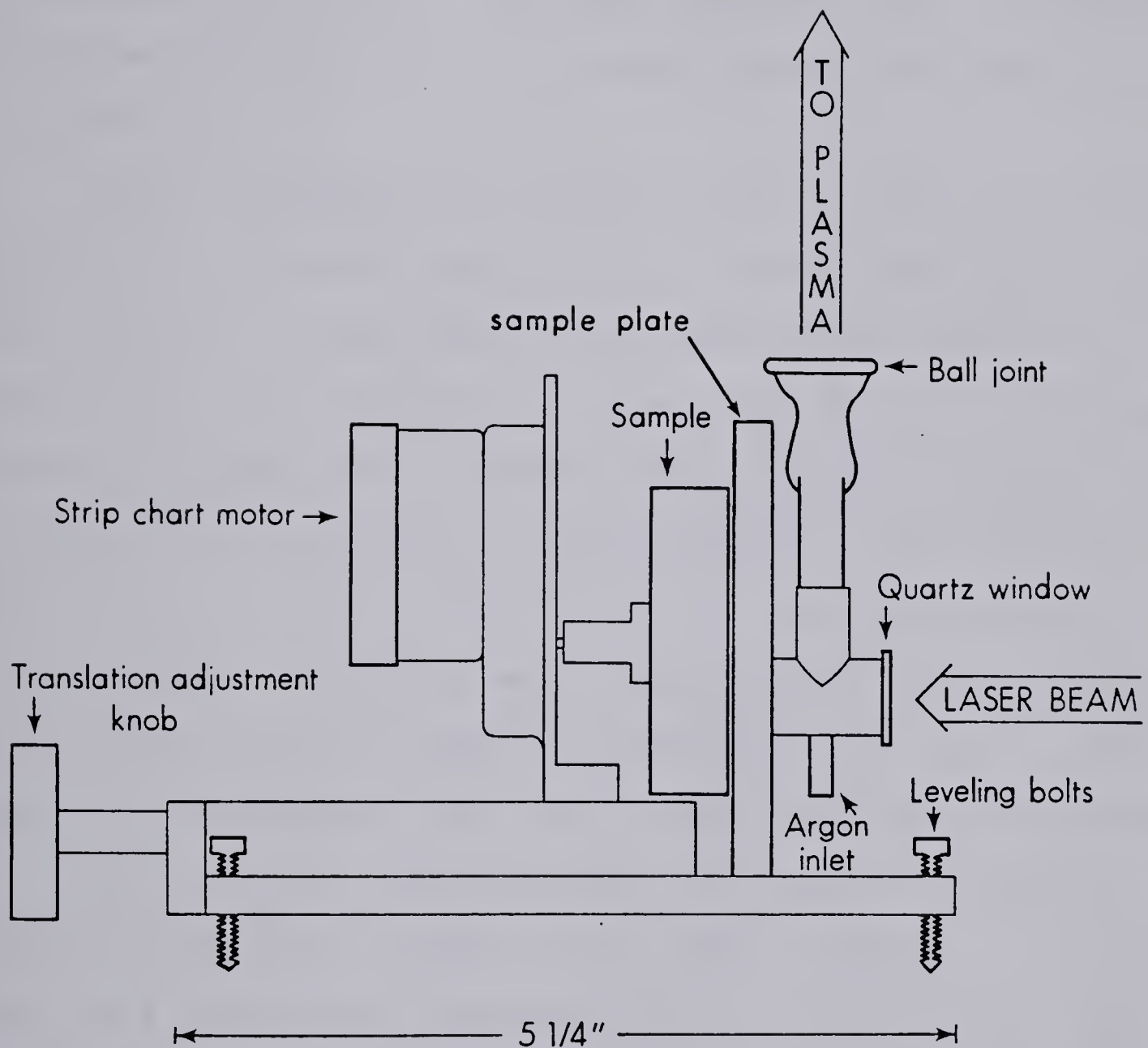


FIGURE 14. Disc Type Sample Chamber

torch and the laser beam is again focused through the optical window on the sample surface. Provisions are also made for rotation of the sample to provide a fresh surface, except in this case the sample is rotated with a 2 RPM strip chart motor instead of by hand. With the electric motor, the sample could be rotated inside the plasma chamber with the plasma in operation.

Sample thickness is compensated for by adjusting the position of the motor along a track behind the sample plate. This ensures a tight seal of the sample face against an O-ring in the rear surface of the sampling plate, preventing argon and sample loss. Before the O-ring was installed, up to 80% of the argon and a large fraction of the vaporized sample in the aerosol was lost around the sample surface. Varying sample diameters were accommodated by manual adjustment of the vertical position of the electric motor. This was not a convenient operation but was performed infrequently.

After lengthy sampling runs, a coating of condensed material plated the inside of the optical window. Since the laser was essentially unfocused when it reached the window a significant amount of its energy was reflected, resulting in a subsequent reduction in sample size. To remedy this, an extension to the sample chamber was added directly in front of the sampling area. Along with multiple argon inlets it was hoped that the vaporized material could be blown away before it reached the window. The additional length was found to make little difference, resulting in neither a decrease

in plating on the window or a decrease in signal due to an increase in dead volume. The chamber size was returned to normal and a high velocity argon inlet pointing directly across the sample face into the bottom of the torch was installed. This final configuration greatly improved the problem of sample plating on the window.

The majority of the experiments utilized the disc sample chamber and it was found to perform adequately for all types of samples examined.

D. Optical System

The optical arrangement used in the experiment is detailed in Figure 15. The ruby laser and right angle prisms were mounted on a rail bed identical to the rail bed mount for the plasma and monochromator setup. The two systems were separated by a room divider. The beam was directed through a hole in the partition (courtesy of Acme Hammer and Saw Corp., Hales Corners, Wisconsin), through a 120 mm focal length focusing lens and into the sample chamber.

The emission from the plasma was observed at 18 mm above the load coil of the ICP throughout the entire experiment to avoid problems with spatial emission common to plasmas (64,65). A four to one image of the plasma was formed by the 100 mm focal length imaging lens on the entrance slit of the monochromator.

The dispersive system was a Heath (GCA/MacPherson EV-700) diffraction grating monochromator with a 100 μm entrance slit and a one inch 1024 element photodiode array

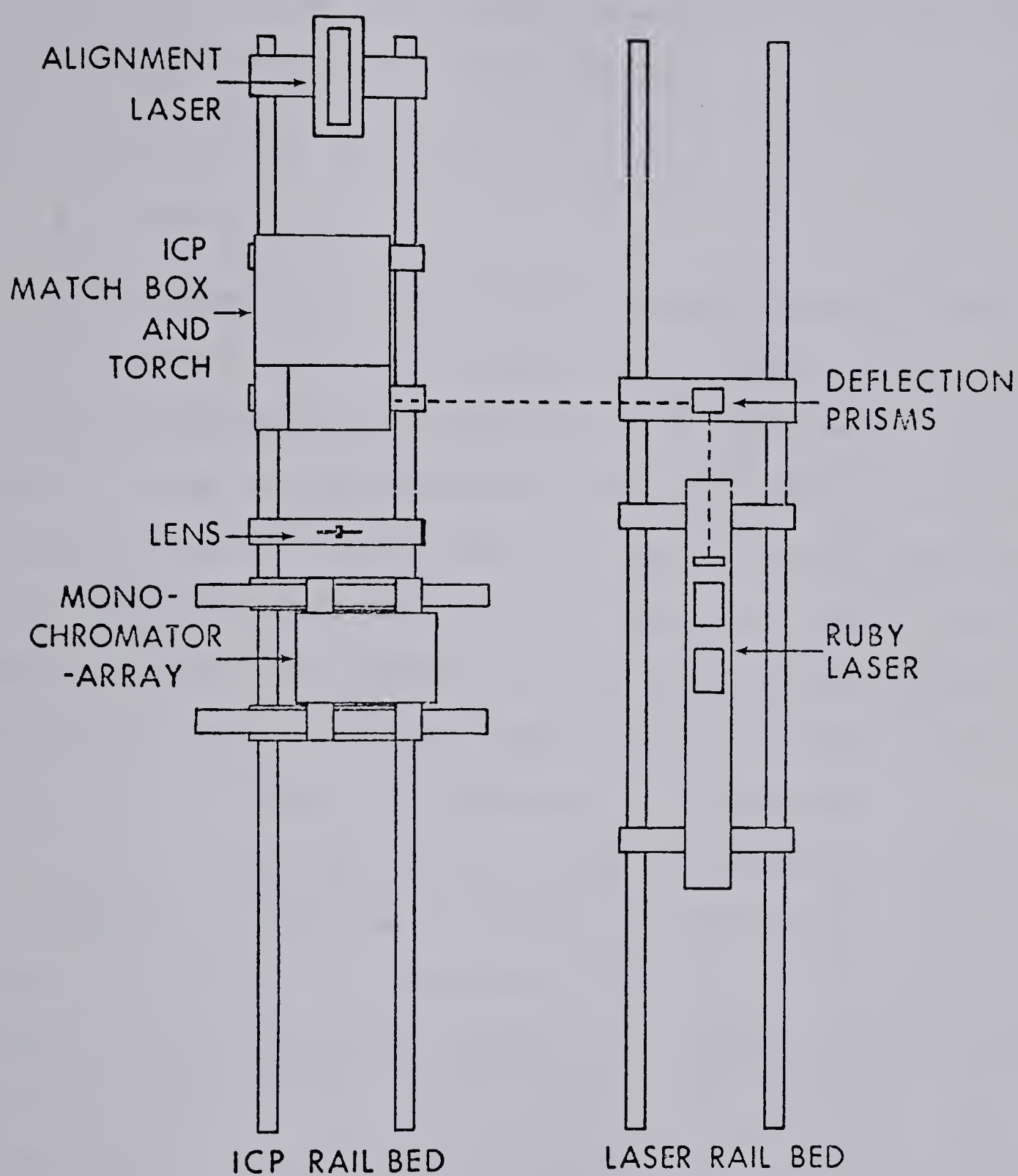


FIGURE 15. Optical Arrangement of the Laser, Plasma and Spectrometer

detector mounted in the focal plane. The dispersion of the monochromator in the focal plane was 0.5 nm/nm allowing a 50 nm spectral coverage with the diode array.

E. The Diode Array Detector

1) Introduction

To complement the multielement capabilities of the ICP emission source, the use of a self scanning silicon photodiode array has been examined (66). The diode array has been found to be an effective multielement detector with nanosecond response times and a wide spectral range. The photomultiplier tube (PMT), the most common type of detector used in multielement systems, is superior in sensitivity to the array, resulting in better detection limits but is restricted for multielement use to large spectrometers by its physical size. Each PMT can only cover one spectral line so background corrections are difficult, requiring a detector at a position that receives only background radiation. The array facilitated coverage of a 50 nm spectral window in a region from 200 to 1000 nm with a resolution of 0.05 nm/diode when installed on a compact Heath 1/3 meter monochromator.

2) Instrumentation

The linear self scanning silicon photodiode array used in the experiment was obtained from the Reticon Corporation, 910 Benica Ave., Sunnyvale, CA. 94086. It consisted of 1024 discrete diodes 0.43 mm (0.017") high on a 25.4 μ m (0.001") spacing which results in a density of 39.4 diodes/mm and a

length of 26.01 mm (1.024"). The electronics described by Horlick (66) allow scan times from 0.1024 sec to 23.296 sec.

Due to the intensity of the signal, data were collected and the array rezeroed to prevent possible saturation of the diodes by the most intense emission lines.

F. Data Collection

1) Introduction

The spectral signal produced by the laser pulse lasted from two to ten seconds depending on the emission characteristics and the concentration of the element under observation. As stated before, the array was scanned every 0.1024 sec to prevent saturation and the information collected and stored. The final form of the data depended upon the computer system used.

2) PDP-11 System

Initial collection of data during the testing of the system was carried out with a Digital Equipment Corporation (DEC, Maynard, Mass.) computer model PDP 11/10. Each scan was collected from the array and stored individually on hard disc, allowing retrieval for the examination of scans in chronological order to determine if any time behavior existed. The spectrum could be plotted, displayed and a hard copy obtained with a DEC VT55 terminal (Digital Equipment Corporation). Due to the time needed by the computer to store the spectra on disc, the shortest scan time that could be read and stored without skipping scans was 0.8 seconds. This

resulted in saturation of the most intense lines.

3) PDP 8 System

To obtain quantitative data, the information from the diode array was collected by a PDP 8/e computer (Digital Equipment Corporation) at a 0.1024 sec scan rate. The scans were collected and summed by the computer during the lifetime of the transient signal. A background spectrum of an equal number of scans was then collected and subtracted to produce the final spectrum which was then scaled and displayed on an oscilloscope. If desired, the information could be stored on DEC magnetic tape for later retrieval or plotted on a HP model 7045A X-Y recorder (Hewlett Packard Corp., Palo Alto, California).

With the program available (DP1000, Appendix A) any number of diodes (from 1 to 1000) of the array could be scanned. If the internal standard and the element of interest had emission lines that were near to each other, considerable computing time could be saved by using a narrower range of the array.

CHAPTER III

SAMPLE TYPES

A. Aluminum Samples

The majority of analytical determinations were carried out on aluminum standards supplied by the Aluminum Company of America. These samples were the disc type, 2.5 inches in diameter and ranging in thickness from 0.40 to 1.12 inches. The samples fell into two categories, aluminum alloys with a larger content of alloyed materials (Table 9) and aluminum alloys with trace amounts of added materials (Table 10).

B. Brass Samples

Three National Bureau of Standards brass samples were used for the generation of analytical curves. The content of major and trace elements is listed in Table 11.

C. Nonconducting Samples

A brief examination of biological nonconducting samples was made. The majority of work was conducted upon a Philippine mahogany sample (again courtesy of Acme Hammer and Saw Corp.) in which carbon was used as an internal standard.

TABLE 9
High Alloy Aluminum Samples

Standard	Alcoa Number	Si	Fe	Cu	Mn	Mg	Ni	Zn	Ti
HA	SS-380-6	8.78	.81	3.58	.45	.17	.30	.34	.092
HB	SS-360-C	9.17	.80	.31	.22	.52	.26	.25	.079
HC	SS-355-Z	4.88	.37	1.25	.089	.53	.057	.10	.12
HD	SS-356-B	7.48	.37	.092	.11	.32	.053	.10	.17
HE	SS-333-C	8.72	.67	3.73	.46	.31	.30	.24	.085
HF	SS-A132AA	11.85	.77	1.02	.070	1.26	2.52	.058	.057
HG	SS-D132-A	9.30	.77	3.03	.30	.82	.90	.26	.092
HH	SS-319E	6.23	.68	3.83	.58	.18	.20	.35	.10
		Cr		Pb		Sn			
HB	SS-360-C	.057		.16		.062			
HC	SS-355-Z	.046							
HF	SS-A132-AA	.005							

TABLE 10
Low Alloy Aluminum Samples

Standard	Alcoa Number	Si	Fe	Cu	Mn	Mg	Zn	Ti
LB	SA-1507	.001	.001	.0013	<.0002	<.0002	.001	.001
LC	SS-1507-A	.068	.10	.021	.005	.002	-	-
LE	SA-909	.061	.082	.031	.031	.030	.030	.030
LF	SA-1170	.23	.56	.10	.027	.009	.039	.039
LG	SA-1169	.10	.26	.21	.076	.038	.021	.021
LH	SA-816	.027	.024	.025	-	.0007	-	-

	Cr	Ni	V	Pb	Sn	Ga
LB	<.0002	<.0002	.001	.001	-	.001
LE	.027	.034	-	.030	.026	-

TABLE 11

Brass Samples

Standard Number	Cu	Zn	Pb	Fe	Sn	Ni	Al	Mn
B1	59.0 ₈	40.0 ₈	0.032	.004	.74	.025	2	.005
B2	61.2 ₁	37.3 ₄	0.18	.037	1.04	.098	-	-
B3	64.9 ₅	34.4 ₂	0.063	.050	.39	.033	-	.025

CHAPTER IV

INITIAL SYSTEM CHARACTERIZATION

A. Time Studies

1) Introduction

A brief study was carried out on the emission lifetimes of various elements vaporized by the ruby laser. The study was performed to determine the maximum amount of time needed for observation and to determine if there was any anomalous time behavior that may be indicative of selective volatilization or matrix effects.

2) Experimental

Vaporization was produced by the laser in the free running mode. The plasma emission from the sample was observed with the 1024 diode array and PDP 11 computer system previously described. As was stated before, because of computer limitations, the fastest speed the diode array could be run was a scan every 0.8 seconds but it was also possible to run the array at a 0.1024 second scan rate and to only collect every eighth scan. The latter method of array operation was chosen because it gave us an idea of relative peak intensities and prevented saturation of the array in most instances.

Measurements were completed on many spectral regions (50 nm widths) of steel, stainless steel, brass, aluminum and copper samples. In most cases, ten scans of 0.8 seconds each were sufficient to cover the entire time of emission,

however in a few cases the very intense lines of elements known to emit strongly with plasma excitation were found to last from 10 to 15 seconds. In these instances it was necessary to increase the number of scans to accomodate the extra time, but for the most part the emission signal lasted 3 to 5 seconds. With the computer program used, each scan could be examined individually on a CRT screen or plotted on a Zeta plotter for measurement.

3) Spectral Results

All of the materials and regions studied show similar time behavior. Of over 500 scans collected not one could be positively identified as having unexpected behavior.

Figure 16 displays eight spectra, all spaced 0.8 seconds apart from the region centred around 300 nm (275 nm to 325 nm) of the high alloy aluminum sample HA. The first scan (#1) was taken before any emission began and was used as a background for subtraction. The first spectrum to be seen in Figure 16, a result of scan #2 minus scan #1 (2-1), is flat, indicating that scan #2 was also taken before emission began. The second spectrum (3-1) shows intense emission from the Al 309.3 nm and 308.2 nm lines. The Cu 324.8 nm line, Si 288.2 nm line and the Mg 280.3 nm and 279.5 nm lines all show strong emission but are weaker than aluminum. Weak emission is seen from Mn 294.9 nm, Mn 293.9 nm and Mn 293.3 nm as well as the Mg 285.2 nm line.

In the third spectrum (4-1) the aluminum is now strongly saturated while Cu, Si and the Mg doublet show intense emission.

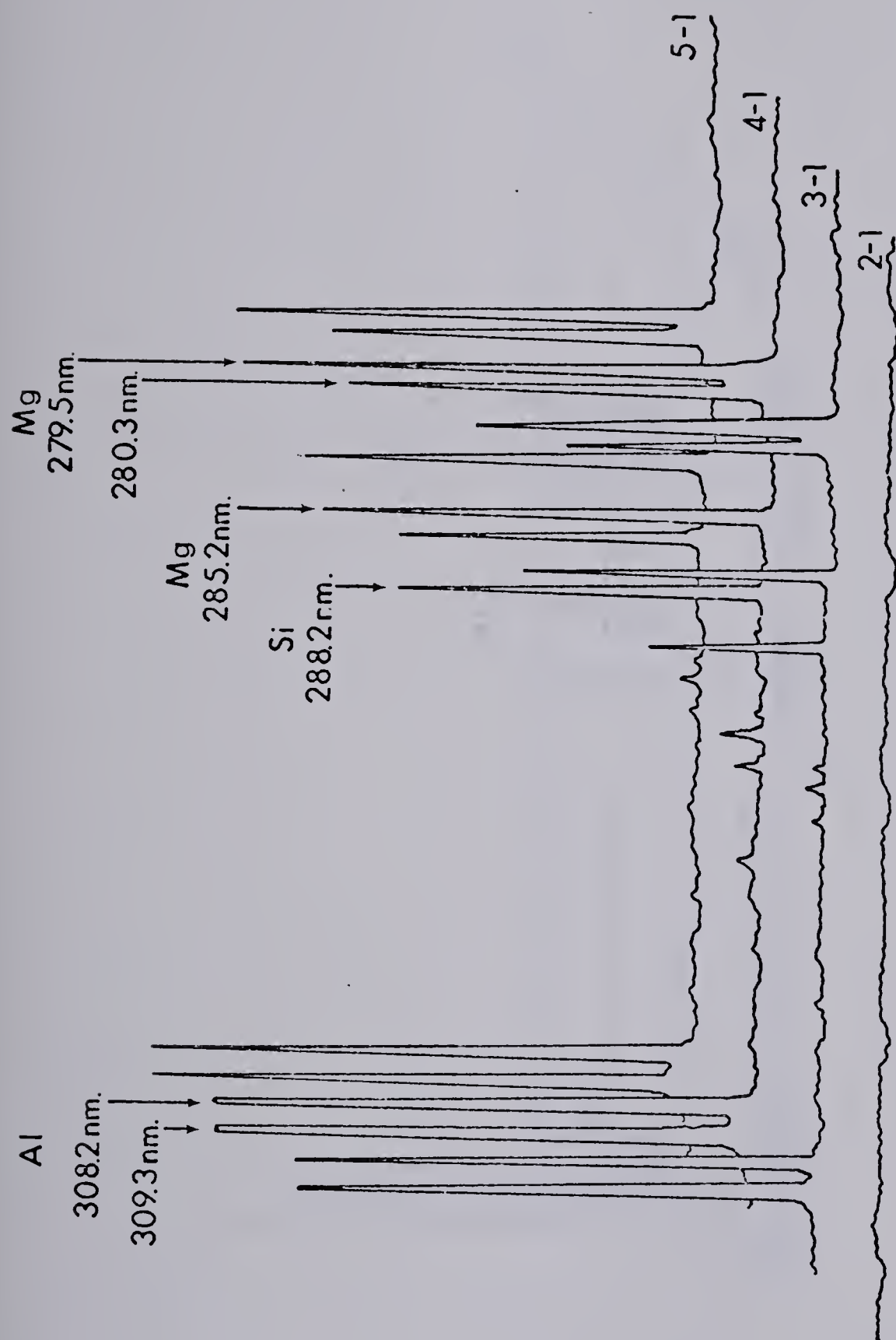
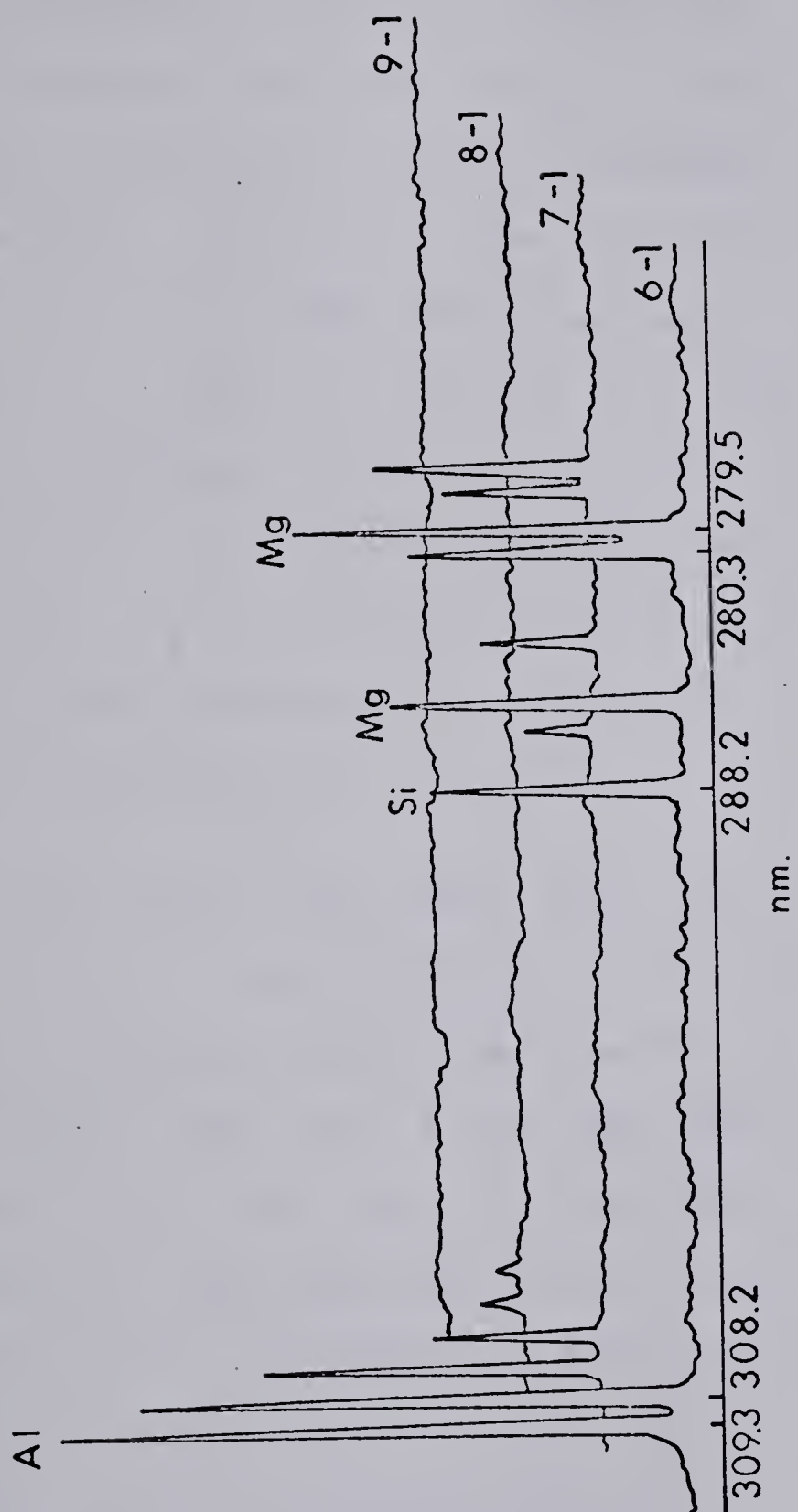


FIGURE 16. Time Behavior of the Laser Solid Sampler



The Mn triplet and the weaker Mg line are also seen to be more intense. It can be empirically stated that all of the lines increase in size by a relatively constant factor.

The fourth spectrum (5-1) is similar to the second indicating a reduction in overall intensity after approximately 2.5 seconds. Within the time resolution of the experiment all of the lines reach their maxima at the same time. A constant decrease in intensity at a rate slower than the initial increase can be seen in spectra five (6-1), six (7-1) and seven (8-1) with the spectrum eight (9-1) totally flat. The total time of emission in this case is approximately 4.5 sec for most elements.

4) Conclusions

The overall time behavior of the laser vaporized samples into the ICP is not noticeably time dependent. If an integrating detector collecting data for the entire emission lifetime is used, all of the analytical information will be collected and there will be compensation for any small differences in time behavior that may occur. Table 12 shows the empirical time behavior of the emission lines of sample HA in the region from 275 nm to 325 nm.

B. Qualitative Wavelength Studies

1) Introduction

To determine the effectiveness of laser vaporization into an ICP as a multielement technique, the emission of several 50 nm regions for many samples were investigated. It

TABLE 12

Time Behavior of Sample HA

Scan Number	Time After Emission (sec)	Al 309.3 nm	Peak Heights in mm		
			Mn 294.9 nm	Si 288.5 nm	Mg 279.5 nm
2-1	0.0	0	0	0	0
3-1	0.8	91(sat.)	3.5	30	61
4-1	1.6	91 (sat.)	7.5	62	91(sat.)
5-1	2.4	91(sat.)	3.4	51	81
6-1	3.2	91(sat.)	2.0	47	56
7-1	4.0	49	1.0	17	31
8-1	4.8	7	0	0	0
9-1	5.0	0	0	0	0

was thought that if the system proved useful for qualitative analysis it could be developed to give quantitative information. The initial testing verified the use of laser vaporization and ICP emission spectroscopy as a useful qualitative tool.

2) Experimental

As in the time studies, the laser was operated in the free running mode with the information collected by the PDP 11 computer and 1024 diode array. The array was run at 0.1024 second scan time with every eighth scan collected and stored by the computer. Steel, stainless steel, aluminum, brass and copper samples were studied in the wavelength region from 190 nm to 450 nm. Most of the useful analytical information occurred in the region from 200 nm to 325 nm.

3) Spectral Results

Figure 17a,b,c presents the spectrum obtained for the high alloy aluminum sample HA. A 135 nm wide spectral range from 190 nm to 325 nm is covered. The major lines have been identified by comparison with known standard samples and are labelled above the peaks. Many of the smaller lines were also identified but not included in the figure because of space limitations.

4) Conclusions

The vast majority of the elements in the sample, regardless of concentration, were positively identified by their emission spectra. A comparison of Figure 16 and Figure 17c,

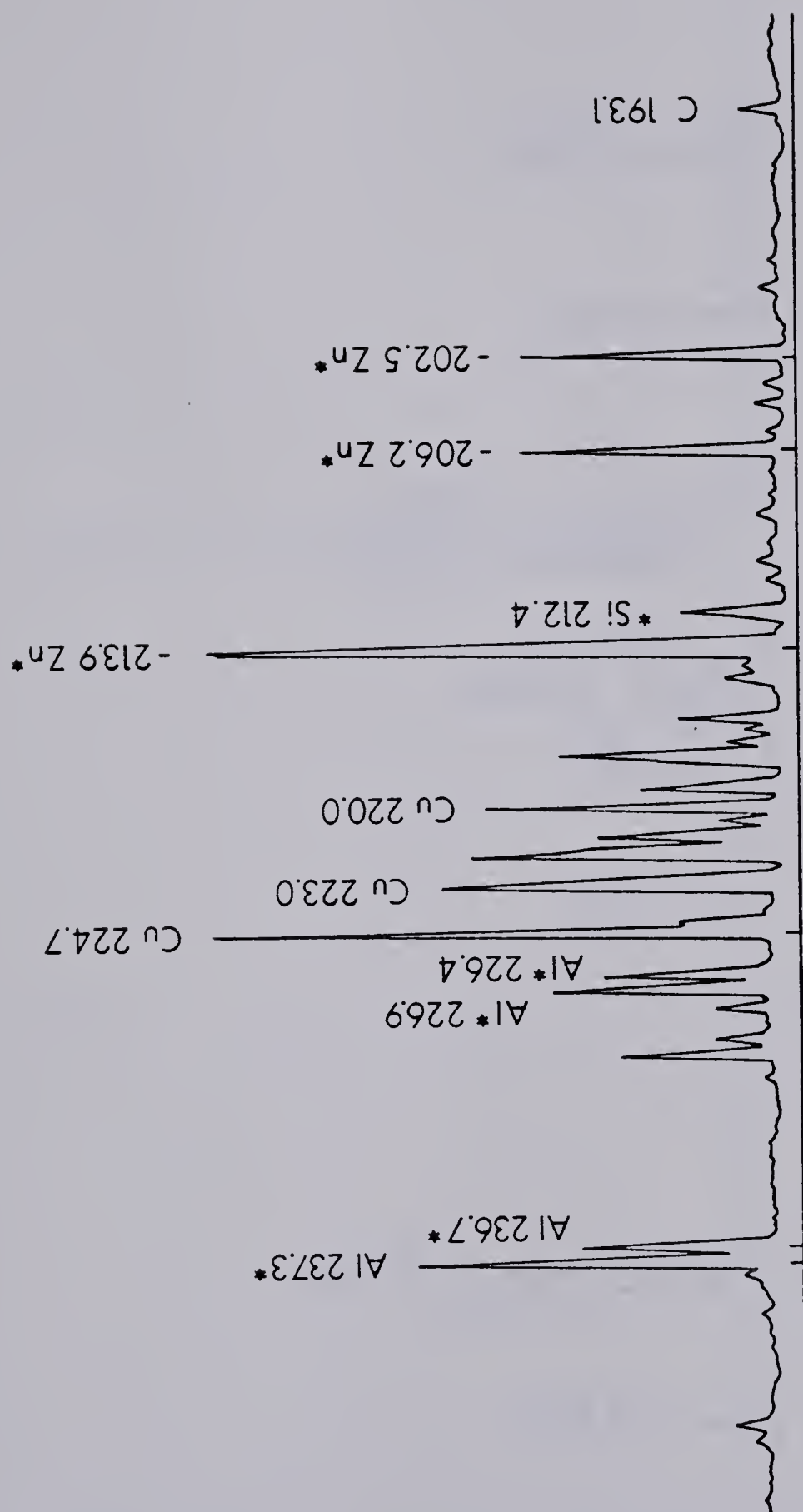


FIGURE 17a. Emission Signal from Sample HA

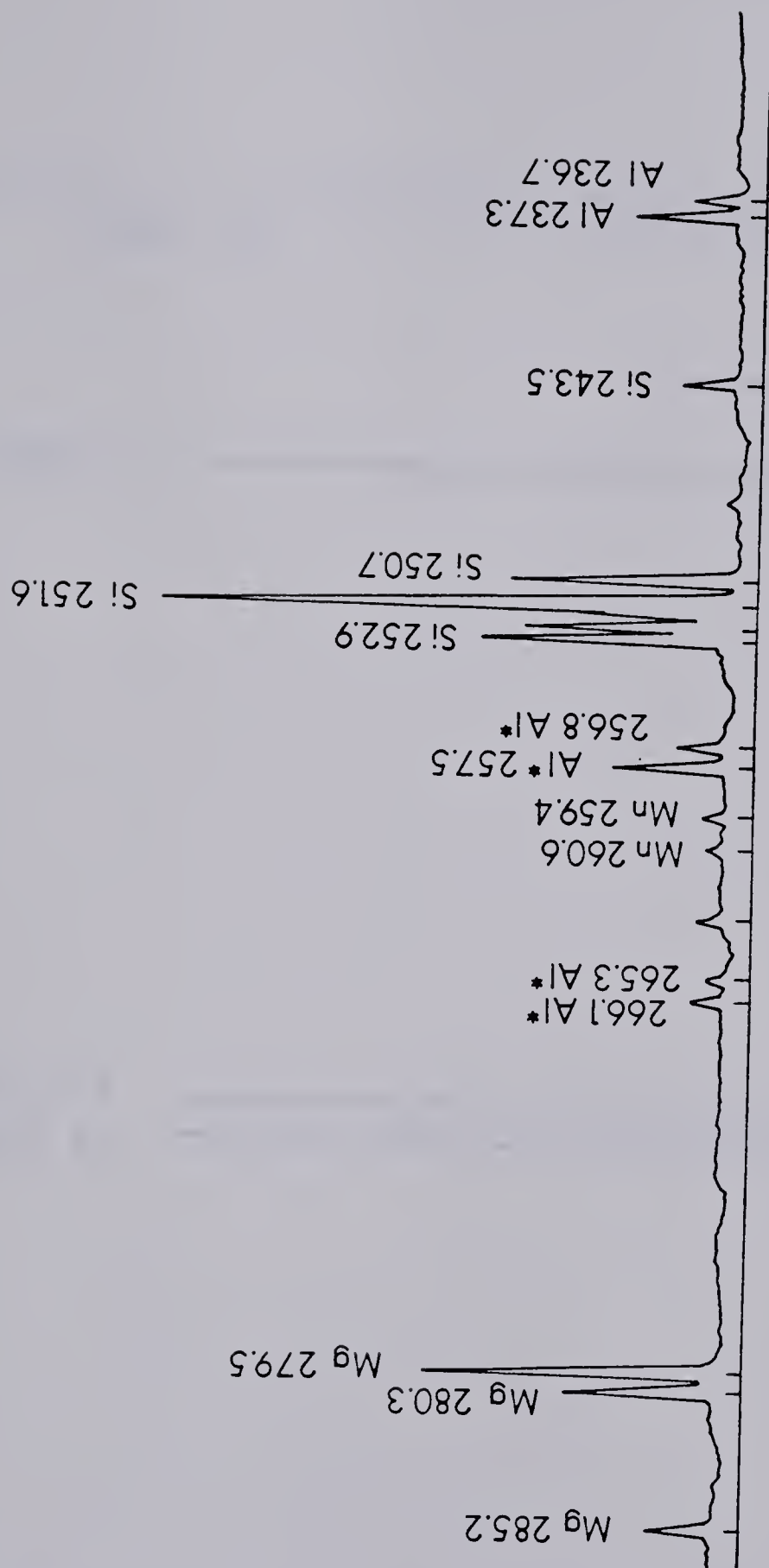


FIGURE 17b. Emission Signal from Sample HA

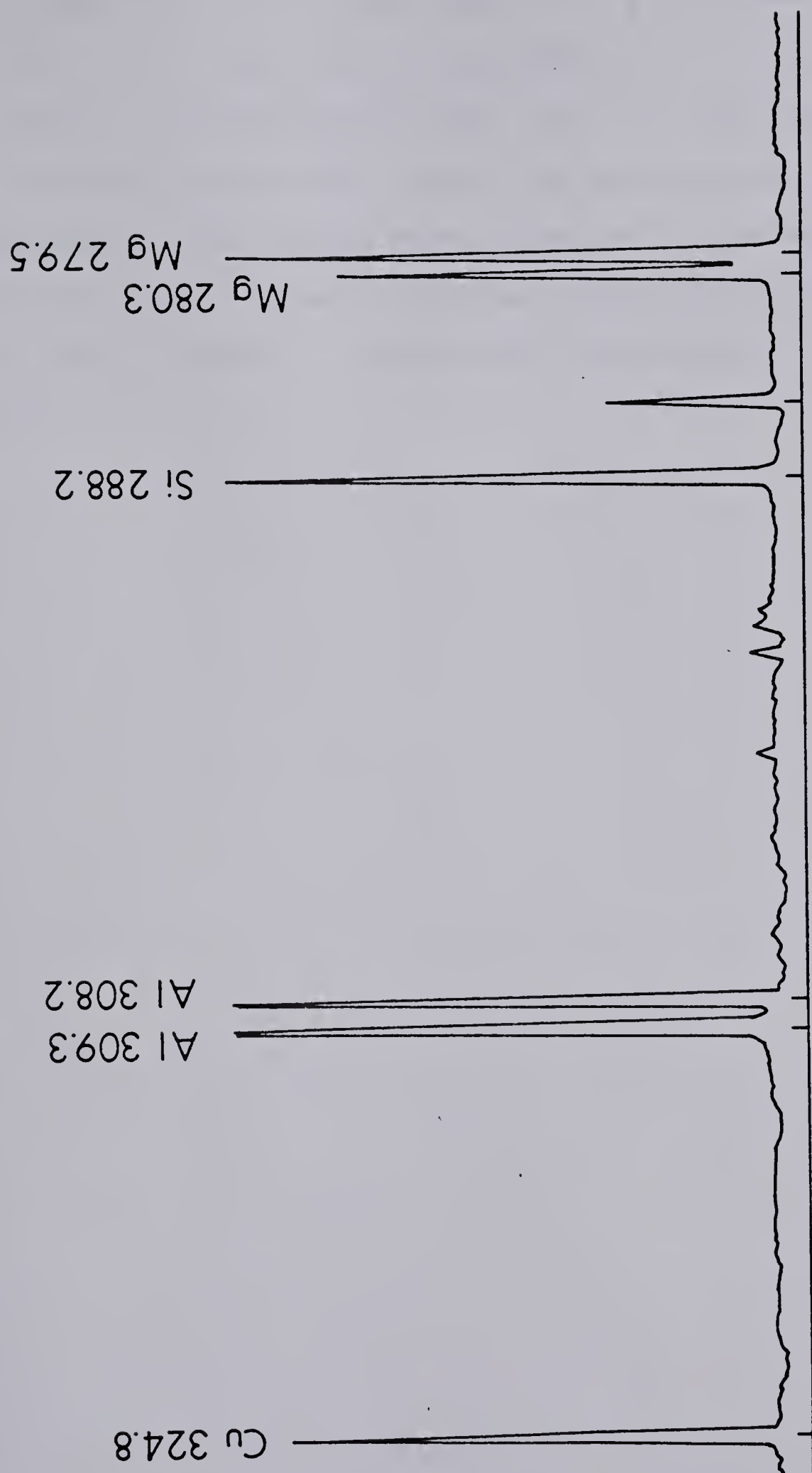


FIGURE 17c. Emission Signal from Sample HA

both of sample HA, will reveal different peak sizes for the same lines. This was a result of summing one out of eight scans and not collecting much more than 2% of the information. While the system was proved useful for qualitative results, new experimental techniques were necessary to increase the precision of the experiment and a new computer data collection system was needed to collect the information in its entirety.

CHAPTER V

SAMPLING TECHNIQUE

A. Introduction

In the last section it was stated that the PDP-11 computer system could not be depended upon to give quantitative results. For this reason, the PDP-8 system previously described was designed to collect and store all the information produced by the sampling system. It was apparent that while the increase in the precision of the data was significant, the change in computer system alone would not be enough if performance equal to the A.C. spark was to be realized.

Methods of increasing the precision of the sampling process by modifications in the plasma and laser operating procedures were investigated. Literature research on previous laser vaporization techniques pointed to areas in laser performance that would affect the sampling process. These methods, described in the next two sections, enabled an increase in performance to a level as precise as some of the best previous spectroscopic methods.

B. Laser Operation

1. Timing and Number of Shots

i) Introduction

A key factor in the stability of the laser output power is the firing repetition rate. If, after a period of warmup, a ruby laser is fired with the shots spaced equidistant in

time the precision of the power delivered by the laser greatly improves. In an attempt to increase the overall precision of the laser vaporizer/ICP system, the optimum number of laser shots per crater as well as the optimum time between shots was determined. A quick repetition rate and the minimum number of shots were desirable to reduce the total time of determination.

ii) Experimental

The experiment was performed on high alloy aluminum samples HA, HB and HC because it was felt that matrix effects might exist and the system should be optimized for the sample that will receive the largest amount of study. Also, for the same reason, the wavelength region investigated, from 305 nm to 282 nm, was used throughout the experiment. The operating temperature of the laser was set to 60 °F and the laser power supply set at 4.23 KV for the duration of the experiment. The ICP was operated at 2 KW of R.F. power with coolant, auxiliary and aerosol gas flow rates of 18, 0.0 and 1.0 l/min respectively. The height of observation above the load coil was 18 mm and a four to one image reduction system was used to focus on to the entrance slit of the monochromator. The monochromator slits were set at 100 μ m and the diode array run at 0.1024 seconds per scan. The computer collected 250 scans of signal and subtracted 250 scans of background for most of the experiment. The number of scans was initially kept constant even though much shorter scan times could be used for some of the tests. This constant

scan time was intended to eliminate any unfair contribution of electronic noise to the tests requiring longer scan times. To discover if there was any benefit to shorter scan times, an experiment was also performed involving 100, 150 and 200 scans per spectrum. At 0.1024 seconds per scan, the time required to collect the information was 10.24, 15.36 and 20.48 seconds respectively.

All of the laser shots in a single spectrum were four seconds apart for the "number of shots" experiment. After the results for optimum number of shots were obtained the determination of optimum time between shots was completed using two shots per crater. A time of two, four, six, eight or ten seconds elapsed between shots and a time of 2.5 minutes passed between subsequent sampling operations. The 2.5 minutes were necessary to take the background spectrum, perform the subtraction and plot the results. For each spectrum, 150 scans of both signal and background were collected.

iii) Results

In determining the optimum number of shots per crater, it was found that the signal to noise ratio increased with increasing number of laser firings. The spectrum produced by one shot (Figure 18) when compared with the spectrum produced by two shots was found to have a smaller signal to noise ratio and the appearance of more noise in the background. The actual background levels in both spectra are the same but the intensities of the emission peaks are different. Since the computer normalizes the largest peaks, the bottom spectrum only appears to have more noise.

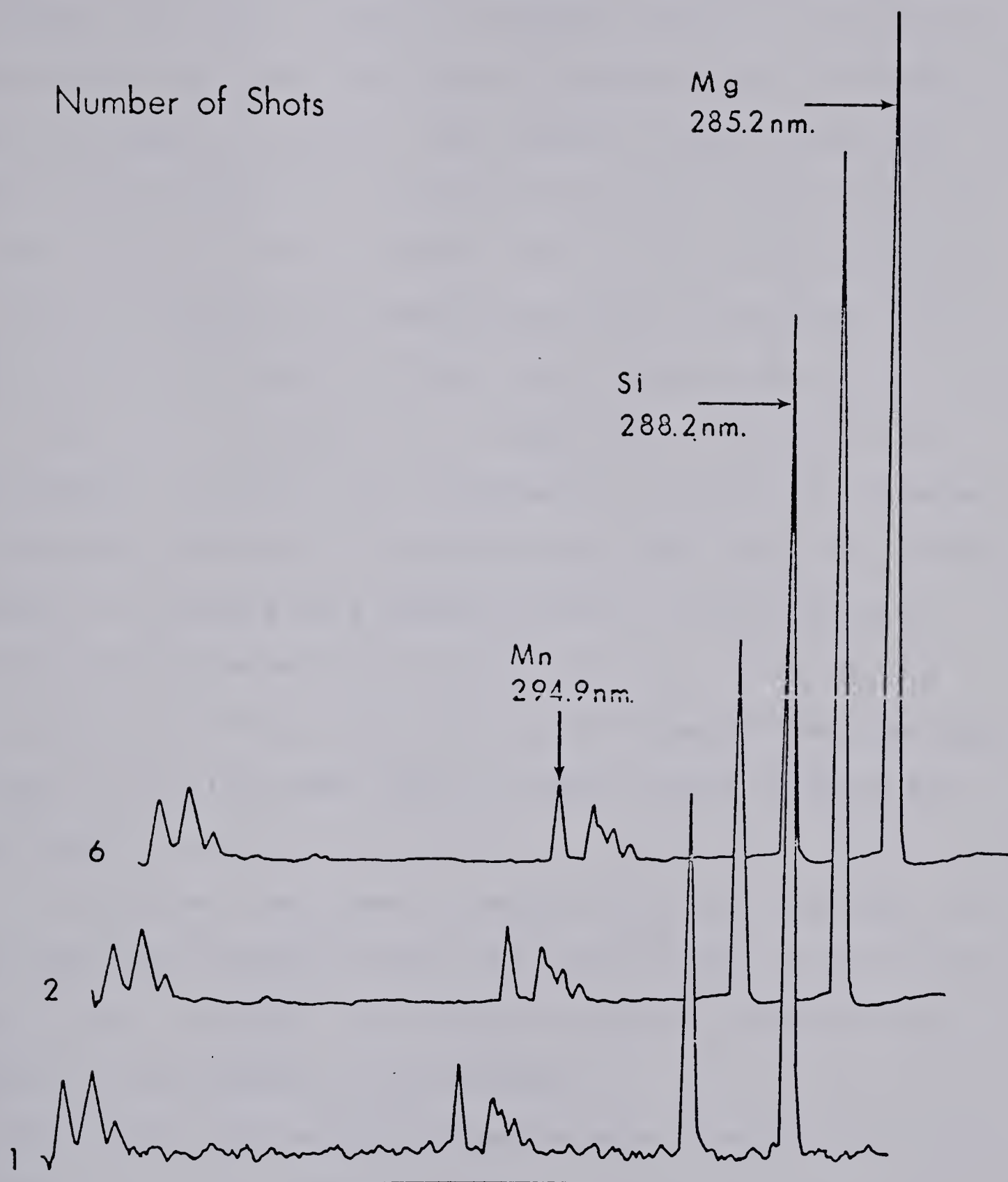


FIGURE 18. Effects on the Emission Signal by the Number of Laser Shots

Spectra were also taken of signals produced by three to eight shots with the spectrum produced by six shots shown in Figure 18, scan 3. While a slight increase in signal to noise ratio was found, the rate of increase was not linear with the number of shots. This can be attributed to the loss of laser power resulting from the high repetition rate. For the amount of time expended and the undoubted reduction in laser lifetime by the high firing rate it was concluded that the optimum number of shots per crater was two.

Operating the laser with longer times between pulses to increase the power was attempted but no obvious increase in precision was seen. The particular ruby laser in use was designed to operate at a maximum rate of one pulse every 15 seconds over an extended period of time. This was far too slow to be of any use, but if a different laser were used a higher pulse rate and number of shots would probably be found beneficial.

A very small increase in background noise was noted when 100 scans were compared with 250 scans in the two shot spectrum. This increase, even though not large, showed that the number of scans should be minimized.

As before, the spectra obtained were normalized to the largest peak. The greatest portion of the study was completed on the high alloy aluminum sample HE in which the Mg 285.2 nm line was the most intense. The Si 288.2 nm line was ratioed to magnesium to determine the fluctuation of the peaks with respect to the time between shots. The

best results were obtained with eight and ten seconds between pulses indicating that longer pauses produce the most stable pulses. An examination of the standard deviation of the peak heights showed eight and ten second pauses to have a RSD of approximately 4% while six and four second pauses produced peaks with a RSD of 12% to 10% respectively. The number of peaks used in the comparison is generally eight to twelve.

A comparison of peak heights using the Mn 294.9 nm line ratioed with Mg at 285.2 nm for four, six and eight second pauses was also completed. The comparison upheld the original findings with 8% RSD for the four second pause and approximately 4% for the six, eight and ten second pauses. Table 13 summarizes the results and averages the RSD for both ratios where applicable.

A scan period of 100 scans (10.24 seconds) and two shots per crater with an eight second pause between shots was used for the remainder of the experiment. It may seem that a scan time of 10.24 seconds is too short if the second shot of the laser occurs only 2.24 seconds before the end of data collection but as a result of the low power of the laser in the second shot and the relatively brief lifetime of the lines being observed all emission of interest had ceased prior to the termination of the scans.

2) Q switched versus Free Running

i) Introduction

Several authors have reported an improvement in analytical precision with the use of a Q switched laser on samples

TABLE 13

Relative Standard Deviations of the Emission Peaks
for Various Spaces of Time Between Laser Pulses

TIME	2 sec	4 sec	6 sec	8 sec	10 sec
RSD					
Intensity Mn/Mg	16.82%	8.25%	4.33%	4.65%	3.95%
RSD					
Intensity Si/Mg	-	9.66%	12.21%	4.00%	4.22%
RSD					
Average	-	8.96%	8.27%	4.32%	4.09%

without subsequent excitation. To determine if Q switching would affect the precision of measurement for a sampling only process, a comparison of Pockel's cell versus free running was completed. From previous research by other workers it was felt that an improvement in the reproducibility of the laser output would be found with Q switching but, because of the use of internal standards, it was unclear whether any improvement would be seen in the analytical performance. An improvement in accuracy with the use of the Q switch mode was also possible if selective volatilization and fractional distillation were occurring to a greater extent in the free running mode.

ii) Experimental

Several high alloy aluminum samples were examined in the spectral region containing silicon, manganese and magnesium emission lines from 282 nm to 305 nm. Each sample was examined ten times with two laser shots eight seconds apart so the relative peak heights could be compared. Each examination consisted of 100 scans, 0.1024 seconds in duration with 100 scans, 0.1024 seconds in length, of subtracted background.

To determine the typical sampling size small aluminum samples were weighed on a nanogram analytical balance before and after sampling. To improve the weighing accuracy, each piece of aluminum was sampled in two locations with two laser shots per sampling spot. The subsequent weight difference

in the aluminum was divided by two to obtain the weight of a single crater. This experiment was performed in both the free running and Q switched modes of operation.

iii) Spectra and Results

The resulting spectra were normalized and plotted by an X-Y recorder. The normalization process simplified the comparison of peak heights for reproducibility. If an internal standard is to be used effectively, the emission peaks of the standard must retain the same peak height relative to those of the sample regardless of laser fluctuation. The expected result, an improvement in precision with Q switch operation, was not supported. Data gathered showed little difference in the precision of peak height measurements for the free running or Q switched modes. This indicates that an internal standard is an effective method for compensation of the laser power fluctuations in the sampling only laser vaporization process.

Examination of the normalized spectra of low alloy aluminum sample LG produced by both the Q switched and free running laser (Figure 19) reveals the Q switched mode produced spectra with a much higher background signal. As before, the background intensity of the two signals are the same but the peak heights and the signal to noise ratio are not. The low signal to noise ratio for the Q switched laser incorrectly indicates better detection limits for the free running laser.

In these spectra, sample size has not been taken into

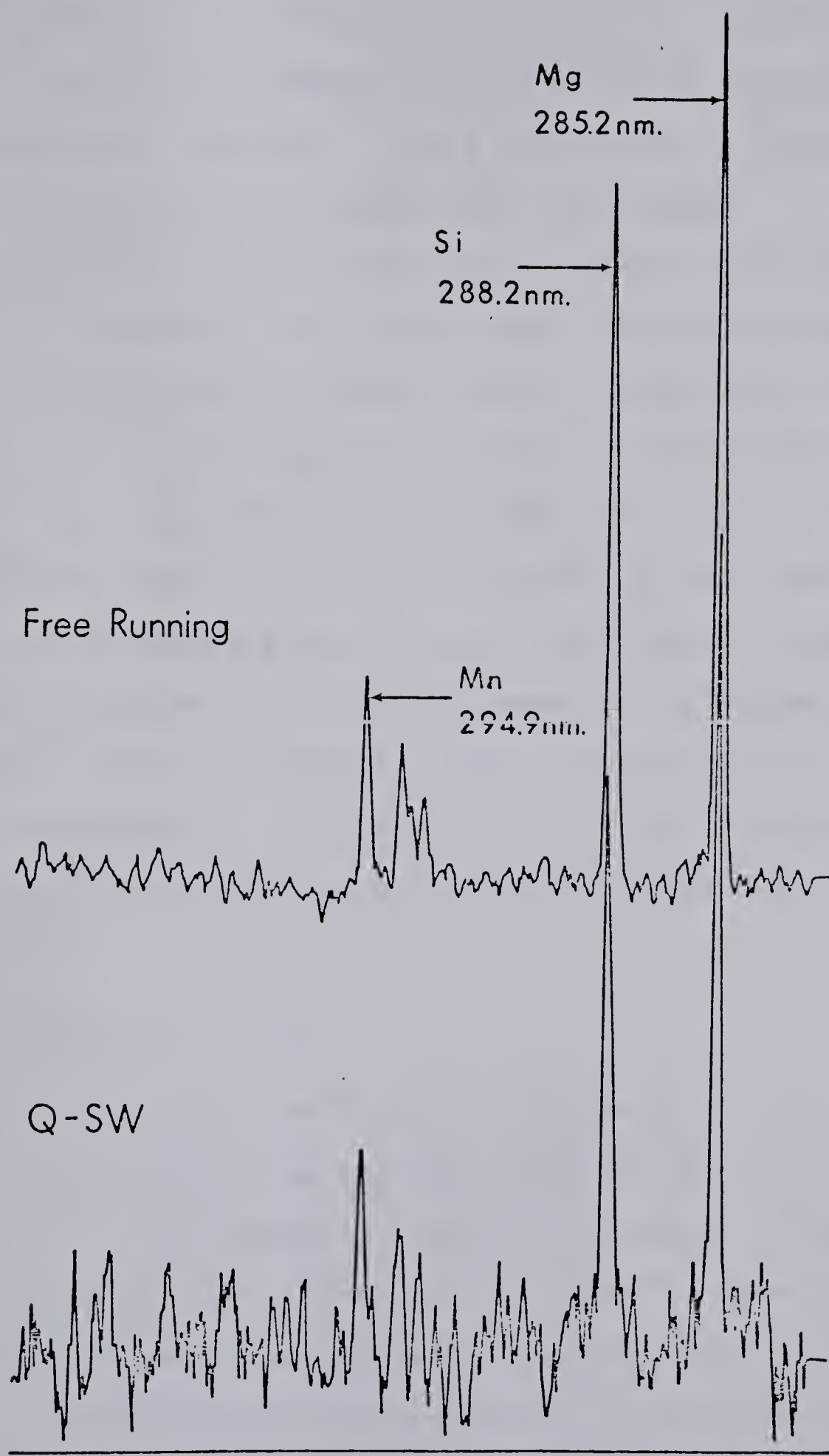


FIGURE 19. Comparison of the Emission Signals for Free Running or Q switched Modes of Laser Operation

account. The size of the sample removed in the Q switched mode is approximately 25 μg while in the free running mode 500 μg of material is removed from an aluminum surface. The free running mode therefore ejects about twenty times as much material that can be swept into the plasma.

A comparison of detection limits for both modes of operation to be discussed later will reveal that the Q switched mode is actually able to detect smaller quantities of material but these lower detection limits are only useful for microsampling. The free running laser when coupled to an ICP excitation source is able to make use of the unexcited portion of the sample and as long as the plasma is able to completely vaporize and excite the sample the largest possible sample size is desirable. When coupled with an ICP, the laser vaporizer is most efficient in the free running mode unless a very small sample ($<0.2\text{mm}$ surface area) is to be determined.

3) Effects of Focus

A brief study on the effects of focus was completed to determine if a wider sampling area could be used to reduce the effects of inhomogeneity within the sample. Earlier findings in this study indicated that sample size and not peak laser power was the most important factor in the detection capabilities of the system. In the aspect of precision, either mode of sampling, high or low power, produced results of similar precision. Since the power of the laser seemed not to be too important, the decrease in energy

density resulting from increasing the focal area on the sample surface might not have created additional problems from selective volatilization. However, adverse effects were seen when the spot size was increased from a diffraction limited spot to spots 1.5 and 3.0 mm in diameter (Figure 20). With the spectra normalized to the silicon peak located at 251.6 nm, a drastic change could be seen in both pairs of aluminum lines located near 237 nm and 257 nm.

The reason for the change in the ratio of silicon to aluminum intensity was not investigated in depth. It was sufficient to learn that the focus must be kept as constant as possible. To keep the effects of a change of focus as small as possible, a long focal length lens was bolted to the back of the plasma chamber and the sample chamber was secured firmly inside.

The aluminum rod powder adapter, built for use in the rod sample chamber, was affected most by these results. The laser beam had to be defocused to a spot size 3 to 4 mm in diameter to prevent cratering of the aluminum substrate. If the focus was kept constant, powdered samples could still be effectively examined provided powdered standards were used and examined under exactly the same conditions of focus.

4) Summary

Parameters that were effective in increasing the precision of the laser vaporizer/ICP solid sampling system were determined. The best results were obtained with a free running ruby laser delivering two shots per crater with eight

Focusing effect

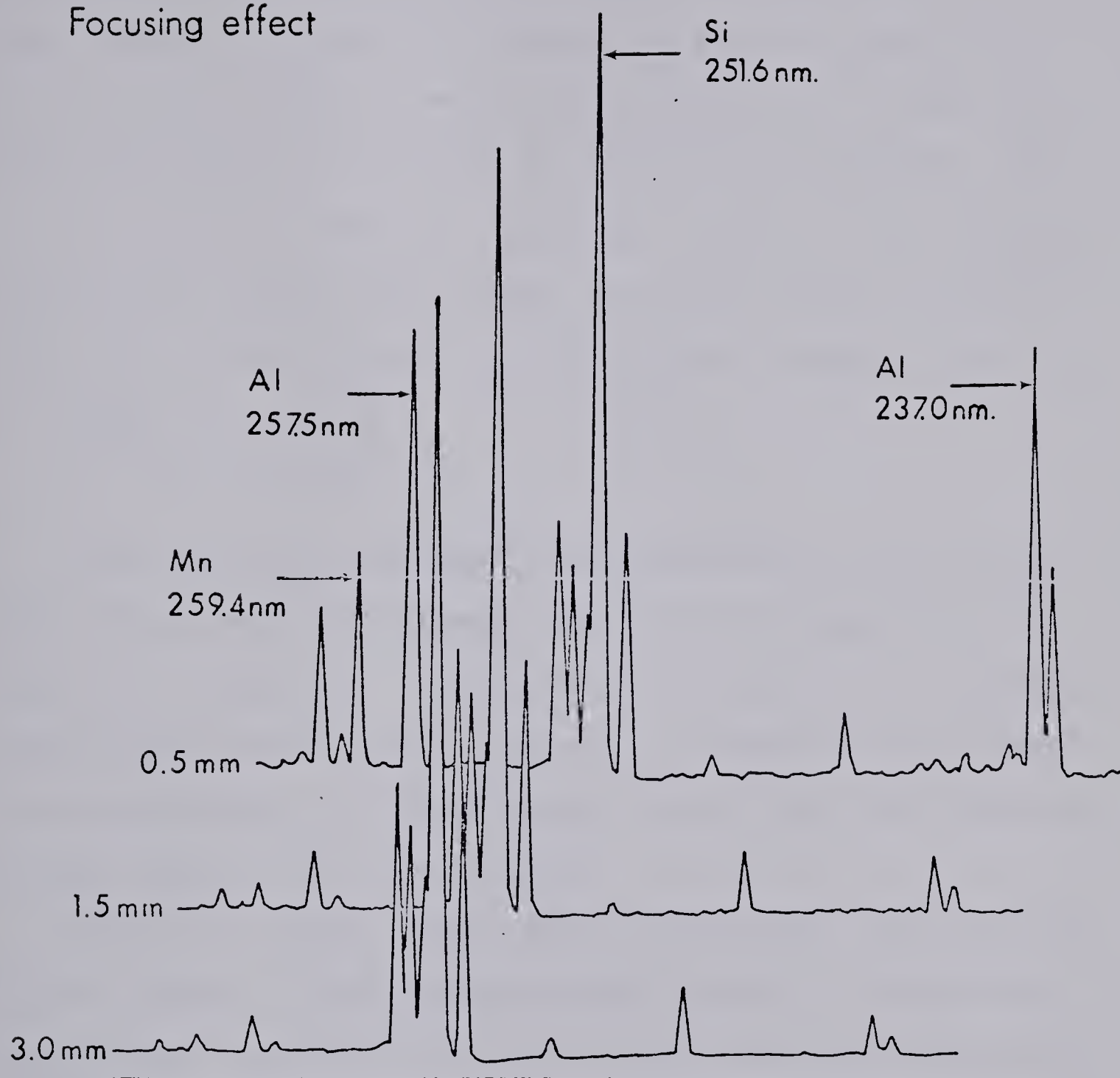


FIGURE 20. Effects of Focus on Aluminum Sample HG

seconds between the shots. The number of scans of sample and background were 100 at 0.1024 seconds each, with the background being subtracted from the sample spectrum for the final result. A sample determination was completed every 2.5 minutes to allow time to plot the data and to keep the repetition rate of the laser as constant as possible. For a large number of samples, and using ratios of many elements and emission lines, the overall precision of the system at this point ranged from 3% to 10% with an average of 5%.

C. Plasma Conditions

1) Introduction

The inductively coupled plasma excitation source has been extensively investigated (69,70) with regards to its operating parameters. It was not the intention to reinvestigate these parameters but rather to determine what effect the introduction of a solid sample could have upon them and to what degree they were altered.

Areas of interest were height of emission and flow rate of the aerosol. These subjects were studied to determine the optimum conditions for laser solid sampling into an ICP. Previous studies of the plasma have investigated in detail topics such as the effect of R.F. power and the effect of flow rate of the coolant gas. It was felt that the ICP would perform the same with respect to these last parameters and only factors that may be affected by the sampling process were of interest.

2) Height of Observation

It has been determined that the emission lines of various elements have optimum viewing regions at different locations in the plasma (70). An area of observation can be chosen that will deliver reasonable results for all elements concerned. If a fairly long region of the plasma is observed there will be no problem with spatial emission. However, with the four to one image reduction and the 0.43 mm (.017") high diode array used in the experiment the area of observation was a rectangle 0.4 mm wide and approximately 1.6 mm high. With an observation area this small, it is possible to obtain different results depending on the region of plasma observation; therefore it was necessary to seek a position where a good signal for all of the emission lines of interest could be obtained.

A good height for observation in the plasma for solution samples has been determined to be from 18 mm to 20 mm above the load coil. To determine the best viewing height for the transient laser signal, a region 6 mm in length centered 19 mm above the load coil was investigated. The array was positioned at 16 mm and moved up in 1.5 mm intervals to obtain five different regions of observation. Ten spectra consisting of 100 scans, two laser shots eight seconds apart and 100 scans of subtracted background were taken at each position. As before, the wavelength studied was from 282 nm to 305 nm.

The intensities of the emission lines studied varied with position of observation as reported in the literature. The precision of peak height was measured for the ten spectra taken at each position and the result found to be the same in all of the positions, approximately 3% to 10%. This indicated that while peak height was dependent on the region of observation, the precision was not.

Emission lines of the elements of interest for this particular experiment, the silicon, magnesium and manganese lines in the wavelength region from 282 nm to 305 nm, were compared to determine the optimum region for the observation of their emission. Peak heights of similar size will reduce measurement errors, so a region where the peak heights were most similar, 18 mm above the load coil, was chosen.

It was felt that the precision of the laser vaporizer/ICP system could still be improved beyond the 5% average now attained. To determine if the small region of observation of the 0.43 mm high diode array was responsible for a part of the loss in precision, the change in the maximum emission intensity of an aluminum or magnesium line versus time and height above the load coil was studied. The shock of the high speed introduction of the expanding sample plume into the plasma could lift the plasma similar to an auxiliary gas and change the position of observation, thereby changing the ratio of emission intensity.

A vertical 256 element diode array similar in all

respects except sensitivity to the 1024 element horizontal diode array was used to examine the plasma for changes in the maximum emission position during sampling. Due to the reduced sensitivity of the older 256 element array, the study was completed on the intense aluminum and magnesium lines located at 309.3 nm and 279.6 nm respectively. The plasma was observed approximately 0.0, 0.5, 1.0, 1.5, 2.0, 3.0 and 4.0 seconds after emission had begun.

As expected, the aluminum and magnesium lines were found to have maximum emission at different heights above the load coil, but there was no deviation in the position of maximum intensity with respect to time. In Figure 21 a comparison of normalized aluminum peaks is shown and the lack of difference in shape and position of maximum can be seen.

The expansion of the laser sample plume into the plasma seems to have little effect on the emission position of the elements in the plasma. The sampling process does not disturb the plasma and in this respect is not responsible for a decrease in precision of the laser vaporizer/ICP solid sampling system.

3) Flow Rate of Aerosol

A comparison of several aerosol flow rates from 0.5 to 5.0 L/min was completed. As a general trend, the increase in flow rate resulted in a reduction of time the sample spent in the plasma as well as a reduction in signal intensity. This fact could be useful in reducing the emission intensity of some lines, but it was found that neutral density filters

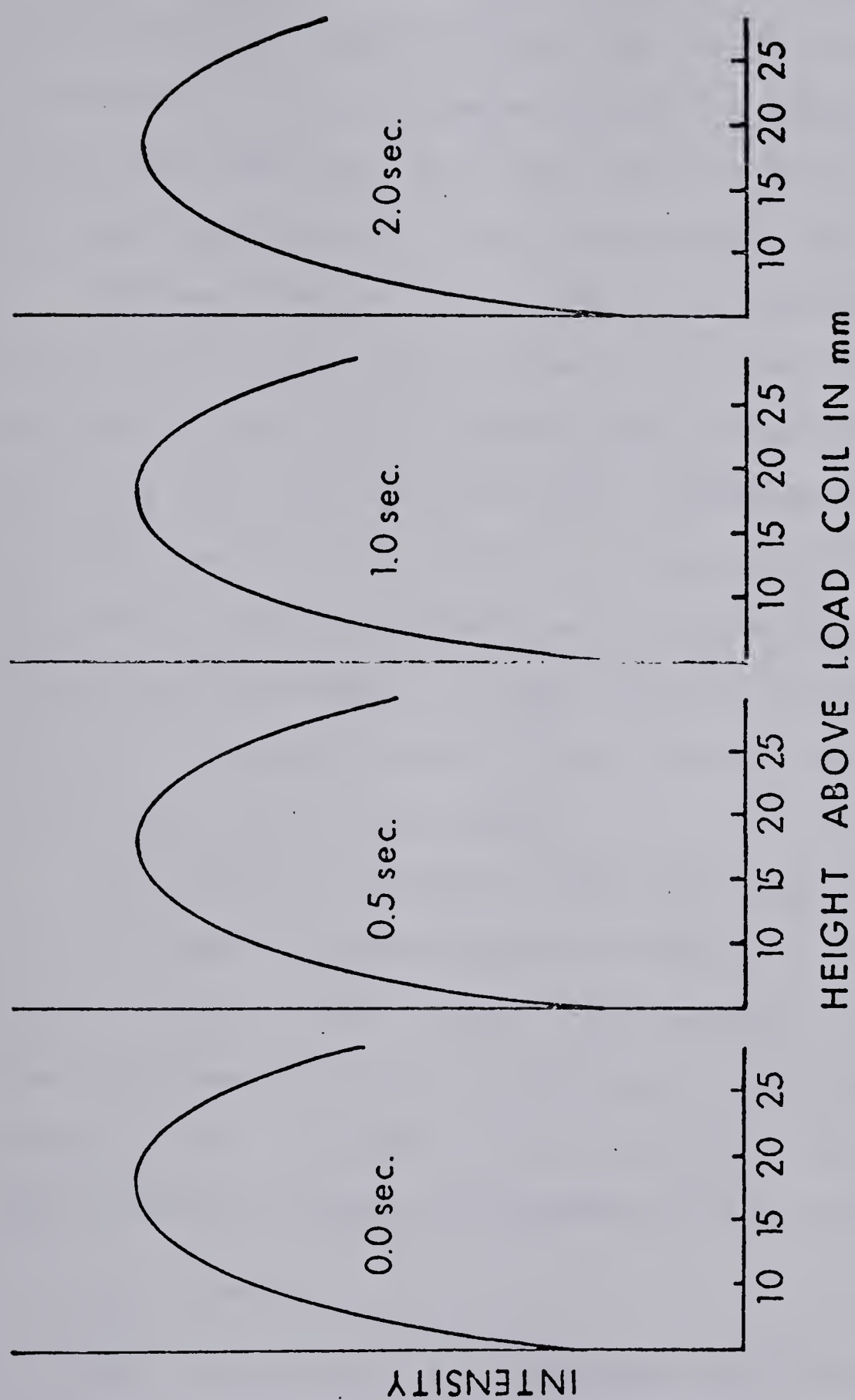


FIGURE 21. Vertical Emission Profiles of Aluminum
as a Function of Time

could be used much more reproducibly.

From the investigation, it was found that the aerosol flow rate can slightly change the position of emission in the plasma. Visual examination of the sample chamber indicated that the flow rate made little difference in the amount of sample material that was transferred into the plasma.

Without further investigation it was decided that the flow rate of the aerosol acted in the same manner for both the solid sampling and liquid nebulizing systems. The aerosol flow rate was controlled by a Matheson 603 Rotameter to 1.0 L/min with 10% precision. It was felt that if the flow was controlled as precisely as possible, the height of emission would be steady. A flow rate of 1.0 L/min was chosen because it is the standard flow rate for the design of the torch used in the experiment.

If a problem remained with a flow rate controlled to 10%, it could be corrected by the use of a mass flow controller or a wider diode array. Unfortunately, at the time of the experiment it was not possible to take these additional steps and the remainder of the experiment was completed using the Matheson rotameter for aerosol gas control.

4) Summary

The solid sampling laser vaporizer/ICP system has no effect on the operating conditions of the plasma. The best performance was obtained when standard conditions for solution nebulization were followed. No improvement was seen

over the 5% average precision already achieved before the experiment. It can be assumed that for plasma systems other than the one used in this experiment, the optimum conditions for solid sampling are the same as those for solution sampling.

CHAPTER VI

ANALYTICAL RESULTS

A. Introduction

After the optimization and initial characterization of the laser vaporizer/ICP system was completed, the analytical capabilities of the system were assessed. For the majority of the work, the previously discussed region from 305 nm to 282 nm was investigated. Analytical calibration curves based on ratioed intensities of silicon, magnesium and manganese signals have been obtained and the precision, accuracy and analytical properties of the system summarized.

B. Aluminum Samples

As noted previously, aluminum samples with both high and low amounts of trace components were examined. In the alloy with a large percentage of trace components, eight samples were used and six calibration curves obtained. These curves consisted of ratios of Si/Mg, Mn/Mg and Mn/Si lines; three of which were produced by the free running laser and three produced by the Q switched laser. The comparison between Q switched and free running mode was made in an attempt to obtain the most linear calibration curve.

The three high alloy curves for the free running mode are shown in Figures 22, 23 and 24 and the statistical results are collected in Table 14. For the high alloy Q switched samples, the calibration curves can be seen in Figures 25, 26 and 27 with the statistical results also listed in Table 14.

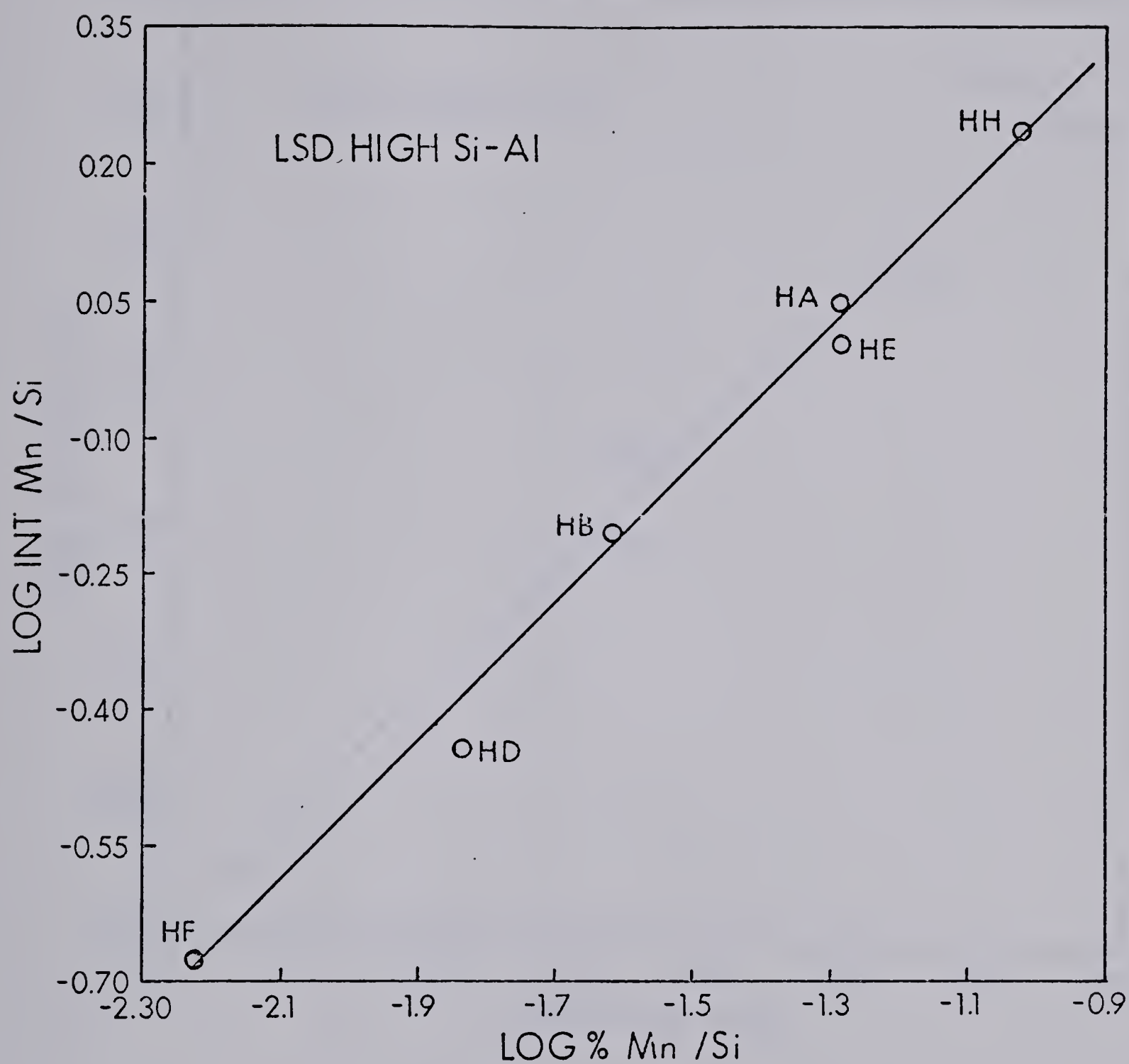


FIGURE 22. Calibration Curve of Mn/Si in the Free Running Mode

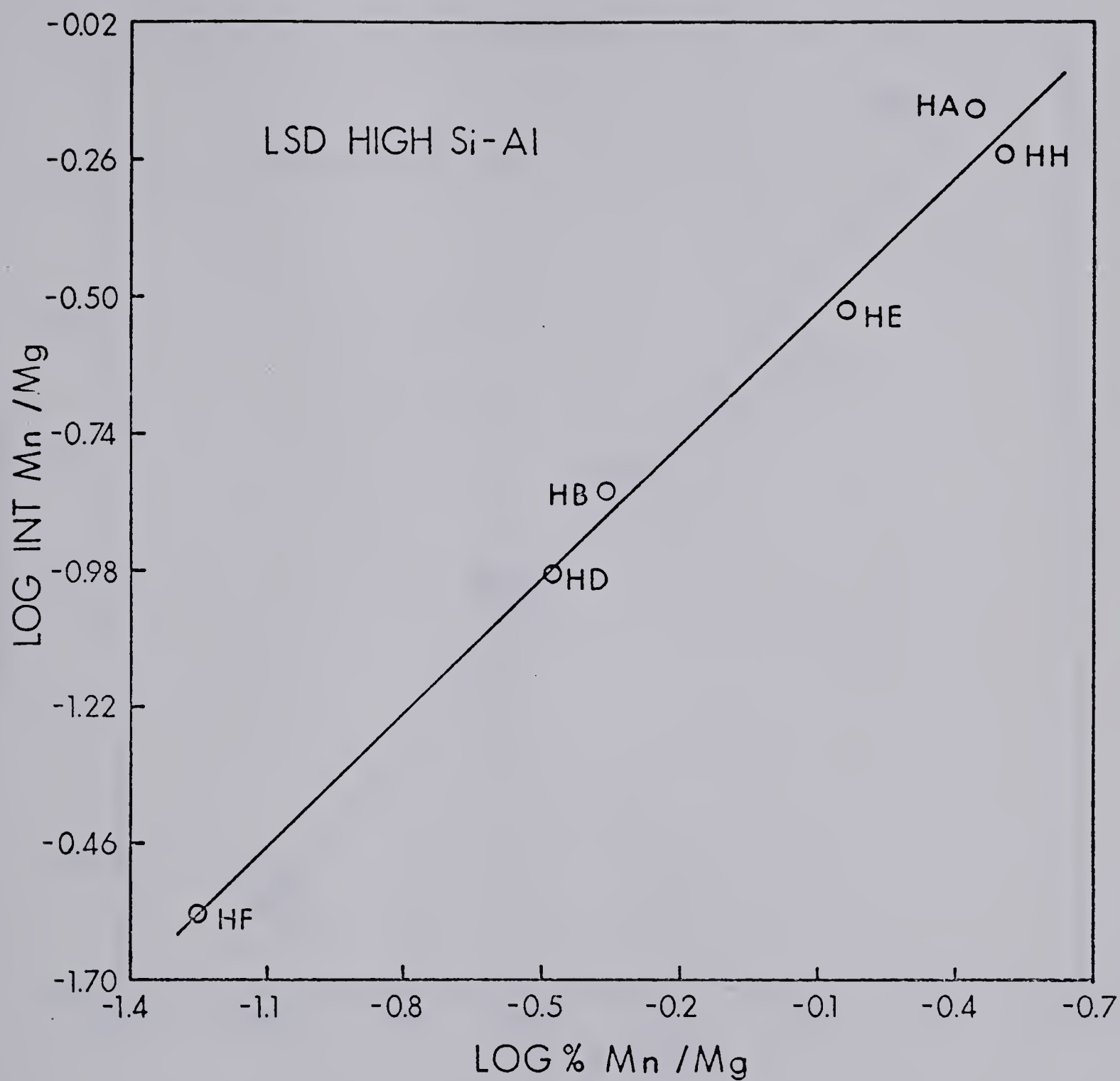


FIGURE 23. Calibration Curve of Mn/Mg in the Free Running Mode

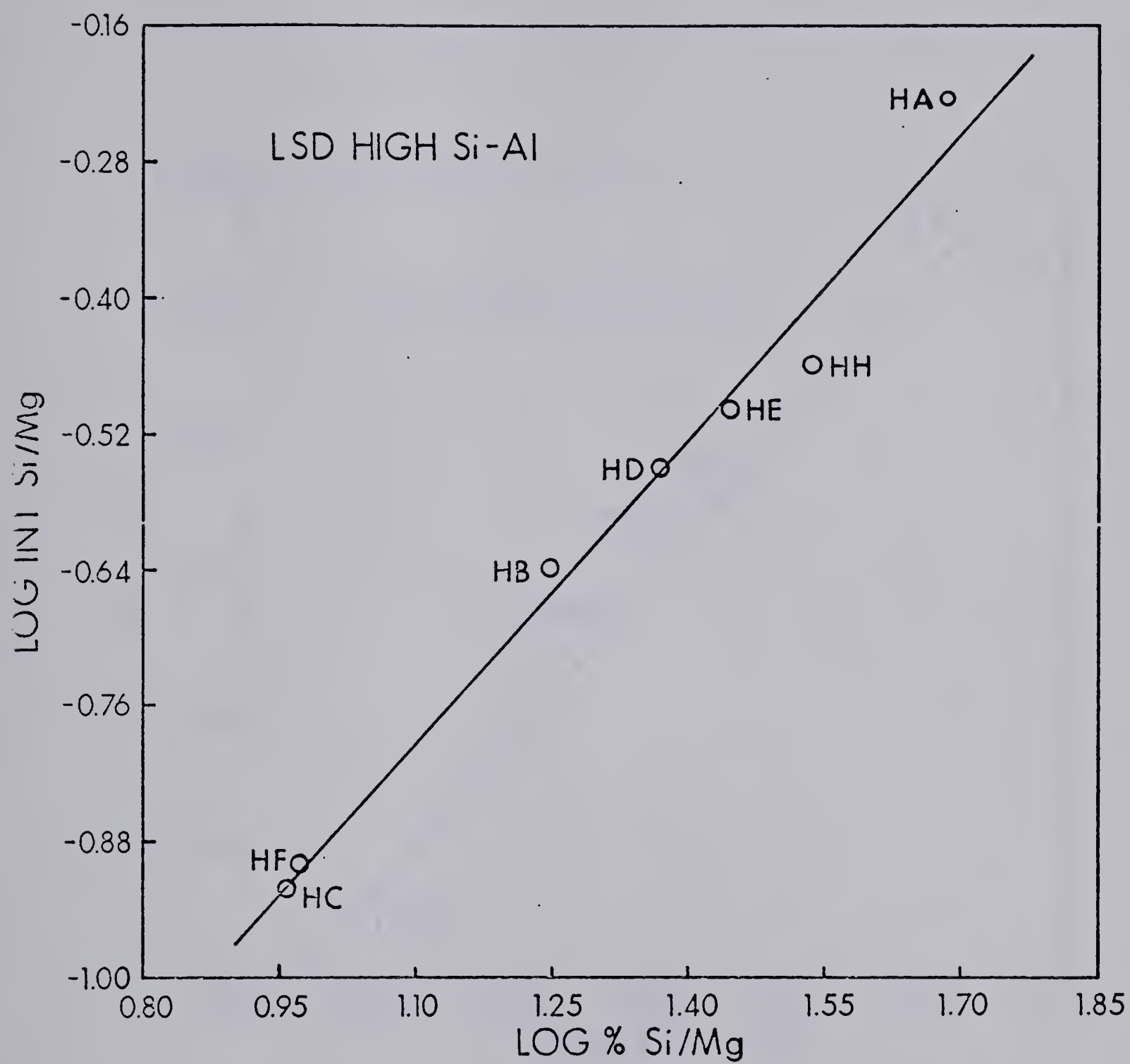


FIGURE 24. Calibration Curve of Si/Mg in the Free Running Mode

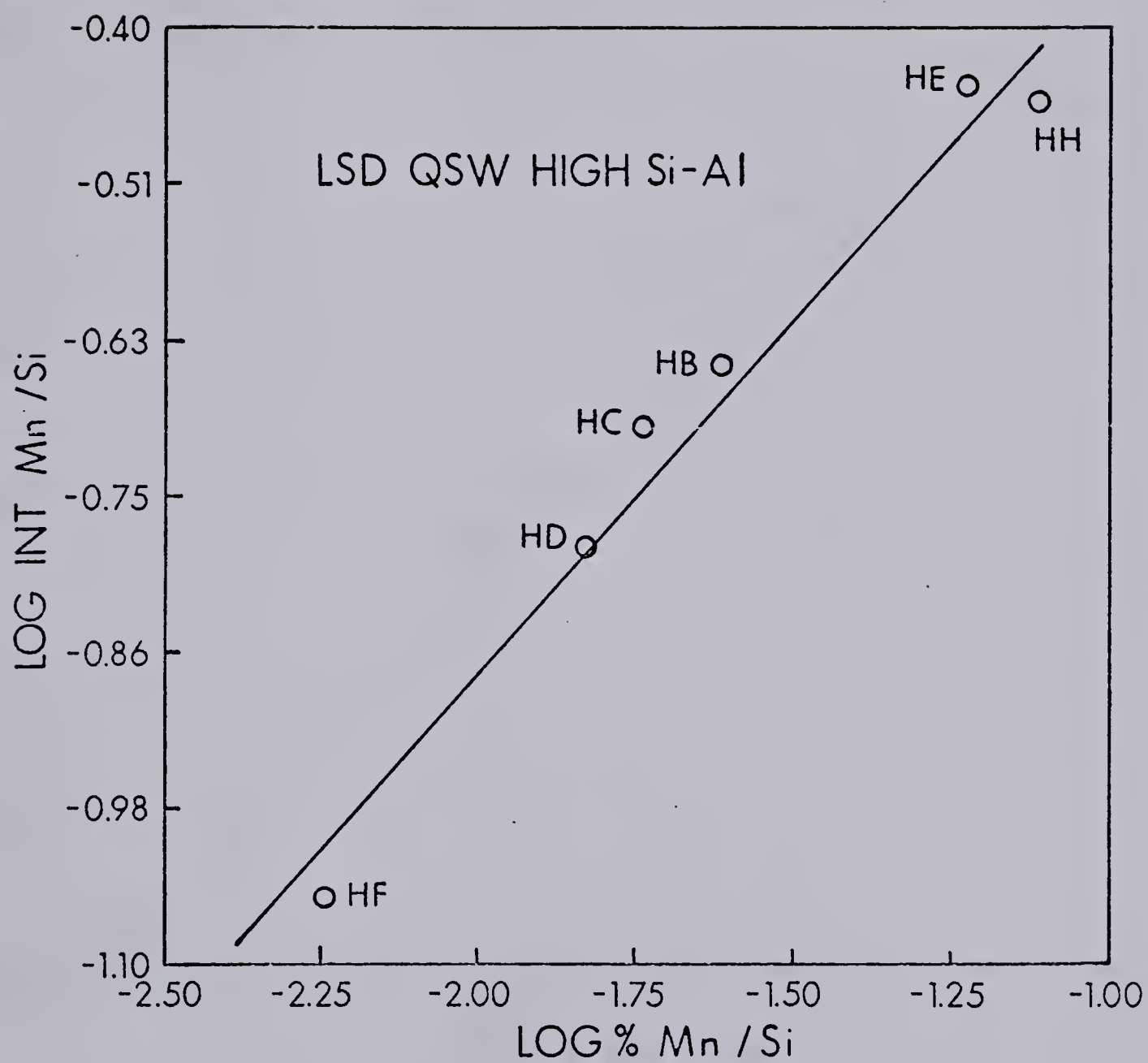


FIGURE 25. Calibration Curve of Mn/Si in the Q
switched Mode

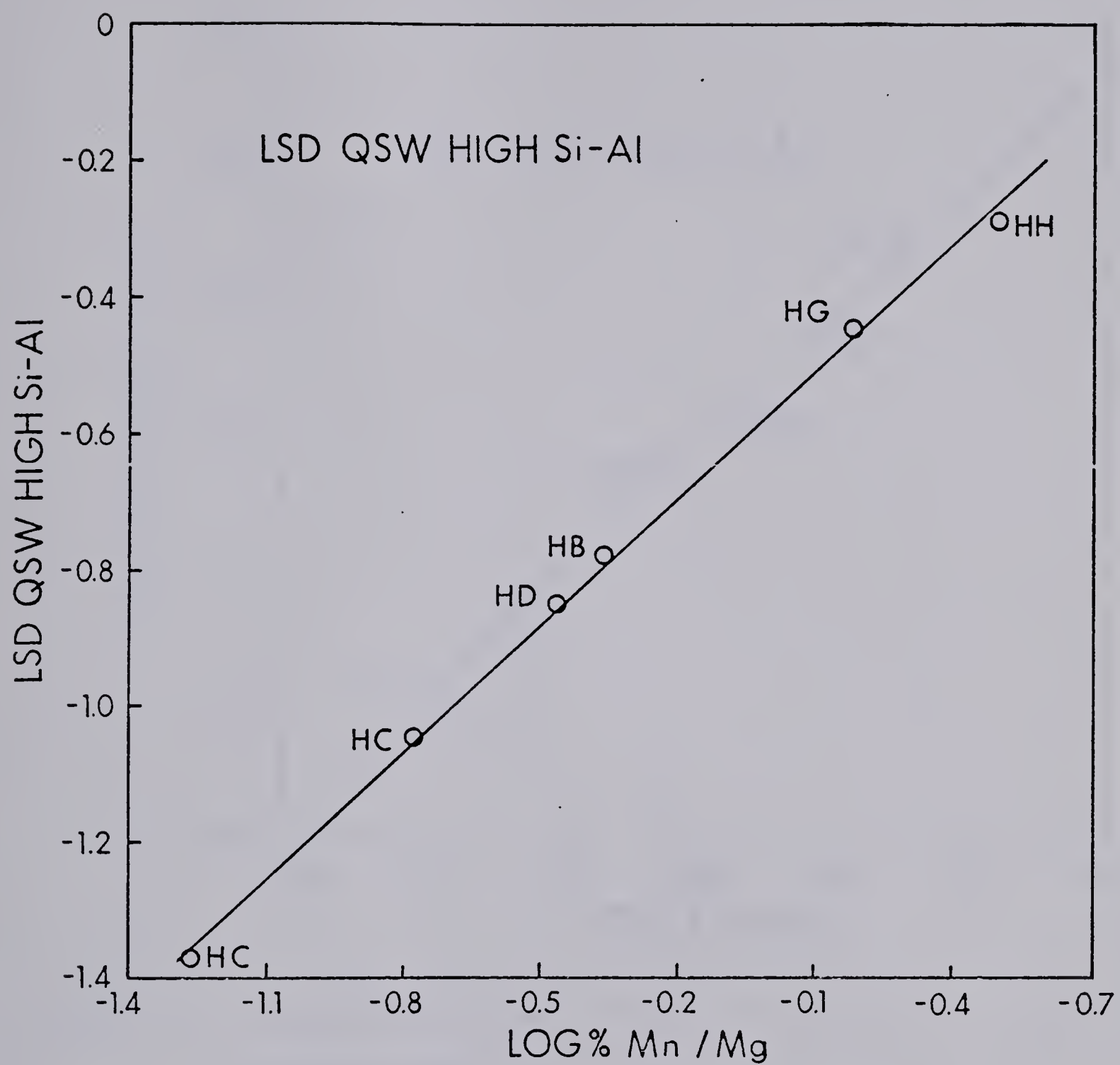


FIGURE 26. Calibration Curve of Mn/Mg in the Q
switched Mode

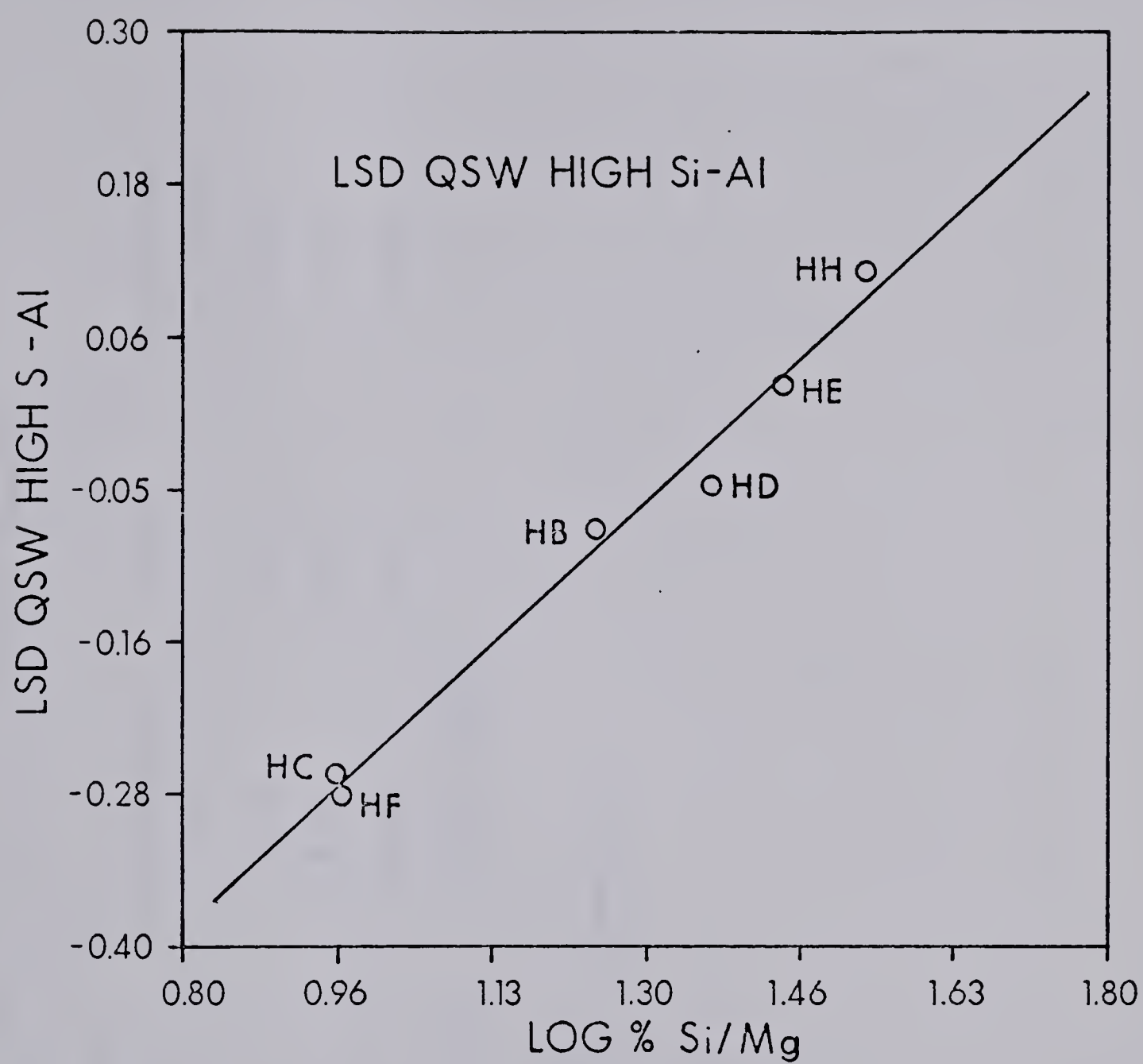


FIGURE 27. Calibration Curve of Si/Mg in the Q
switched Mode

TABLE 14
Statistical Data for Aluminum Samples

Ratio	Free Running		Q Switched	
	Slope	Correlation	Slope	Correlation
Mn/Si	0.764	0.9930	0.685	0.9891
Mn/Mg	0.837	0.9786	0.594	0.9908
Si/Mg	0.868	0.9857	0.526	0.9695
Mg/Al [*]	0.483-1.03	0.9211-.9966		

*Free running only, ranges given

In the comparison of free running versus Q switched operation, the free running laser was found to produce calibration curves with slopes slightly closer to unity but because of the small number of samples no conclusive result was obtained. Both modes of operation have similar correlation coefficients (the correlation of the points to the line) and no great advantage of either system was found. For reasons discussed previously, the free running mode remained the method of choice.

Analytical data, when plotted on a log concentration versus log intensity plot, will produce curves with a slope of one if there are no interfering conditions such as self absorption or matrix effects. Examination of Table 14 reveals slopes of the analytical curves to be between approximately 0.5 and 1.0 for all of the samples and modes used. The plasma as an emission source has been shown to be relatively free of self absorption effects therefore some other explanation of the nonunity slopes must be found.

An examination of the literature (38,71,72) shows that other authors using laser vaporization have obtained calibration curves with slopes between 0.75 and 0.50. As these results were obtained from examining the sample plume alone it was assumed that the nonunity slopes were due to self absorption. Since the same results are obtained when the laser vaporizer is coupled to an ICP source it is unlikely that the slope is due to self absorption but due instead to some aspect of the sampling process produced by the laser itself. It is possible that the changing matrix of the samples could be responsible

for the slope of the line.

The aluminum samples with only trace amounts of alloyed materials should have similar matrix characteristics in all six samples studied. These samples were examined by comparing the strong emission line of the trace element magnesium at 279.5 nm with the weak aluminum line located at 266.1 nm. The calibration curve (Figure 28) has a slope of .483 (Table 14) and shows a large amount of curvature even in a log log plot. If the lower concentration samples are removed from consideration, the slope improves from 0.483 to 0.618 with the removal of LB (Figure 29), from 0.618 to 0.773 with the removal of LH (Figure 30) and to 1.03 with the removal of LC.

To discover if the curve was reproducible, the experiment was repeated several times. The same results were produced each time. In the low concentration region, the curve becomes almost flat, indicating enhanced emission for the trace elements. However, Osten and Peipmeier (51) have reported similar sloped curves when the laser plume is examined for atomic absorption. It would seem that the curve is a result of the sampling process as well. The slopes obtained with the laser vaporizer/ICP system show an improvement over the 0.75 to 0.50 range reported previously. This improvement in slope may be explained by the additional vaporization and excitation power of the ICP over other previously used sources.

The curves of the upper and lower concentration ranges of the aluminum samples may be coupled to produce an S shaped curve. This type of curve could be indicative of the sampling

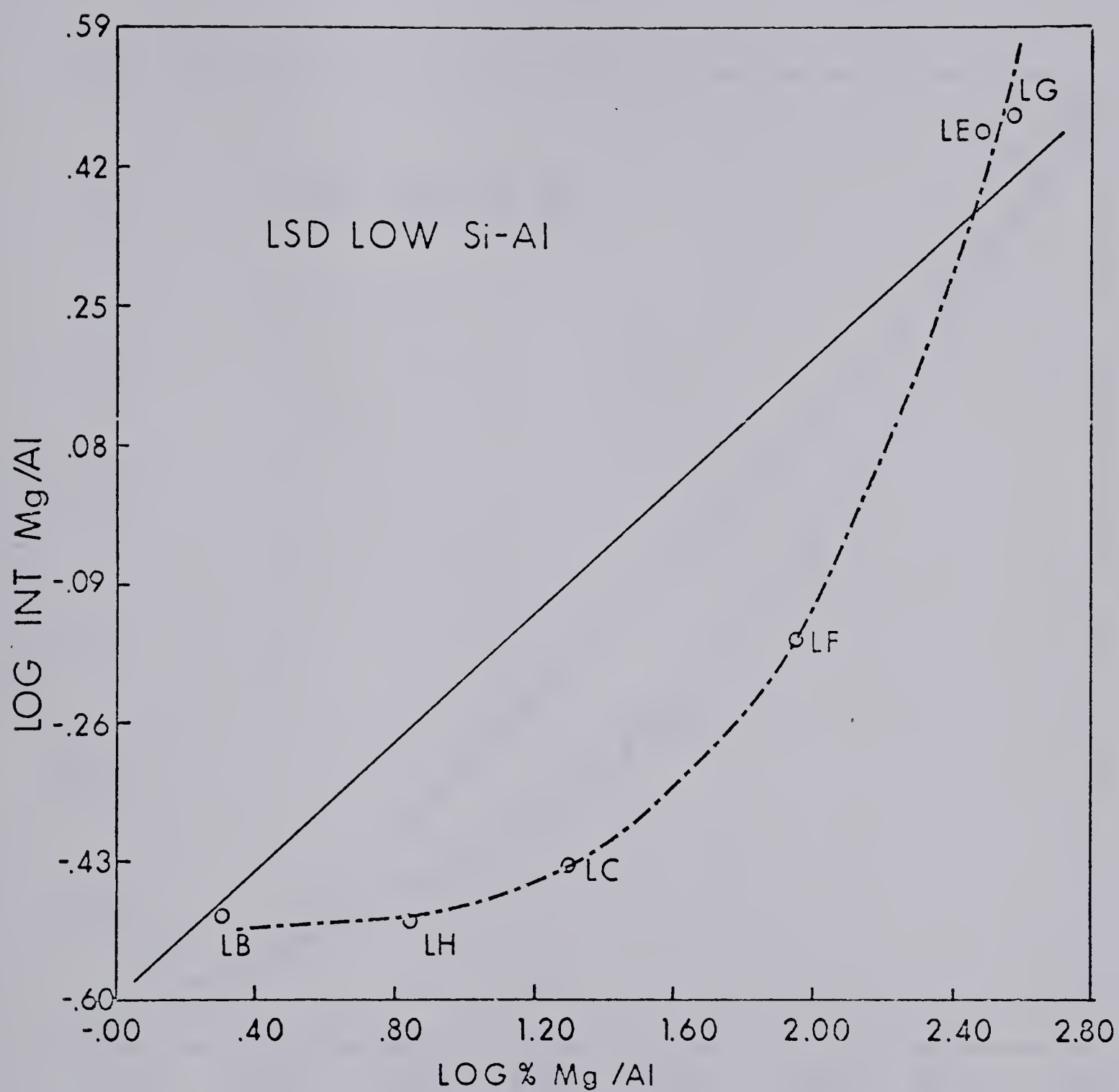


FIGURE 28. Calibration Curve of Low Alloy Aluminum
Samples with all Points Included

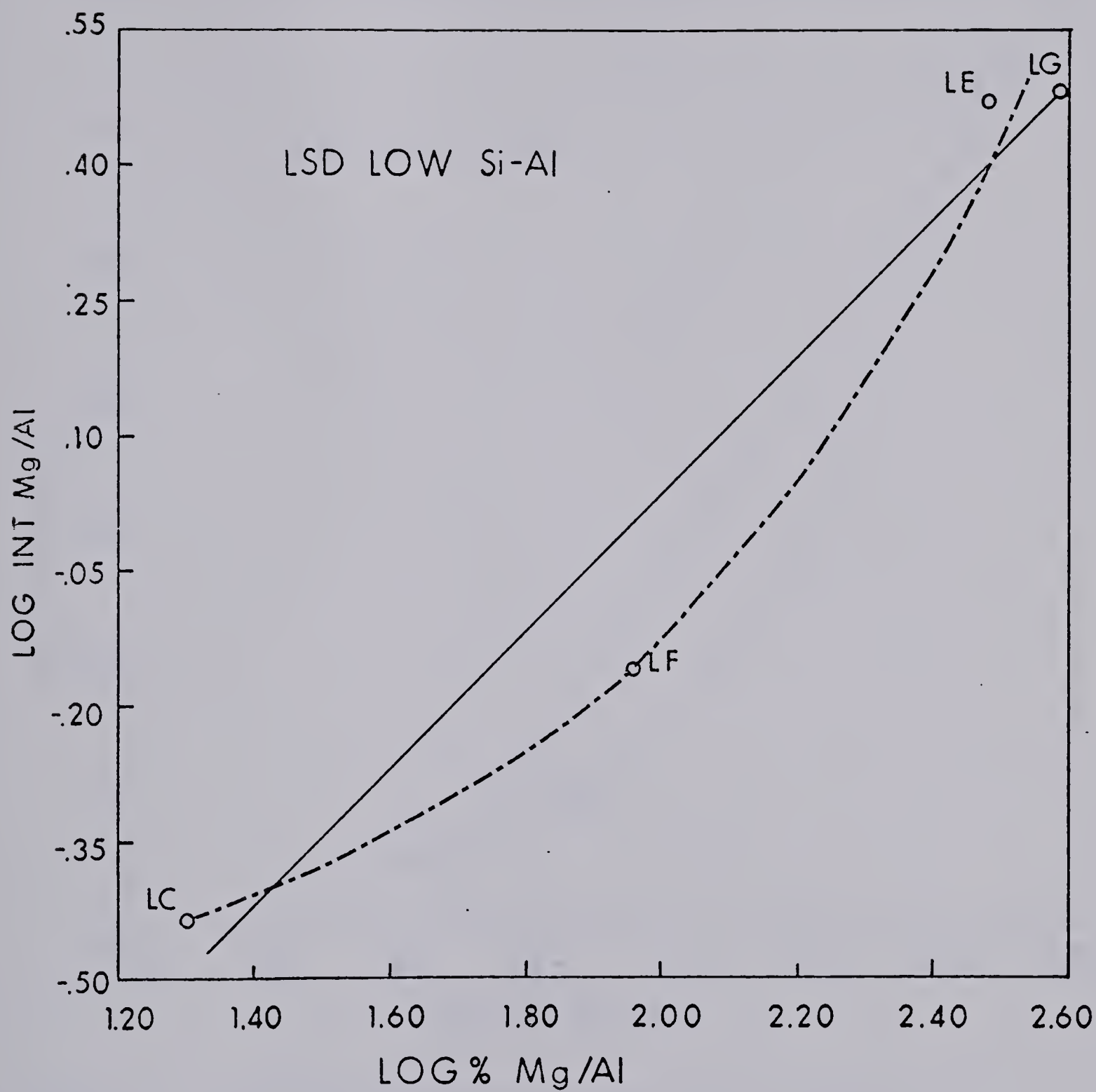


FIGURE 29. Calibration Curve of Low Alloy Aluminum
Samples with LB not included

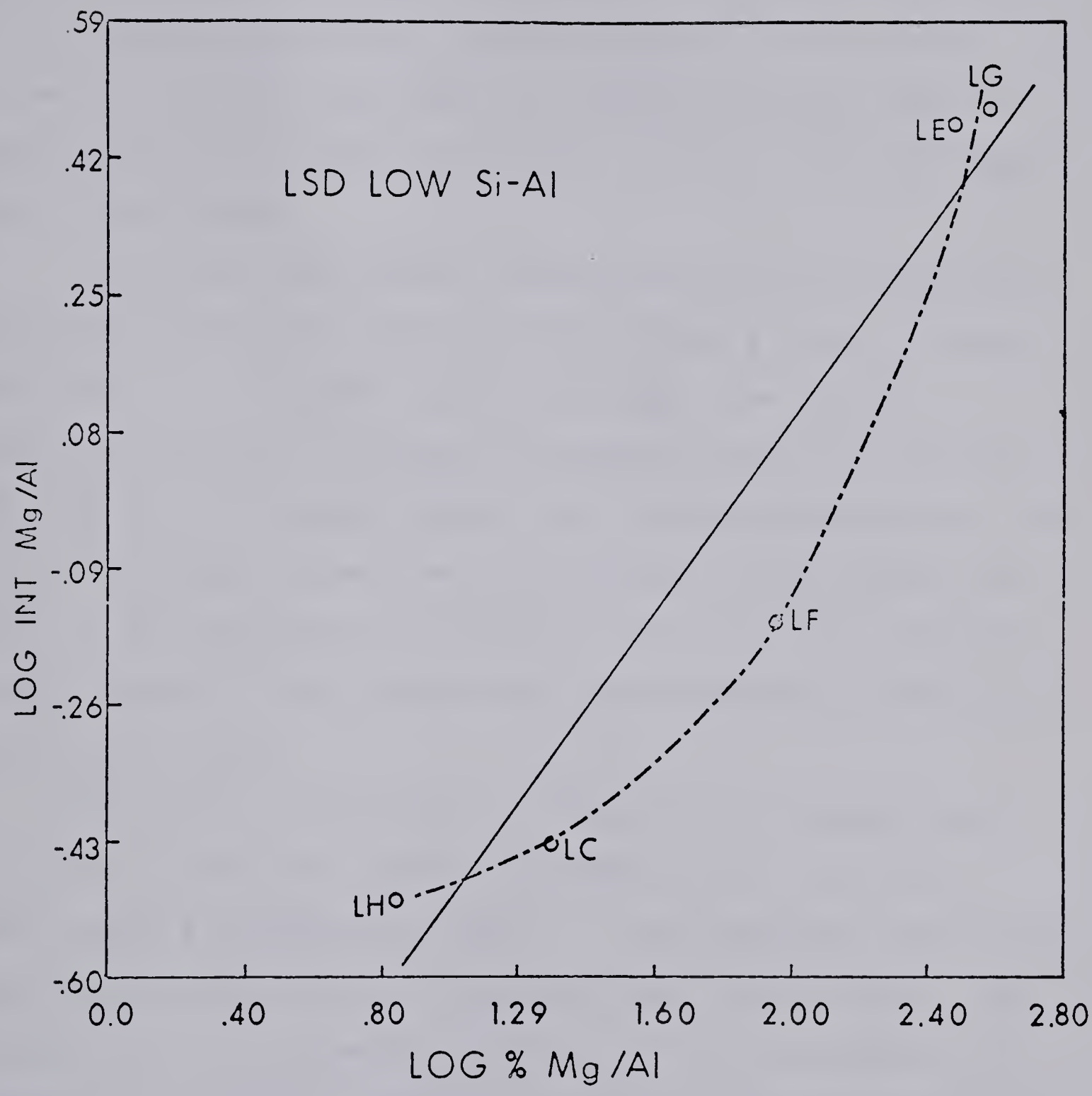


FIGURE 30. Calibration Curve of Low Alloy Aluminum
Samples with LB not Included

method of the laser, but at this point there is no direct evidence to support a curve of this shape over a large concentration range. It may not be valid to compare the ratio of the Mg/Al lines to the ratio of Mg/Mn or to any other element. To fully understand the sampling process and the shape and slope of these analytical curves, a detailed study must be performed.

Fortunately analytical information can be obtained from nonunity curves with little problem except a slight loss in precision. As the slope approaches zero, the difference in distance on the graph between two samples of different composition becomes smaller and the measurement error increases in size. This loss in precision is not serious except in the low concentration end of the low alloy aluminum sample curve; in that region only semiquantitative determinations can be made.

For a free running laser, the precision obtained over a period of 500 shots was in the order of 5% (Table 15). Each number represents the RSD of a sampling run of ten individual spectra for the emission lines of interest. This overall accuracy compares favorably with or is superior to previous techniques. Figure 31 displays the type of precision obtainable when the system is optimized and a homogeneous sample is investigated. Overall results showed that complex sampling processes are occurring but the system can be used successfully and the sampling effects disregarded if suitable standard curves are used.

TABLE 15

RSD of Peak Heights for Various
Samples and Ratios

Sample	Mn/Si (%)	Si/Mg (%)	Mn/Mg (%)	Mg/Al (%)
HA	1.79	2.29	3.26	-
HB	2.05	5.81	6.50	-
HC	5.44	4.53	1.74	-
HD	4.28	7.94	4.00	-
HE	4.15	4.09	7.45	-
HF	5.98	5.32	2.87	-
HH	5.16	9.40	6.90	-
LB	-	-	-	3.12
LC	-	-	-	5.89
LE	-	-	-	5.72
LF	-	-	-	1.64
LG	-	-	-	8.63
LH	-	-	-	3.12
Average	4.12	5.61	4.67	5.17

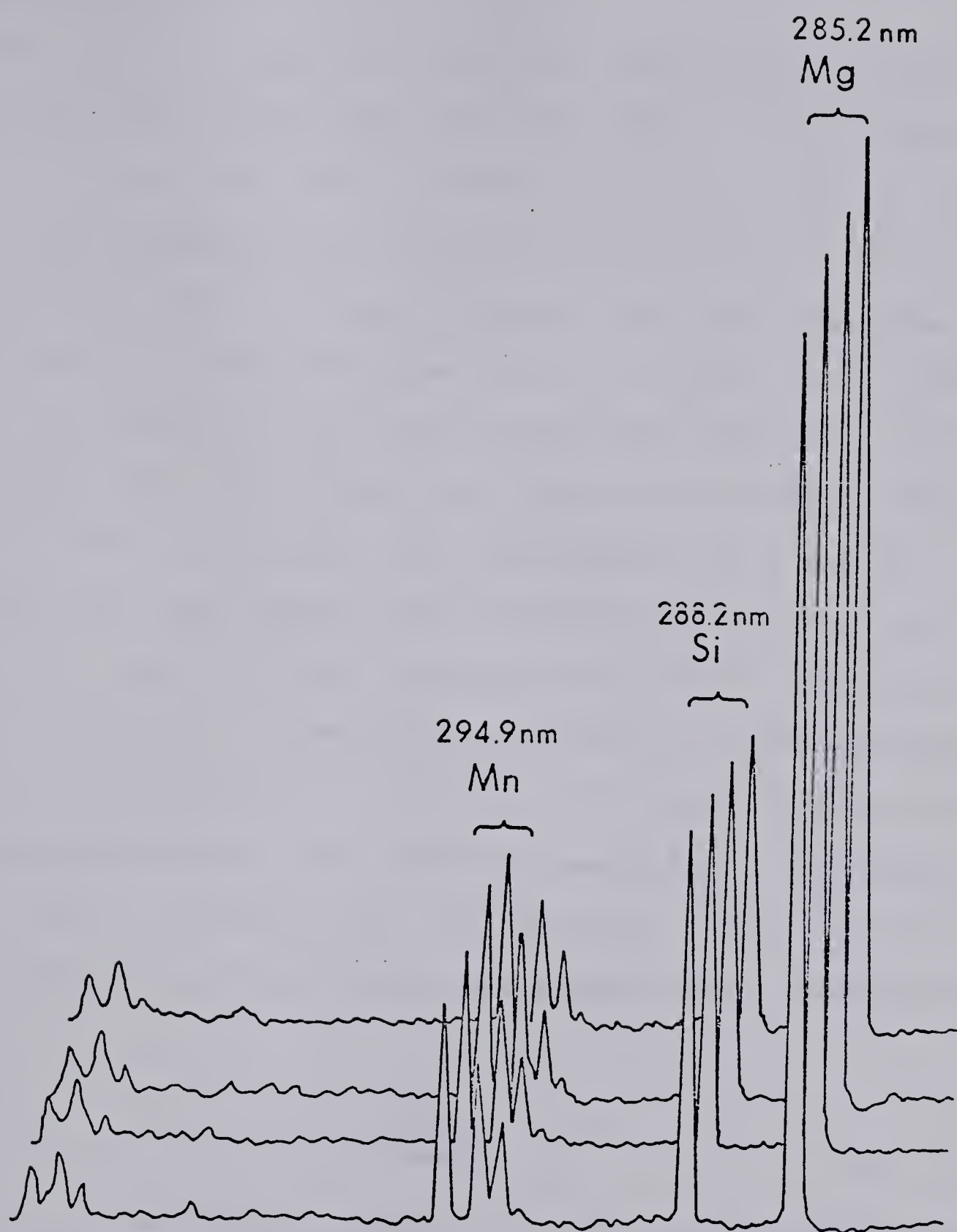


FIGURE 31. Spectra showing the Reproducibility that can be Obtained with Homogeneous Samples

C. Detection Limits

An important figure of merit for an analytical system is the magnitude of the smallest detectable level of an element. A system with 100% accuracy and precision is of little use if the elements that are being determined are present below the detection limit. In this respect, the laser vaporizer/ICP system excels by producing low detection limits for a large number of elements. Many other techniques have lower detection limits than this system, but these other methods are expensive, difficult or can only determine a few elements.

The detection limits were estimated by comparing the height of a peak of known concentration with the size of the background noise. The minimum detectable peak was defined according to convention as twice the standard deviation of the background level. The standard deviation of the background can be estimated with good accuracy as 0.20 of the peak to peak distance of the background signal (74). Using the formula

$$D_L = \frac{2C\sigma_B}{\text{Signal}} \quad 6-1$$

where D_L is the detection limit, C is size or concentration of the sample introduced (found by weighing in this case), σ_B is the standard deviation of the background and signal is the intensity of the signal in units similar to σ_B . In this case the units for σ_B and signal were mm, taken directly from the spectrum. D_L is in the same units as C (grams).

The detection limits for several elements in both the

free running and Q switched mode were calculated (Table 16). These results can be compared with other methods listed in earlier tables. The lowest detection limit obtained was 0.55 pg for magnesium when sampled in the Q switched mode. As mentioned earlier, the signal level for the Q switched laser is smaller than for the free running laser when compared to similar background levels, however the sample size for the Q switched laser is significantly less; equation 6-1 takes the sample size into account. If the emission from the plasma increased linearly with sample size, the free running signal should be correspondingly larger than the Q switched signal. Since the detection limits are not the same, sampling can be said to be more efficient in the Q switched mode, but this increase in efficiency does not make up for the large increase in sample size of the free running mode. The actual percentage of a trace component that can be determined is lower for the free running mode because more of the trace element is introduced into the plasma. Sampling would be completed in the Q switched mode if the smallest possible sample size, such as in sampling of art objects, were desired.

It is interesting to note that these detection limits were obtained with a photodiode array. With the increased sensitivity of the PMT, detection limits two orders of magnitude lower would be obtained; this should be taken into account when comparing results to other techniques. The recent availability of diode arrays with increased sensitivity would also improve overall performance.

TABLE 16

Detection Limits for Selected Elements

Element	Wavelength (nm)	Q Switched Detection Limits (pg)	Free Running Detection Limits (pg)
Mn	294.9	1.3	15.5
Mg	279.5	0.55	6.0
Si	251.6	1.0	12.5
Zn	213.9	0.82	9.5
Cu	324.7	0.91	11.8
		Q switched Detection Limits (ppm)	Free Running Detection Limits (ppm)
Mn		0.057	0.031
Mg		0.024	0.012
Si		0.043	0.05
Zn		0.036	0.018
Cu		0.040	0.024

D. Brass Samples

The copper to zinc ratios of three brass samples were determined and produced overall results superior to that obtained with the aluminum samples. The slope of the analytical curve on a log-log plot was 1.07 with a correlation factor of 0.9921 (Figure 32). The reproducible curve indicates that the nonunity slopes for the aluminum samples may be the result of matrix effects of that alloy. Unfortunately, only three brass samples covering a narrow concentration range of copper and zinc were available. It is not known whether the slope would remain at one if the range of concentration was extended. The range of copper and zinc generally found in brass alloys is covered by the range used in the experiment, therefore the laser vaporizer/ICP technique is well suited to the study of these alloys.

The precision of the brass spectra ranged from 1.2% to 5.3%, with an average of 3.3% (Table 17). This is remarkable, not only because of the improvement over the aluminum alloys, but because these results were obtained with only six spectra per sample instead of the usual ten.

Since only three brass samples were available, it was not possible to obtain information on the accuracy of the laser vaporizer/ICP system for this alloy. The correlation factor can be considered an indicator of accuracy, assuming that future samples will behave similarly to the previous ones. In this case the correlation factor of 0.9912 is nearly as good as the best aluminum value, indicating an accuracy of

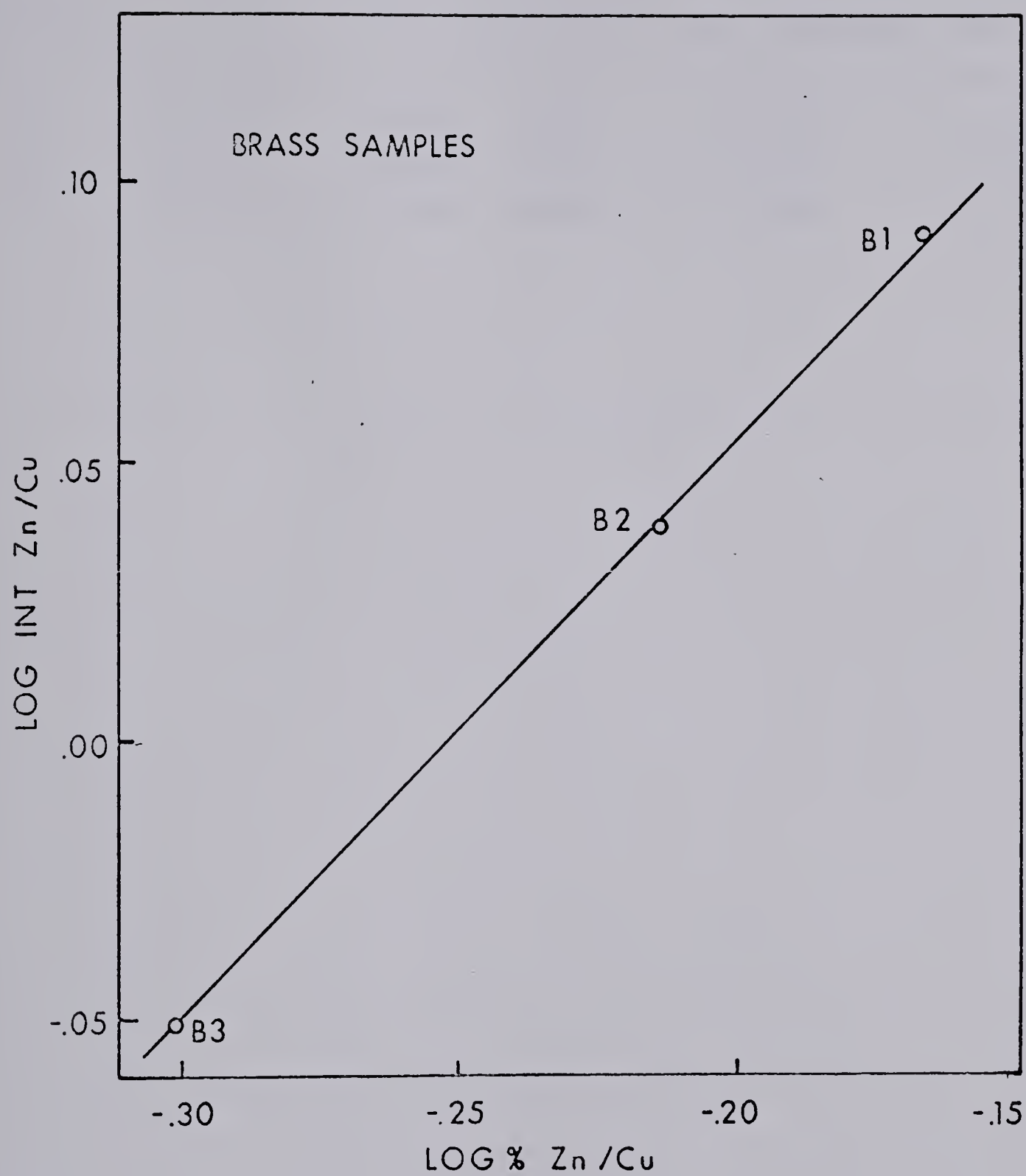


FIGURE 32. Calibration Curve for NBS Brass Standards

TABLE 17

Analytical Data For Brass Samples

Standard	% Zn/Cu	log %	Intensity	log Intensity	RSD
B1	0.6784	-.1685	1.233	0.0910	5.3%
B2	0.6100	-.2164	1.092	0.0382	3.31%
B3	0.4921	-.3080	0.8855	-.0528	1.2%

3% or better.

All of the other elements listed in Table 11 claimed to be in the NBS sample were positively identified in the brass spectrum. No quantitative information was obtained from these peaks but the analytical information was present. Figure 33 displays a typical spectrum of the NBS brass sample B1.

E. Nonconducting Samples

A qualitative study involving Philippine mahogany, Douglas Fir and spruce was completed using carbon as internal standard for wavelength calibration. Tentative identification was made of several trace elements including magnesium, iron, copper and calcium. Molecular bands of CO, NH and CN resulting from the wood sample also appeared in the spectrum and could possibly be used in obtaining the empirical formula of the sample.

A typical spectrum of mahogany covering the region from 240 nm to 290 nm is shown in Figure 34. The assignment of the lines is not absolute but positive identification could be made with the use of wavelength calibration standards. A good method for the inclusion of a standard would be to soak the wood in a solution containing a dissolved salt such as CuNO_3 . Comparison of the spectra with and without the copper standard could lead to the positive identification of the copper lines in the spectra.

Even though quantitative data has not been obtained, the

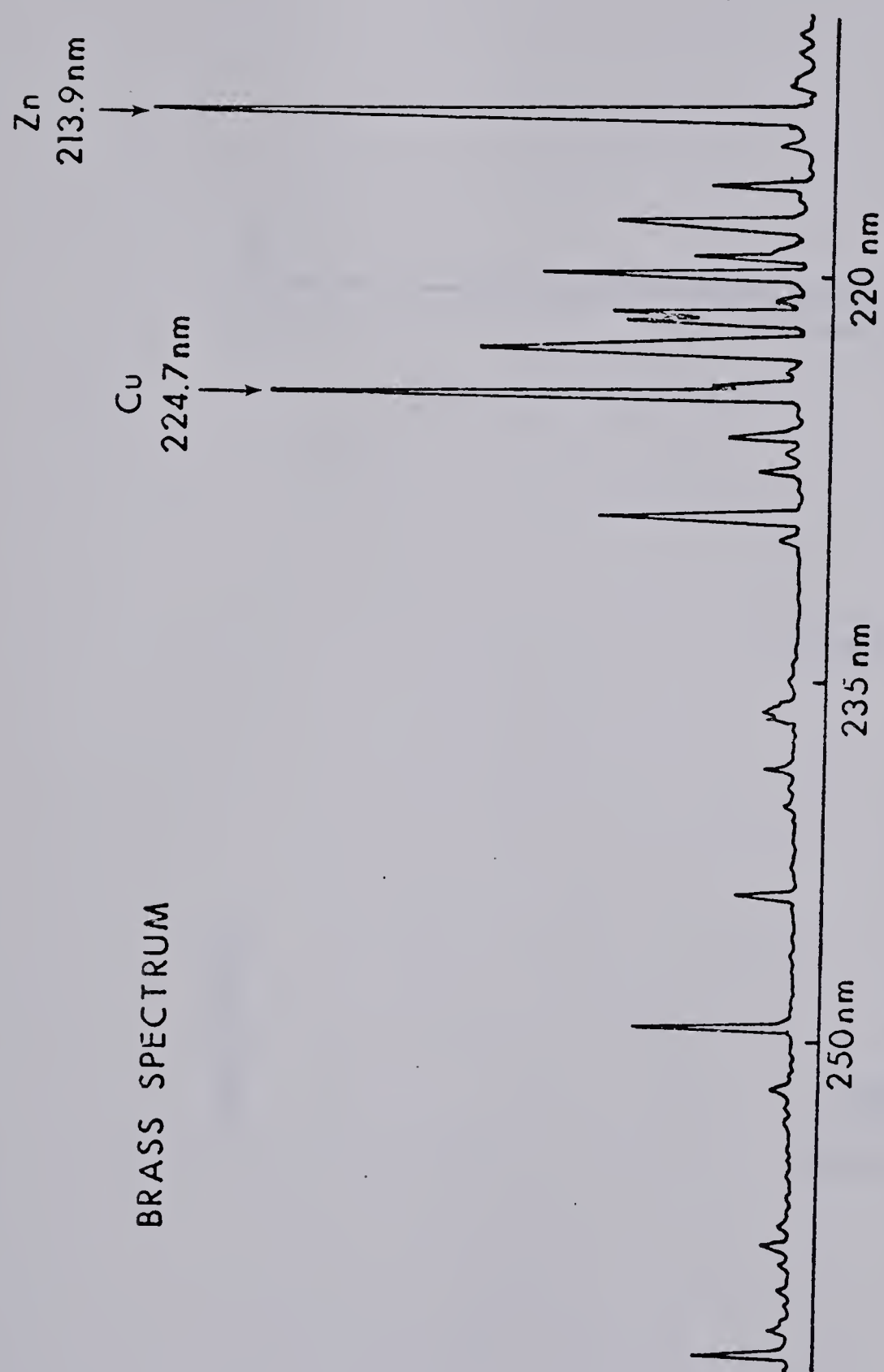


FIGURE 33. Brass Spectra

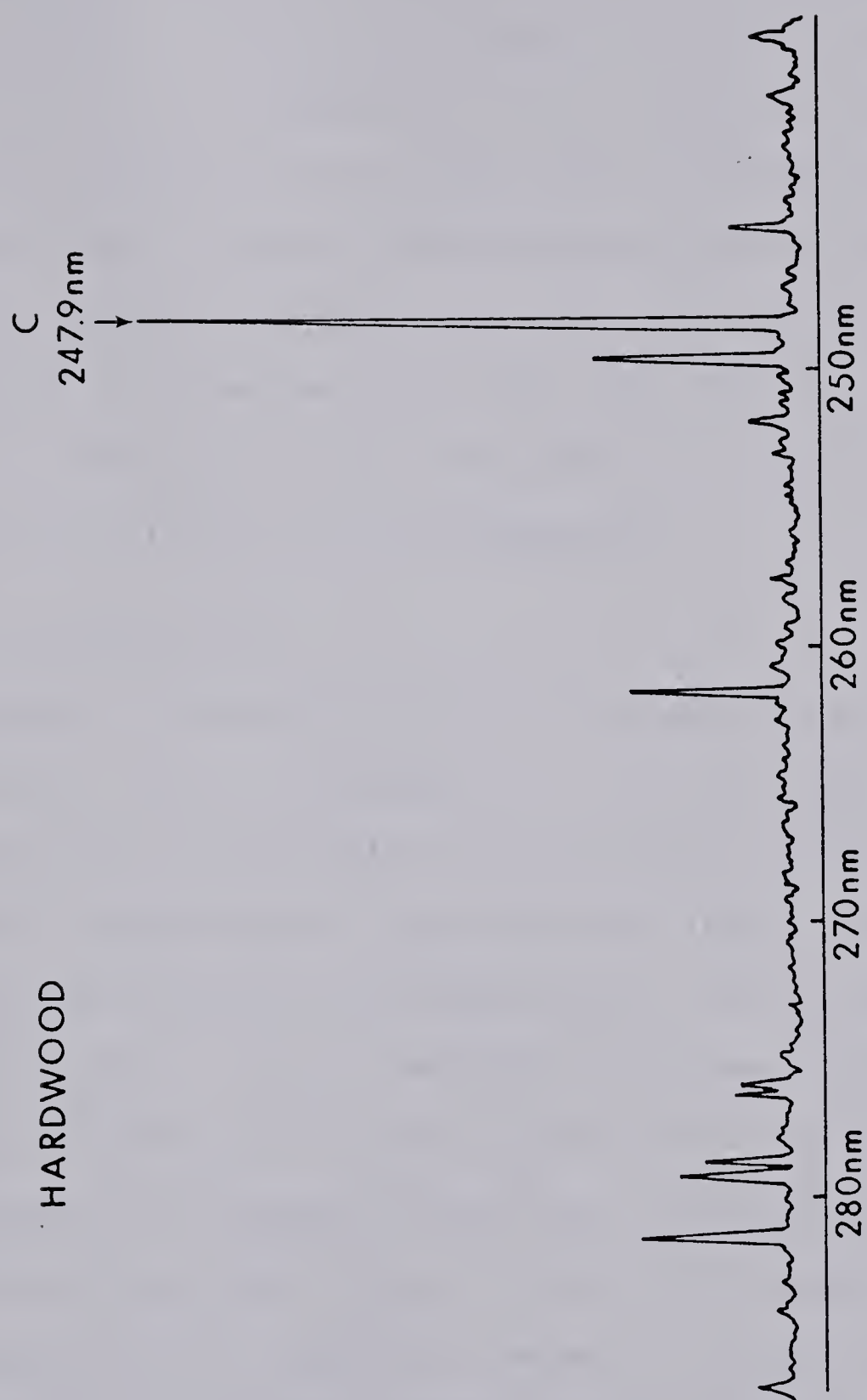


FIGURE 34. Wood Spectra

feasibility of investigating nonconducting samples has been established. It is reasonable to expect the same magnitude of detection limits and precision that can be obtained from the alloy samples. A possible problem in sampling nonconducting samples is the inhomogeneity of the material under study. In biological material such as wood the distribution and concentration of trace elements would vary within the cell but would remain constant from cell to cell. If the area sampled is large enough to cover several cells and the investigation is confined to one type of cell (eg. xylem or ploom) there should be little problem with inhomogeneity.

F. Sample Inhomogeneity

The largest remaining problem with regard to precision of measurement is sample inhomogeneity. In some instances, this can be as high as 20% (73) over an area as small as a laser crater. Examination of spectra will indicate the change of sample concentration as the sampling proceeds along the surface of an alloy. It is reasonable to expect random fluctuation in the spectra if random processes such as laser power fluctuation or plasma flicker were responsible for the error. Instead a gradual change in emission intensity can be seen, suggestive of a gradual change in concentration. Fifteen spectra of low alloy sample LD, listed in Table 18 show the gradual decrease in intensity of the magnesium lines from spectrum five to spectrum seven, a gradual increase from spectrum seven to spectrum ten and reasonably constant heights for the remainder of the peaks. The relative standard

TABLE 18

Sample Inhomogeneity: Measurement of Peak Heights

Spectrum	Height of Mg (mm)	Spectrum Number	Average	RSD (%)
1	103	1-4	103.2	0.87
2	102	11-15	103.2	0.87
3	104	5-10	87.66	6.8
4	103	overall	97.00	8.8
5	91			
6	86			
7	78			
8	84			
9	90			
10	97			
11	104			
12	103			
13	104			
14	104			
15	102			

deviation of peaks one through five and ten through fifteen is a respectable 2.1%. This is comparable to the best values possible with homogeneous samples. The overall relative standard deviation is 9.1%, comparable to other poor values obtained.

Unfortunately samples in nature have no inherent homogeneity and this aspect may limit the ultimate success of the system for sampling geological, biological or other solid samples. A solution to the problem would be to increase the number of samples taken. This would also increase the sampling time and defeat part of the purpose of the laser as a rapid solid sampler. A larger laser pulse capable of covering a region large enough to neutralize the effects of inhomogeneity would overload the plasma and a significant portion of the sample would be wasted. The solution with the most promise is a total consumption system using a CO₂ laser or other high power CW laser to totally vaporize a macro sample. If an integrating detector were used, the effects of selective volatilization often seen in conjunction with a CO₂ laser would be compensated for.

G. Conclusion

In a recent article (75) van Deijck et al. made an assessment of the laser microprobe analyser as a tool for quantitative analysis in atomic emission spectroscopy. The authors dissuaded readers from the use of the spark cross excited laser microprobe for quantitative analysis, citing poor overall precision (16%) and calibration curves with small slopes as reasons for their decision. From this experiment, it has been concluded that the ICP can be used in place of the spark source, resulting in an overall increase in performance. Precision of the laser vaporizer/ICP system is approximately 2% for homogeneous samples and generally 2% to 5% for other metal alloys. The calibration curves have slopes from 1.1 to 0.6 and while some of the curves are not linear, all can be used for analytical purposes. Performance equal to or better than arc and spark techniques can now be expected.

The laser vaporizer/ICP system also offers some unique advantages over previous techniques. Their favorable characteristics can be summarized in four points:

- 1) Ability to handle conducting or nonconducting samples
- 2) Little or no sample preparation
- 3) Short determination time
- 4) Good analytical results with detection limits, precision and accuracy comparable to the standard techniques of D.C. arc and A.C. spark. Through the use of internal standards, crater size and laser power fluctuations have been compensated for, causing an increase in the reproduci-

bility of the sample spectrum. The system is well suited to routine analytical investigations such as quality control but still has the ability to handle samples of unknown composition.

Improvements in lasers and operating procedures that will increase the general utility of the system can still be expected. The area of nonconducting samples including biological, geological and inorganic substances remains to be investigated. In spite of the research that remains to be completed the major goal, the ability to introduce solid samples into the plasma, has been achieved. The combination of a laser as a source of sample vapor and an ICP as a source of additional vaporization and excitation has proven itself a viable technique for the quantitative examination of all types of solid samples.

Bibliography

1. C.E. Harvey, "Spectrochemical Procedures", (Applied Research Laboratories, Sunland, California, 1950).
2. C.E. Harvey, "Semiquantitative Spectrochemistry" (Applied Research Laboratories, Sunland, California, 1964).
3. R.M. Barnes, ed., "Emission Spectroscopy", (Halsted Press, Stroudsburg, Pennsylvania, 1976).
4. C. Alkemade, Appl. Opt., 7, 1261 (1968).
5. B.V. L'vov, Spectrochim. Acta, 33B, 153 (1978).
6. R.E. Sturgeon, Anal. Chem., 49, 1255A (1977).
7. F.J. Langmyhr, Analyst, 104, 993 (1979).
8. S. Greenfield, H. McGeachin and P.B. Smith, Talanta, 23, 1 (1976).
9. P.W.J.M. Boumans, ICP Newsletter, 5, 181 (1979).
10. R.M. Dagnall, P.J. Smith, T.S. West and S. Greenfield, Anal. Chim. Acta, 54, 397 (1971).
11. H.C. Hoare, R.A. Mostyn, Anal. Chem., 39, 1153 (1967).
12. E.D. Salin and G. Horlick, Anal. Chem., 51, 2284 (1979).
13. G.F. Kirkbright and R.D. Snook, Anal. Chem., 51, 1938 (1979).
14. A.M. Gunn, D.L. Millard and G.F. Kirkbright, Analyst, 103, 1066 (1978).
15. J.P. Walters, Appl. Spectrosc., 23, 317 (1969).
16. T.H. Maiman, Nature, 187, 493 (1960).
17. F. Breck and L. Cross, Appl. Spectrosc., 16, (1962).
18. H. Moenke and L. Moenke-Blankenburg, "Laser Micro-Spectrochemical Analysis", translated by R. Auerbach, (Adam Hilger, London, 1973).
19. I. Harding-Barlow, K.G. Snetsinger and K. Keil, "Laser Microprobe Instrumentation in Microprobe Analysis", C.A. Anderson, ed., (Wiley-Interscience, New York, 1973).

20. K. Laqua, "Analytical Spectroscopy Using Laser Atomizers" in Analytical Laser Spectroscopy, N. Omenetto, ed., Chemical Analysis vol. 50, (Wiley-Interscience, New York, 1979).
21. M. Margoshes, "Application of the Laser Microprobe to the Analysis of Metals", in Microprobe Analysis, C.A. Anderson, ed., (Wiley-Interscience, New York, 1973).
22. R.M. Barnes, Anal. Chem., 46, 150R (1974).
23. R.M. Barnes, Anal. Chem., 48, 106R (1976).
24. R.M. Barnes, Anal. Chem., 50, 100R (1978).
25. J. Eichler and H. Lenz, Appl. Opt., 16, 77 (1977).
26. J.F. Ready, Appl. Phys. Lett., 3, 11 (1963).
27. J.F. Ready, Phys. Rev., 137, A620 (1965).
28. J.F. Ready, J. Appl. Phys., 36, 462 (1965).
29. W. Bogerhausen and R. Vesper, Spectrochim. Acta, 24B, 103 (1969).
30. H. Klocke, Spectrochim. Acta, 24B, 263 (1969).
31. K.W. Marich, W.J. Treytl, J.G. Hawley, N.A. Peppers, R.E. Meyers and D. Glick, J. Phys. E, 7, 830 (1974).
32. N.A. Peppers, E.J. Scribner, L.E. Alterton, R.C. Honey, E.S. Beatrice, I. Harding-Barlow, R.C. Rosen and D. Glick, Anal. Chem., 40, 1179 (1968).
33. H. Human, R. Scott, A. Oakes and C. West, Analyst, 101, 265 (1976).
34. R.H. Scott and A. Strasheim, Spectrochim. Acta, 25B, 311 (1970).
35. R.H. Scott and A. Strasheim, Spectrochim. Acta., 26B, 707 (1971).
36. E.H. Pepmeier and H.V. Malmstadt, Anal. Chem., 41, 700 (1969).
37. N.G. Basov, O.N. Krokhin, and G.V. Sklizkov, Appl. Opt., 6, 1814 (1967).
38. S. D. Rasberry, B.F. Scribner and M. Margoshes, Appl. Opt., 6, 87 (1967).
39. A.B. Whitehead and H.H. Heady, Appl. Spectrosc., 22, 7 (1968).

40. J.M. Baldwin, Appl. Spectrosc., 24, 429 (1970).
41. V.V. Pantaleev and A. Yankovskii, Zh. Prikl. Spectrosc., 3, 1 (1965).
42. N.V. Korolev, V.V. Ryukhin and G.B. Lodin, Zh. Prikl. Spectrosc., 19, 21 (1973).
43. E.F. Runge, S. Bonfiglio and F.R. Bryan, Spectrochim. Acta, 22, 1678 (1966).
44. Lamma 500 from Inficon Leybold-Heraeus In., East Syracuse, New York, 13057.
45. S.D. Raspberry, B.F. Scribner and M. Margoshes, Appl. Opt., 6, 81 (1967).
46. C.D. Alkemade, Spectrochim. Acta, 27B, 185 (1974).
47. A.J. Saffir, K.W. Marich, J.B. Orenberg and W.J. Treytl, Appl. Spectrosc., 26, 469 (1972).
48. T. Ishizuka and Y. Uwamino, Anal. Chem., 52, 125 (1980).
49. V.G. Mossotti, K. Laqua and W.D. Hagenah, Spectrochim. Acta, 23B, 197 (1967).
50. T. Ishizuka, Y. Uwamino and H. Sumahara, Anal. Chem., 49, 1339 (1977).
51. D.E. Osten and E.H. Pepmeier, Appl. Spectrosc., 27, 165 (1973).
52. T. Kantor, L. Polos, P. Fodor and E. Pungor, Talanta, 23, 585 (1976).
53. L.N. Kaporskii and G.S. Musatova, Zh. Prikl. Spectrosc., 8, 681 (1968).
54. A.V. Karyakin and V.A. Kaigorodov, Zh. Anal. Khim., 23, 930 (1968).
55. C.A. Sacchi and O. Svelto, "Basic Principles of Lasers" in Analytical Laser Spectroscopy, N. Omenetto, ed., Chemical Analysis, vol. 50 (Wiley-Interscience, New York, 1979).
56. M. Margoshes and B.F. Scribner, Anal. Chem., 38, 297R (1966).
57. M. Margoshes and B.F. Scribner, Anal. Chem., 40, 223R (1968).

58. M.L. Franklin, Ph.D. Thesis, University of Illinois (1969).
59. W.J. Treytl, K.W. Marich, J.B. Orenberg, P.W. Carr, D.C. Miller and D. Glick, *Anal. Chem.*, 43, 376 (1971).
60. E.H. Pepmeier and D.E. Osten, *Appl. Spectrosc.*, 25, 642 (1971).
61. R.H. Wednt and V.A. Fassel, *Anal. Chem.*, 37, 920 (1965).
62. S. Greenfield, I.L. Jones and C.T. Berry, *Analyst*, 89, 713 (1964).
63. V.A. Fassel and R.N. Kniseley, *Anal. Chem.*, 46, 1155A (1974).
64. T.E. Edmonds and G. Horlick, *Appl. Spectrosc.*, 31, 536 (1977).
65. G. Horlick and M.W. Blades, *Appl. Spectrosc.*, 34, 229 (1980).
66. G. Horlick, *Appl. Spectrosc.*, 30, 113 (1976).
67. I. Harding-Barlow and R.C. Rosen, "Application of the Laser Microprobe to the Analysis of Biological Materials", in *Microprobe Analysis*, C.A. Anderson, ed., (Wiley-Interscience, New York, 1973).
68. K. Keil and K. G. Snetsinger, "Applications of the Laser Microprobe to Geology" in *Microprobe Analysis*, C.A. Anderson, ed.; (Wiley-Interscience, New York, 1973).
69. P.W.J.M. Boumans and F.J. de Boer, *Spectrochim. Acta*, 27B, 391 (1972).
70. S.S. Bersman and J.W. McLaren, *Appl. Spectrosc.*, 32, 372 (1978).
71. W.J. Tretyl, J.B. Orenberg, K.W. Marich and D. Glick, *Appl. Spectrosc.*, 25, 376 (1971).
72. H. Schroth, *Z. Anal. Chem.*, 261, 21 (1972).
73. W. van Deijck, J. Balke and F.J.M.J. Maessen, *Spectrochim. Acta*, 34B, 1979 (1979).
74. H.V. Malmstadt, C.G. Enke, S.R. Crouch and G. Horlick, "Optimization of Electronic Measurements", (Benjamin, Menlo Park, California, 1974).
75. W. van Deijck, J. Balke and F.J.M.J. Maessen, *Spectrochim. Acta*, 34B, 359 (1979).

76. W.J. Boyko, P.N. Keliher and J.M. Malloy, Anal. Chem., 52, 53R (1980).
77. H.H. Bauer, G.D. Christian and J.E. O'Reilly, "Instrumental Analysis", (Allyn and Bacon, Toronto, Ontario, 1978).

APPENDIX A

DP1000


```

COMMON FJ
DIMENSION J(1024),JJ(1024),FJ91024)
SOPDEF KCF 6030
SOPDEF DBSK 6502
SOPDEF DBCI 6503
SOPDEF DBRI 6504
SOPDEF DBCO 6505
SOPDEF DBSO 6506
SOPDEF SODF 6531
SOPDEF SCGC 6535
SOPDEF RBCF 6536
3 WRITE(1,502)
502 FORMAT(/'BACKGROUND SUBTRACTION? Y OR N')
READ(1,507)JB
K=0
WRITE(1,500)
500 FORMAT('ENTER NO. OF SCANS AND POINTS, 2I3')
READ(1,501)N,NP
501 FORMAT(2I3)
S CLA
S TAD /N /ENTER NO. OF SCANS
S CIA /NEGATE N
S DCA SCAN /STORE NO. OF SCANS
S TAD /NP /ENTER NO. OF DATA POINTS
S CIA /NEGATE NPT
S DCA POINT /STORE NO. OF DATA POINTS
S CLA CLL
15 DO 1 I=1,NP
JJ(I)=0
1 J(I)=0
S CLA CLL
S TAD SCAN /GET THE NO. OF SCANS
S DCA 12 /SET THE SCAN COUNTER
SGO, TAD POINT /GET NO. OF DATA POINTS
S DCA 10 /SET POINT COUNTER
S TAD K0177 /GET STARTING ADDRESS
S DCA 11 /SET STORAGE ADDRESS
S TAD K0177 /GET STARTING ADDRESS
S DCA 13 /SET STORAGE ADDRESS
S TAD K1177 /GET STARTING ADDRESS OF UPPER FIELD
S DCA 14
S CMA
S DBC1 /CLEAR INPUT BUFFER
S CLA
SSTART, DBSK /CHECK FOR START FLAG
S JMP START
S DBRI /READ INPUT BUFFER
S DBCI /CLEAR INPUT BUFFER
S SPA
S JMP START
S CLA CLL
S SCGC
SCLOCK, SODF /CHECK FOR CLOCK FLAG

```



```

S      JMP      CLOCK
S      SCGC                      /READ INPUT BUFFER
S      RBCF                      /CLEAR INPUT BUFFER
S      CLL RAR
S      TAD I 11
S      SPA
S      JMP      HIGH
S      DCA I 13
S      ISZ      14
S      JMP      CHECK
SHIGH, AND      K3777
S      DCA I 13
S      ISZ I 14      /INCREMENT UPPER FIELD
SCHECK, ISZ      10
S      JMP      CLOCK
S      ISZ      12
S      JMP      GO
S      CLA CLL
      R=FLOAT(N)
      IF(K-0)10,10,11
10     DO 100 I=1,NP
      FJ(I)=2048*FLOAT(JJ(I))+FLOAT(J(I))
100    FJ(I)=FJ(I)/(R*51.1)
      GO TO 16
25     IF(JB-1632)9,13,9
13     WRITE(1,503)
503    FORMAT(/'STRIKE CR WHEN READY')
      READ(1,507)JG
      K=1
      JB=0
      GO TO 15
11     DO 14 I=1,NP
      FB=2048*FLOAT(JJ(I))+FLOAT(J(I))
      FB=FB/(R*51.1)
14     FJ(I)=(FJ(I)+.05)-FB
16     WRITE(1,588)
588    FORMAT(/'OUTPUT:TTY:1;DTA1:2;SCOPE:3;RECORDER:4;CONTINUE:5')
      READ(1,509)NO
509    FORMAT(I3)
      GO TO(21,22,23,23,25)NO
21     WRITE(1,505)(FJ(I),I=1,NP)
505    FORMAT(10(F6.3,1X))
      GO TO 16
22     WRITE(1,510)
510    FORMAT('ENTER FILE NAME, A6')
      READ(L,511)FILE
511    FORMAT(A6)
      CALL OOPEN('DIA1',FILE)
      WRITE(4,505)(FJ(I),I=1,NP)
      CALL OCLOSE
      GO TO 16
23     AMAX=FJ(1)
      DO 17 I=2,NP

```



```

18      IF(FJ(I)-AMAX)17,17,18
17      AMAX=FJ(1)
      CONTINUE
      AMIN=FJ(1)
      DO 19 I=2,NP
      IF(FJ(1)-AMIN)20,20,19
20      AMIN=FJ(1)
19      CONTINUE
      S=AMAX-AMIN
      IF(4-NO)9,26,27
26      DO 28 I=1,NP
28      J(I)=(FJ(I)-AMIN)*1000/S
      GO TO 29
27      DO 30 I=1,NP
30      J(1)=(FJ(1)-AMIN)*850/S
      J(1)=500
      J(2)=1000
      J(3)=500
SSET,   CLA
S       TAD      POINT      /GET NO. OF POINTS
S       DCA      10         /SET POINT COUNTER
S       TAD      K0177      /GET STARTING ADDRESS
S       DCA      11         /SET STARTING ADDRESS
SPLOT,  CLA CMA
S       DBCO                      /CLEAR OUTPUT BUFFER
S       CLA
S       TAD  1   11          /GET DATA POINT
S       TAD      K2000      /SET OUTPUT FLAG
S       DBSO                      /DATA TO OUTPUT BUFFER
S       KSF                      /CHECK FOR STOP FROM KEYBOARD
S       JMP CONT
S       KCF                      /CLEAR KEYBOARD BUFFER
S       JMP      /16         /EXIT
SCONT,  ISZ      10         /CHECK POINT COUNTER, SKIP IF ZERO
S       JMP      PLOT      /GET NEXT POINT
S       JMP      SET       /START OVER
29      WRITE(1,512)
512     FORMAT('ENTER DELAY, I3')
      READ(1,509)NT
S       CLA CLL
S       TAD      POINT      /GET NO. OF POINTS
S       DCA      10         /SET POINT COUNTER
S       TAD      K0177      /GET STARTING ADDRESS
S       DCA      11         /SET STARTING ADDRESS
31      DO 32 I=1,NT
32      JG=1*1
S       CLA CMA
S       DBCO                      /CLEAR OUTPUT BUFFER
S       CLA
S       TAD  I   11          /GET DATA POINT
S       TAD      K2000      /SET STROBE
S       DBSO                      /SET OUTPUT BUFFER

```



```
S      CLA
S      ISZ      10      /CHECK POINT COUNTER, SKIP IF ZERO
S      JMP      /31      /CONTINUE
      WRITE(1,513)
513    FORMAT('REPEAT PLOT,Y OR N')
      READ(1,507)JG
507    FORMAT(A1)
      IF(JG-1632)16,29,18
SK0777, 0777
SK2000, 2000
SPOINT, 0000
SK3777, 3777
SK1177, 2177
SK0177, 0177
SSCAN, 0000
9      WRITE(1,506)
506    FORMAT('// 'DO YOU WISH TO REPEAT, Y OR N')
      READ(1,507)JG
      IF(JG-1632)4,3,4
4      CALL EXIT
      END
```


B30280